Evaluation of ^{1}H NMR- and GC/MS-based metabonomics for the assessment of liver and kidney toxicity

Dissertation zur Erlangung des
naturwissenschaftlichen Doktorgrades
der Julius-Maximilians-Universität Würzburg

vorgelegt von
Maximilian Sieber
aus Nürnberg

Würzburg, 2009

Eingereicht am: .....
bei der Fakultät für Chemie und Pharmazie

1. Gutachter:.....
2. Gutachter:.....
der Dissertation

1. Prüfer:.....
2. Prüfer:.....
3. Prüfer:.....
des öffentlichen Promotionskolloquiums

Tag des öffentlichen Promotionskolloquiums: .....

Doktorurkunde ausgehändigt am:.....

Table of contents

1 Introduction

Histopathology is still the standard for the assessment of drug candidate toxicity in animal experiments, required for preclinical safety testing. Histopathological evaluation not only requires large numbers of animals, but also trained specialists. Therefore, for cost reduction and animal welfare reasons, there is an urgent need for the development of novel non-invasive methods for toxicity screening.

The existing urinary and plasma parameters measured routinely with clinical chemistry analysis are too insensitive as well as too unspecific to be used for toxicity assessment alone. For example, the most commonly used clinical markers of renal injury, blood urea nitrogen (BUN) and serum creatinine, do not detect kidney damage until 70-80% of the renal epithelial mass is lost. Urinary analysis has three advantages: urine is not subjected to such a close homeostasis as plasma or other body fluids and alterations due to perturbations of metabolic processes should show up earlier than in plasma, urine samples can be collected non-invasively, and urine is available in comparably large quantities. However, the sensitivity and specificity of increased glucose and decreased osmolarity, the urinalysis parameters indicating renal damage in clinical chemistry analyses, are not satisfactory.

The omics technologies provide a promising approach for urinary analysis, combining modern computer-assisted data acquisition with multivariate statistical modeling. In the omics-cascade, going from genomics via proteomics to metabonomics, metabonomics is the phenotypic end. It focuses on small molecules and is therefore well suited for urinary analysis. There are two potential routes to a metabonomics approach for urinary analysis: a pattern recognition approach for sample classification based solely on the differences of ^{1}H NMR spectra or GC/MS chromatograms of treated animals and controls, and the identification of new biomarkers of toxicity found by a mechanistic understanding of the observed alterations of sample composition.

In this thesis, urinary metabonomics is applied to several rodent toxicity studies to assess whether urinary metabonomics may serve as a complementary tool to “classical” histopathology and clinical chemistry for the detection of drug candidate toxicity.

2 Background

2.1 Conventional methods for the non-invasive detection of nephro- and hepatotoxicity

2.1.1 Clinical chemistry parameters

Kidney and liver function can be assessed routinely by clinical chemistry parameters and histopathology. While blood and urine parameters can be sampled repeatedly and non- or minimal-invasively, these parameters lack sensitivity. Histopathology, while being sensitive and specific, requires sacrifice of the animal.

Clinical chemistry parameters monitoring renal function are blood urea nitrogen (BUN) and serum creatinine which increase when the kidney's ability to filtrate and excrete these compounds is reduced, together with a decrease in urine specific gravity or osmolarity and an increase in urinary glucose, occurring when the concentration of urine and the reabsorption of glucose from the filtrate are impaired. However, such alterations can be observed only when the kidney is already substantially damaged [1].

Liver injury specific clinical chemistry parameters are the increase of alanine amino transferase (ALAT) in serum if aspartate amino transferase (ASAT) increases in parallel, however, an ASAT increase in serum may also be observed for muscle damage. Liver injury may lead to low BUN, but disturbed hepatic function may not be observed until half of the functional liver mass is lost. Increased serum and urine bilirubin and increased serum bile acids together with increased alkaline phosphatase (ALP) and gamma glutamyl transferase (GGT) indicate bile duct damage and cholestasis [2].

2.1.2 Histopathology

The liver consists mainly of hepatocytes and bile ducts. The most common pathological lesions observed in the liver are apoptosis or necrosis and proliferation of hepatocytes, as well as lesions of the bile duct. Bile duct lesions observed are mainly necrosis or hyperplasia of the bile ducts and cholangiofibrosis.

Compared to the liver, the kidney possesses a complex anatomy. The kidney consist of various parts with different functions. The glomerulus, the proximal convoluted tubule, the pars recta, the thin limbs of the loop of Henle, the thick ascending limb of the loop of

Henle, the juxtaglomerular apparatus, the distal convoluted tubule, the collecting duct and the interstitium.

The glomerulus is responsible for the filtration of molecules from the blood, based on molecule size, configuration and charge. Transport decreases in the order from cationic, neutral to anionic molecules.

In the proximal convoluted tubule, active transport of sodium, calcium, potassium, phosphate as well as organic acids takes place, to recover these ions and molecules from the urine. The proximal tubule epithelial cells exhibit a high P450 mixed function oxigenase activity, and organic anion transporters are highly expressed as well, therefore it is an important place for xenobiotica metabolism. The proximal tubule endothelial cells also possess a very active cytosis and lysosomal apparatus. All these factors predestine the proximal convoluted tubule as primary target for many nephrotoxins [1].

2.1.3 Novel protein biomarkers for kidney and liver injury

To complement the classical clinical chemistry parameters and histopathology, there are a number of novel protein-based biomarkers with potential for the detection of kidney and liver injury. Kidney injury molecule 1 (KIM1) is a renal tubular protein elevated in experimental animals with acute kidney injury. Urinary neutrophil gelatinase-associated lipocalin (NGAL), urinary interleukin 18 (IL-18) and urinary *N*-acetyl-ß-*D*-glucosaminidase (NAG) perform well for the diagnosis, early detection and prognosis of acute kidney injury [3]. This is also the case for clusterin and osteopontin [4; 5].

For the early non-invasive detection of liver damage, some novel serum parameters are proposed. Increase in glutamate dehydrogenase (GLDH), serum F protein hydroxyphenylpyruvate deoxygenase (HPD), glutathione-*S*-transferase alpha (GSTα) and Arginase I correlate with hepatic injury. Malate dehydrogenase (MDH), like ALT, is a periportal enzyme released into serum. Purine nucleoside phosphorylase (PNP) is located in endothelial cells, Kupffer cells and hepatocytes and is released during necrosis of these cells. Paraoxonase 1 (PON1) is reduced in serum upon hepatic injury [2]. Besides bilirubin and bile acids, no robust urinary parameter indicating liver injury has been found yet.

Table 2.1.3.1: *"Classical" clinical chemistry parameters and novel protein-based biomarkers for the detection of kidney and liver damage. Especially for the detection of liver damage, a robust urinary parameter still remains to be found.*

	kidney		liver	
	serum	**urine**	**serum**	**urine**
clinical chemistry	blood urea nitrogen (BUN)	glucose	alanine amino transferase (ALAT)	bilirubin, bile acids
	serum creatinine		aspartate amino transferase (ASAT)	
			bilirubin, bile acids	
			alkaline phosphatase	
			gamma glutamyl transferase (GGT)	
novel protein biomarkers	kidney injury molecule 1 (KIM1)	neutrophil gelatinase-associated lipocalin (NGAL)	glutamate dehydrogenase (GLDH)	
		interleukin 18 (IL-18)	serum F protein hydroxyphenylpyruvate deoxygenase (HPD)	
		N-acetyl-ß-D-glucosaminidase (NAG)	glutathione-S-transferase α (GSTα)	
		clusterin	arginase I	
		osteopontin	malate dehydrogenase (MDH)	
			purine nucleoside phosphorylase (PNP)	
			paraoxonase (PON1)	

2.2 Definitions and terminology

2.2.1 Omics and metabolites

The "omics" technologies have gained a large impact in the life sciences in the recent years. Starting with genomics, on the DNA level, transcriptomics and proteomics on the RNA respectively protein level and finally metabonomics on the metabolite level, these technologies are based on the comprehensive analysis of the genome, transcriptome, proteome or metabolome, i.e. the complete set of an organism's or, more generally speaking, test system's genes, transcripts, proteins or metabolites.

Contrary to the "classical" analytical chemistry approach were a targeted analysis is carried out aiming at a small number of compounds which are known or suspected to change within the experimental setting, the metabonomics-approach is different. A global analysis is carried out, using ^{1}H NMR or full scan MS, to access as many metabolites as

possible. Then, using statistical tools, the differences between samples are filtered, thereby allowing the identification of alterations in samples without *a priori* knowledge.

Metabolites in this context are all endogenous intra- and extracellular compounds produced by the organism with a mass of up to 1000 amu. This definition has to be distinguished from the common pharmacological use of the term "metabolite" for drug metabolites, i.e. the degradation or conjugation products of pharmaceutical agents or xenobiotica in general. Throughout this thesis, the term "metabolite" shall be used in the former sense of all endogenous intra- and extracellular compounds of an organism. The complete set of all metabolites in an organism or system is defined as the metabolome [6], in analogy with the genome being the complete set of a system's genes.

2.2.2 Metabonomics vs. metabolomics

There are a number of terms such as metabonomics, metabolomics, metabolite profiling, metabolic fingerprinting etc. found in the literature which are neither well defined nor used consistently. The question which term is appropriate is often more of a philosophical nature, since these definitions try to differentiate between approaches that are based on the same analytical and statistical techniques and are only distinguished by minute differences in their objectives, and are also used interchangeably by different authors.

Metabonomics is defined as the "quantitative measurement of the dynamic multiparametric response of living systems to pathophysiological stimuli or modification" [7] and is often used interchangeably with metabolomics, the "study of global metabolite profiles in a system (cell, tissue, organism) under a given set of conditions" [8; 9]. The notion that metabonomics refers to ^{1}H NMR analysis and metabolomics to MS-based analysis origins from the fact that the pioneers in the field that coined these definitions used ^{1}H NMR analysis respectively MS-based analysis. Metabolic fingerprinting is an "unbiased, global screening approach to classify samples based on metabolite patterns or "fingerprints" that change in response to disease, environmental or genetic perturbations" [9; 10]. "Metabolic fingerprinting" is based solely on pattern recognition, and turns to "metabonomics" or "metabolomics", when the pattern or "fingerprint" is assessed as quantitative metabolite data. Metabolic profiling is the "quantitative analysis of a set of metabolites in a selected biochemical pathway or a specific class of compounds" [9; 10]. It focuses on a subset of the metabolome.

While metabolite profiling is focused on a specific compound class, metabolic fingerprinting is a global approach, trying to analyze a pattern or "fingerprint", but not necessarily with quantitative data or metabolite identification. The omics technologies require quantitative data and identification of the changes with regard to a systems biology approach. However, for practical purposes the distinction between metabonomics, metabolomics and metabolite profiling is of little importance, since the analytical and statistical methods used are highly similar. Therefore, the term "metabonomics" will be used throughout this thesis.

2.3 Analytical platforms

The demand of obtaining a global metabolite profile for metabonomics applications requires a new analytical approach. Instead of focusing on a single analyte or a small group of compounds with similar properties, comprehensive metabolite profiles have to be obtained in a single analytical run. The large progress in the field of instrument technology and computer processing power in the last few years has facilitated the recording of comprehensive metabolite profiles.

2.3.1 ^{1}H NMR for metabonomic analysis

The pioneers of metabonomic applications in the field of toxicology used ^{1}H NMR analysis. They studied alterations in urinary excretion patterns upon administration of renal toxins such as mercuric chloride [11; 12] cadmium chloride [13] and various nephrotoxins [14]. The advantage of ^{1}H NMR technology is that aqueous biological samples such as urine or plasma require only minimal sample work-up. Mostly, only addition of a deuterated standard as chemical shift reference and buffering to reduce pH-dependent shifts of pH-sensitive resonances is required. Although ^{1}H NMR analysis indiscriminately records resonances from all proton-containing compounds in a sample, and thus well fulfills the requirement of "global" profiling, it has three major draw-backs. First, ^{1}H NMR has limited sensitivity and dynamic range compared to GC/MS or LC/MS analysis. It is widely recognized throughout the metabonomics community that in most cases the range of ^{1}H NMR analysis is limited to the 20-30 most abundant molecules in urine, which are often referred to as the "usual suspects" [15]. Secondly, detection of metabolites depends on the proton structure of the compound. Molecules with a large number of chemically equivalent protons such as trimethylamine-*N*-oxide (TMAO) can be detected in relatively

small quantities as their resonance is a prominent singlet. Compounds with many chemically different protons with complicated multiplet resonances such as glucose are still lost in the spectral baseline noise at much higher concentrations. Finally, the missing chromatographic separation of metabolites compared to GC- or LC/MS leads to a large overlap of resonances making metabolite identification difficult.

A fact that is under technical control but has to be considered nevertheless is that the sample solvent, water, produces a dominant resonance of its own. Thus, the recording of ^{1}H NMR spectra requires water suppression, which can be handled well with pulse sequences such as the noesyprd1 pulse sequence contained in the Bruker library. Resonances of compounds of biological interest are found in the chemical shift region of $\delta = 0 – 10$ ppm. However, a range of around 18% of this region of the ^{1}H NMR spectrum has to be excluded from the analysis due to residual water resonances. Fortunately, not too many compounds have resonances in this chemical shift region of $\delta = 4.40 – 6.20$ ppm.

Despite these drawbacks, it must be recognized that ^{1}H NMR analysis is relatively cheap, fast and offers superb reproducibility across different laboratories, and therefore is the analytical technique that can be easily implemented for a routine toxicity screening. Furthermore, the samples are not destroyed during analysis. The wealth of publications on ^{1}H NMR based metabonomics applications across a broad scientific field proves the value of this approach [16].

2.3.2 GC/MS analysis for metabonomic analysis

Until recently, GC/MS-based applications with a metabonomics approach have been mostly used in the plant and cell sciences [17; 18], although the first profiling approaches in the 1970's using a GC/MS platform were intended for clinical uses [19]. A quantitative method for more than 100 compounds found in human urine was published as early as 1991 [20]. Such screening methods are routinely used for screening of inborn errors of metabolism in newborns [21; 22].

The relatively small range of toxicological applications of GC/MS-based metabonomics is probably not so much a question of the analytical technique, but also of fashion: the advent of electrospray ionization (ESI) and the possibilities for LC/MS analysis of aqueous biological samples opened by this new ionization technique moved the focus away from GC/MS in toxicological research. Thus, up to date, only few GC/MS-based metabonomics studies with a toxicological background are published [23; 24].

Although GC/MS requires volatile analytes and thus extensive sample work-up with extraction, drying and derivatization, GC/MS analysis is otherwise well suited for metabolome analysis.

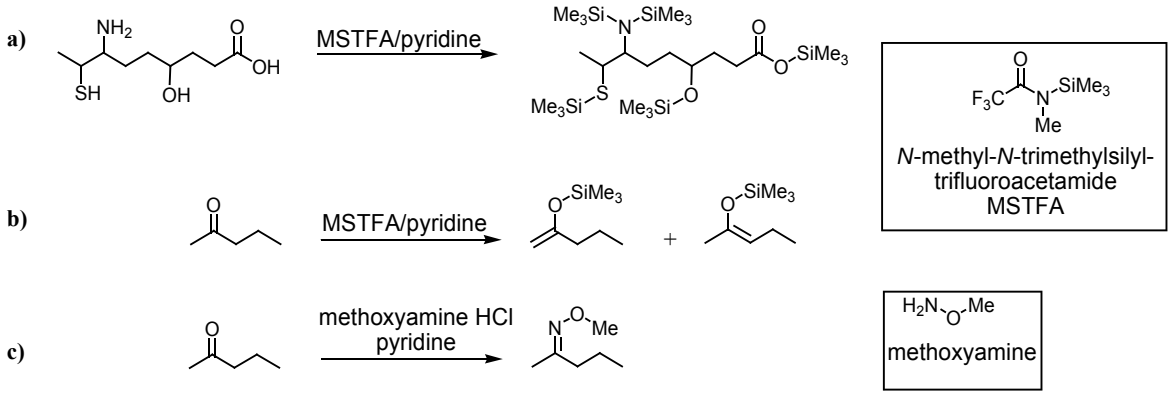

Figure 2.3.2.1*: GC/MS derivatization. Silylation of nucleophilic groups of the metabolites in biological samples increases the volatility and thermal stability of the analytes (a). In order to prevent the formation of isomers by enolization (b), silylation is preceded by a reaction with methoxyamine hydrochloride (c). The resulting oximes stabilize the ketones and aldehydes.*

Comprehensive derivatization methods such as the silylation with *N*-methyl-*N*-trimethylsilyltriflouroacetamide (MSTFA) exist, allowing access to a large number of compounds in body fluid samples by transferring OH-, NH- and SH-groups into stable volatile products (Fig. 2.3.2.1a). Prior to silylation, ketones and aldehydes are converted to oximes in order to avoid isomer formation due to keto-enol tautomery (Fig. 2.3.2.1b and c). A major advantage of GC/MS analysis is the high separation capacity of GC/MS columns, yielding sharp, baseline-separated peaks and good peak forms which enable automated processing by specialized peak picking and alignment software. Furthermore, due to almost 40 years of experience with GC/MS analysis with capillary columns, derivatization agents and artifacts are well investigated [25], and large commercially available databases (Wiley Registry of Mass Spectral Data, NIST Mass Spectral Data Base) exist, allowing the rapid identification of unknown metabolites.

Lately, a number of validated GC/MS methods intended for metabonomic analysis for urine or serum have been published [24; 26; 27], demonstrating the return of GC/MS analysis to metabolite profiling in toxicology. This is also due to the advent of novel

techniques such as two-dimensional GC separation coupled to time-of-flight detection (GC × GC/TOF-MS) [28; 29].

A drawback of GC/MS-based methods is the differential response of different compounds. The derivatization procedure requires optimization, since some endogenous metabolites are more reactive than others, and in some cases one compound forms a variety of different derivates instead of a single product. A general problem with MS-based techniques is the response to the ionization procedure. Some compounds are ionized more easily than others. Therefore, quantification of MS data is more difficult than with ^{1}H NMR data and classical analytical procedures use ^{2}D- or ^{13}C-labeled internal standards for quantification. However, this procedure cannot be implemented easily for an untargeted analysis such as required for metabonomic analysis.

2.3.3 LC/MS analysis for metabonomic analysis

LC/MS analysis has been used in a variety of metabonomic studies in the recent years. However, as LC/MS analytics included only a minor part of this thesis, this method shall only be mentioned briefly in order to complete the discussion of analytical platforms applied to metabonomic analysis. LC/MS has gained importance for metabonomics applications [30; 31], especially after the introduction of ultrahigh pressure liquid chromatography (UPLC) [32] resulting in superior separation, and hydrophilic interaction liquid chromatography (HILIC) [33], allowing efficient separation of highly polar compounds. Advantages are high sensitivity, good chromatographic separation and less sample work-up needed as compared to GC/MS. However, the automatic processing and interpretation of results is hampered by retention time drifts, adduct formation, ion suppression and the lack of databases allowing rapid identification of unknown metabolites based on their ESI spectra.

2.3.4 Combination of analytical platforms

It is important to recognize that ^{1}H NMR spectroscopy and mass spectrometry are complementary tools and that a combination of methods provides wider coverage of metabolites and thus a much more comprehensive picture of the metabolome than any single technique by itself. Using a combination of ^{1}H NMR, GC/MS and LC/MS techniques, Atherton *et al.* [34] were able to identify metabolic perturbations in the PPAR-α null mutant mouse liver as compared to wild-type mice, ranging from decreased

glucose and choline discovered by ^{1}H NMR analysis to increased stearic acid, cholesterol and pentadecanoic acid found with GC/MS analysis. Similarly, plasma analysis using all three analytical platforms provided a more comprehensive metabolite profile of normal and Zucker (fa/fa) obese rats than any methodology would have on its own. For instance, GC/MS revealed an increase in arachidonic acid and tocopherol, whereas a rise in taurocholate in Zucker rats was detected UPLC/MS [35].

2.4 Multivariate data analysis

The modern analytical methods for comprehensive metabolite screening require computerized data collection for the rapid sampling of large amounts of data. These large data quantities have to be filtered by automatized techniques to separate information from noise. Of the thousands of resonances in a ^{1}H NMR spectrum of an urine sample, those which are altered as a consequence of a toxic insult must be filtered. There are various approaches for multivariate data analysis in metabonomics [36], but the most common one, principal component analysis (PCA), is based the projection of variance. The methods for data reduction applied in this thesis are all based on PCA.

2.4.1 Unsupervised models: principal component analysis

Modern analytics produce so called short and fat matrices, meaning that there are much more variables (i.e. metabolites, chromatographic peaks, ^{1}H NMR resonances) than observations (i.e. animals, and their urine samples respectively) in a study. In typical toxicity studies, three groups of animals (n = 5) are observed at three time points, resulting in 45 observations. ^{1}H NMR spectra are typically binned into 250 bins; and at least 500 features (mass/retention time pairs) can be extracted from GC/MS chromatograms. The data structure is a k-dimensional coordinate system with k variables describing each observation (for ^{1}H NMR data: 250 variables describing 45 observations). Moreover, these data tables often contain missing values either because some metabolites simply do not exist in certain samples, for example, if they are only excreted upon treatment or they are not detected, because they are contained in the samples in concentrations near their limit of detection. To analyze this kind of data, PCA is useful, as it is robust against outliers and missing values [37].

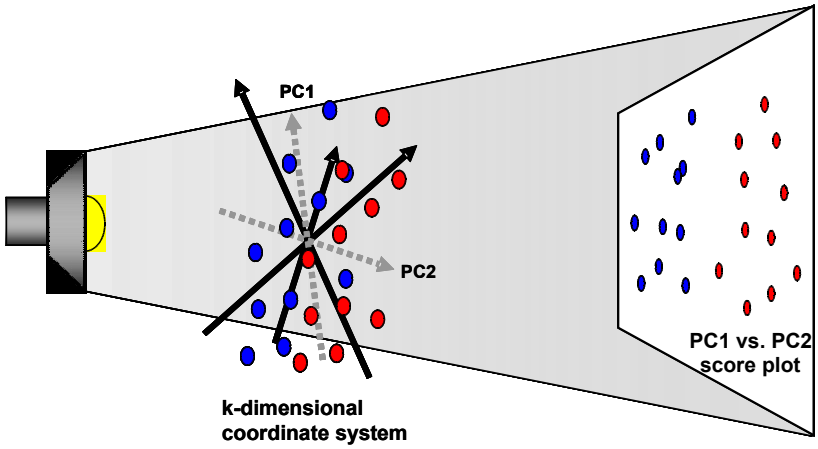

***Figure 2.4.1.1**: Principal component analysis (PCA) is a data reduction method based on the projection of variance. The data, represented by a k-dimensional coordinate system is reduced to a two-dimensional coordinate system, spanned by the principal components (PCs). The first PC is chosen in such a way that the variance along it is maximized. The second PC is orthogonal to the first, and maximizes the variance as well. In this way, the complex data can be visualized two-dimensionally, while retaining a large part of the information which is contained in the data.*

PCA is a multivariate projection method, based on the identification of systematic variation and the maximization of variance. The many partially correlated variables are reduced to few independent, latent variables, the principal components (PCs). Every PC is a linear combination of the original parameters. Consecutive PCs are orthogonal to each other and thus independent. Every observation can therefore be plotted in a two- or three-dimensional coordinate system of latent variables, which still contains most of the spectral or chromatographic information (Figure 2.4.1.1). Since the localization of the scores in the plot is based purely on variance and no other information is put into the model, PCA is called an unsupervised method. PCA is the first method of choice used for metabonomics, before any more complex data analysis methods are employed, since it is robust, unsupervised and can be implemented quite easily [36].

While PCA can be applied to gain a rapid insight into data structure, a problem associated with PCA-based variance analysis is its sensitivity to variables not correlated to the trends investigated, such as analytical variability, sample work-up, analytical artifacts, physiological influences (genotype, sex, age, day time, food etc.) and vehicle or compound metabolites in animal experiments. For the identification of discriminating markers between experimental groups, supervised approaches are superior.

2.4.2 Supervised models: orthogonal projection to latent structures

For closer examination of such samples containing a large variance and possessing only very little discriminating information, a supervised approach often yields superior results. Supervised multivariate analysis means that information on class identity, such as "vehicle control" versus "treated" is included in the statistical analysis. The partial least squares projection to latent structures analysis (PLS) can be seen as an extension of PCA with a regression element. Two blocks of variables (X-block and Y-block) can be brought into relation with each other. The X-block is the *k*-dimensional coordinate system also used in the PCA, while the Y-matrix consists of one or more continuous variables. For a two-class problem such as modeling control versus treated animals in a toxicity study, the Y-block becomes a so called dummy matrix, a single column with two descriptors (0, 1), and the PLS becomes a discriminant analysis (PLS-DA).

Because the results of PLS and PLS-DA are often difficult to interpret, especially when trying to determine which variables contribute most to the class discrimination (or, in the concrete case of toxicity modeling: which metabolites are changed between controls and treated animals as a result of a toxic insult), a further extension of PLS-DA can be made. Under the assumption that the X-block variables contain a certain part of information not correlated to the Y-block describing the class, the X-block variance is modeled in such a way that discriminating information is modeled on the first component t[1]P and orthogonal information, i.e. information not contributing to class separation, is modeled with the second component t[2]O and all following components. This approach is called orthogonal projection to latent structures discriminant analysis (OPLS-DA) [38].

The OPLS-DA approach allows a better analysis of discriminating features, and allows the analysis and interpretation of information not contributing to class separation. Analytical variation, sampling sequence, genetic differences, daytime effects and physiological variation have been found by this approach. Thus, OPLS-DA of metabolite profiles obtained with GC/MS analysis revealed differences between three strains of Zucker rats [39], and a model based on metabolite profiles obtained from human cancer tissue samples could differentiate between colon and rectal cancers [40]. The OPLS-DA models can also be used to identify the variables responsible for class separation and therefore they can be used for identification of potential biomarkers of toxicity. One approach used is the S-plot [41], which plots the covariance (p) against the correlation (pcorr). For a marker, both the contribution to the model expressed in p and the effect and

reliability of this contribution expressed in p(corr) should be high. Thus the potential markers are located on the outer ends of the S-shaped point swarm (Figure 2.4.2.1).

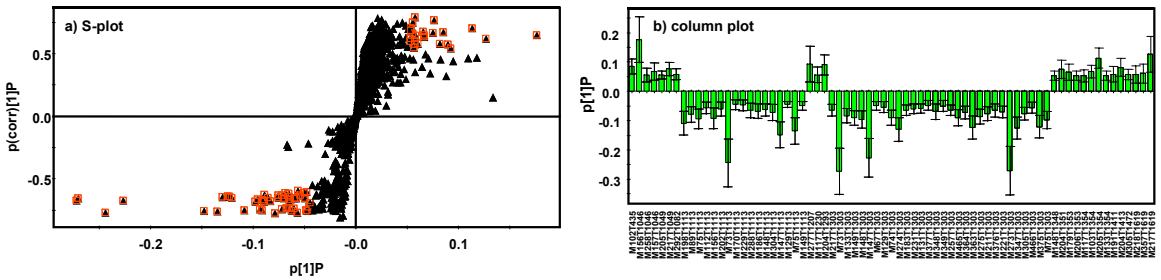

Figure 2.4.2.1*: S-plot (a) and column plot of extracted variables with jack-knifed confidence intervals (b) of an GC/MS data based OPLS-DA model to illustrate the process of marker identification. The S-plot shows the covariance p against the correlation p(corr) of the variables of the discriminating component of the OPLS-DA model. Cut-off values for the covariance of p ≥|0.05| and for the correlation of p(corr) ≥|0.5| were used, the variables thus selected are highlighted in the S-plots with red squares (a). In order not to overinterpret the model, the markers were selected in a conservative manner by investigating only those variables showing a jack-knifed confidence interval less than half of the variable's value (b).*

2.4.3 Binning, peak picking and alignment

Data extraction from the chromatogram to the X-matrix in table format containing the features that can be processed with statistics programs require different software packages. The approaches between ^{1}H NMR and GC/MS are fundamentally different. For ^{1}H NMR data processing, the routine method is spectral binning. The whole ^{1}H NMR spectrum is divided into 0.04 ppm-wide bins, and the total intensity of each bin is recorded. The resulting table contains 250 bins for a 10 ppm wide ^{1}H NMR spectrum. With the multivariate data analysis, alterations in a bin are detected. Subsequently, the compounds contained in these bins responsible for the change in intensity have to be identified.

For GC/MS (and LC/MS) applications, signal processing software extracts the peaks of each mass trace according to certain criteria such as signal to noise ratio, length of the peak etc. These software packages yield tables for statistical analysis containing mass/retention time pairs as peak identity and the corresponding intensity. The software requires some optimization of the extraction parameters, but offers the advantage that the resulting ions can be directly compared to reference compounds and the separation of

overlapping peaks is possible too. A variety of software tools is available for this purpose, such as MetAlign [42], mzMine [43] and XCMS [44]. An overview of the variety of commercially and publicly available software tools is given by Katajamaa and Oresic [45]. Recently, Lange *et al*. systematically tested six peak processing and alignment programs and attested XCMS superior performance concerning both data quality and run time [46].

2.4.4 Normalization and scaling

A problem is the normalization of urinary data prior to analysis. In conventional studies, parameters are normalized to urinary creatinine. For metabonomics analysis, this approach seemed not feasible, especially for nephrotoxic compounds, where creatinine excretion may be altered as toxic response, so another approach is chosen. For most metabonomic studies, GC- or LC/MS chromatograms or ^{1}H NMR spectra are normalized to total integral, meaning that each peak intensity is divided by the intensity of all peaks in one sample. This levels out any differences in sample concentration or MS response, as long as the samples analyzed do not differ too much and any alterations in the peak intensities are small compared to the total intensity of the spectrum. It also circumvents the problem of internal analytical standards in MS-based analyses, since in this way all other compounds act as a standard for the peak analyzed. Even though the normalization to total integral is by no means the optimal procedure, it is easy to implement and yields good results and is therefore used by many researchers. Warrack *et al*. recently tested the differentiation of urine samples obtained from control and treated animals in multivariate models comparing normalization to osmolarity, creatinine and total integral and no normalization, and found that total integral and osmolarity normalization performed best [47].

Centering and scaling is applied to the data prior to multivariate analysis. Data is mean centered, meaning that the mean of each peak intensity across all samples is set to zero. This allows the comparison of peaks with different means. Scaling has influence on the variance of the peaks [36]. No scaling would mean the absolute variance of the peak is used, leading to the dominance of the few large peaks detected. Unit variance scaling set the variance of the peaks to one, giving the same weight to all peaks. This scaling procedure however places too much weight on the noise. A good compromise between no scaling and unit variance scaling is pareto scaling, which weighs the variance according to its square root. This procedure reduces the influence of the high intensity peaks on the

model and at the same time does not overestimate the contribution of the noise to the model [37].

2.5 Applications in toxicology

Metabonomics is increasingly being propagated as a non-invasive method for toxicity assessment. This technology may offer a fast and comprehensive detection of biochemical perturbations in urine or plasma indicative of toxicities and may provide information on mechanisms of toxicity. Metabonomics techniques have been applied to analyze the urinary profiles of various model hepato- and nephrotoxins such as hydrazine and mercuric chloride, and to characterize the toxicities of novel compounds in drug development [15].

2.5.1 ^{1}H NMR-based metabonomics in toxicology

A large number of studies focusing on single compounds have been published in the recent years. Using ^{1}H NMR techniques, decreased urinary Krebs cycle intermediates and increased urinary creatine were identified after acetaminophen treatment in rats [48; 49]. Cadmium induced creatineuria in rats, and complexion of urinary citrate by cadmium was observed [50]. α-Naphthylisothiocyanate-induced cholestasis in rats correlated with creatineuria, taurineuria, bile aciduria and decreased urinary Krebs cycle intermediates [51]. Decreased urinary Krebs cycle intermediates as well as increases in the excretion of creatine, glucose, choline, alanine and 5-oxoproline were observed for bromobenzene-induced liver damage in rats [52]. *N*-Phenylanthranilic acid treatment of rats resulted in an increased excretion of ketone bodies and ascorbate with urine [53].

2.5.2 GC/MS-based metabonomics in toxicology

GC/MS analysis was used to investigate the toxic effects of hydrocortisone in rats, indicating increased catecholamine synthesis and raised levels of urinary alanine and cholesterol [54]. Galactosamine-induced hepatic failure in the mouse was characterized by increased amino acids and Krebs cycle intermediates in plasma [55]. Tetrahydro-corticosterone and 5α-terahydrocorticosterone were identified as putative urinary biomarkers for nonylphenol-induced kidney injury in the rat [56]. Carbontetrachloride-mediated acute liver failure in mice correlated with elevation of gluconeogenic amino acids and depletion of free fatty acids in plasma [57].

2.5.3 LC/MS-based metabonomics in toxicology

LC/MS analysis was applied to studies of nephrotoxicity induced by various heavy metals in rats, indicating decreased urinary levels of xanthurenic acid, kynurenic acid and increased levels of phenolic sulfoconjugates upon treatment [58–60]. Similar effects were also observed after treatment with cyclosporin A [61]. *D*-Serin induced nephrotoxicity in the rat correlated with glucosuria, aminoaciduria, lactaturia and decreased levels of xanthurenic acid [62].

2.5.4 Identification of putative biomarkers

These applications were not only aimed at differentiating between controls and treated groups, but also at biomarker identification. For example, various combinations of elevated and decreased excretion levels of up to 20 metabolites quantified from ^{1}H NMR spectra of urine from rats treated with various nephrotoxins were proposed as putative site-specific biomarkers of nephrotoxicity [14; 63] and hydrazine-induced neurotoxicity [64]. Increased urinary phenylacetylglycine (PAG) excretion was proposed as a biomarker of drug-induced phospholipidosis [65].

2.5.5 Confounders

One problem with studies comprising only one or a few compounds administered are the confounders, which may be altered in correlation with compound administration but are not related to the mechanism of toxicity. In humans, urinary carnosin and anserin excretion increased after meat consumption, betaine and trimethylamine excretion after fish and shellfish consumption and fructose excretion after cherry consumption [66]. A large influence on urinary profiles of rats is now attributed to the intestinal microflora [67; 68], especially the excretion levels of hippurate, 3-hydroxyphenylpropionic acid and phenylacetylglycine vary with alterations in the intestinal microflora. Hippurate and 3-hydroxyphenylacetic acid excretion also varied with diet [69]. Alterations in urinary profiles of rats were also correlated to the female cyclus [70], and age-dependent changes in the urinary excretion of citrate and taurine were observed [13].

2.5.6 Multiple compound studies

The collection of toxin-specific and organ-specific patterns in urinary metabolites would be practicable to build a system for toxicity classification and biomarker

identification [71]. To address these problems and generally evaluate the work-flow of metabonomics studies, a large-scale consortium project was initiated to assess the value of ^{1}H NMR metabonomics studies with a large number of compounds. The aim was also to control the inter-laboratory variance of metabonomics studies. The Consortium for Metabonomic Toxicology (COMET) was formed between six pharmaceutical companies and the Imperial College of Science, Technology and Medicine in London to evaluate the role of metabonomics in xenobiotic toxicity studies [72]. The focus thereby lay on nephro- and hepatotoxicity. The evaluation of more than eighty compounds analyzed with urinary ^{1}H NMR metabonomics during the COMET project resulted in an expert system for prediction of toxicology based on ^{1}H NMR urinary profiles which is able to predict toxicity based on urinary ^{1}H NMR profiles with good predictivity [73].

While COMET was focused on the evaluation of ^{1}H NMR metabonomics in toxicology, the InnoMed PredTox project was designed to evaluate a broader range of novel approaches, including genomics, proteomics and metabonomics approaches for the early prediction of toxicity [74].

In summary, metabonomics approaches have gained large impact in the recent years not only in toxicology but also in various other fields of the life sciences. The pharmaco-metabonomic approach aims to predict outcomes of drug treatment based on the metabolic phenotype of the individual. The concept was demonstrated by the prediction of the magnitude of paracetamol toxicity in rats from the predose urinary ^{1}H NMR profiles [75]. GC/MS based urinary profiles are used in clinical screening of newborns for the detection of inborn errors of metabolism [22]. Furthermore, metabonomics is applied in the fields of plant sciences [76], environmental technology [77], *in vitro* test systems [78] as well as food quality control and nutrition [79].

2.6 Model compounds for nephro- and hepatotoxicity

2.6.1 Gentamicin

The aminoglycoside antibiotic gentamicin is used against life-threatening infections with gram-negative bacteria. Its heterocyclic structure consists of two aminosugars linked to an aminocyclitol ring by glycoside bonds (Fig.2.6.1.1). Gentamicin binds irreversibly to the ribosomal 30S subunit of bacteria and thereby blocks their protein synthesis. The drawback of gentamicin and the aminoglycoside antibiotics in clinical use is their nephrotoxicity, occurring in about 10 % of all cases treated.

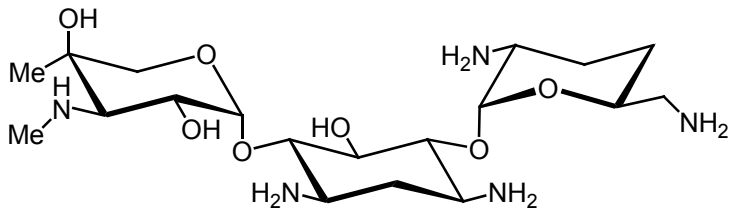

Figure 2.6.1.1: *Chemical structure of aminoglycoside antibiotic gentamicin. It is built up of two aminosugars linked to an aminoglycitol ring by glycoside bonds.*

Gentamicin induces non-oliguric renal failure with a rise in serum creatinine and impaired urinary concentration, accompanied by tubular dysfunction manifested in the release of brush border enzymes and renal wasting of K^+, Mg^{2+}, Ca^{2+} and glucose. Gentamicin is not absorbed from the intestine after p.o. administration and has to be given i.v. or i.p.. It is not metabolized and excreted almost completely over the urine after glomerular filtration. However, a small amount is retained in the tubular epithelium of the S1 and S2 segment of the proximal tubuli. Gentamicin enters the cell by endocytosis mediated by the megalin receptor and accumulates in lysosomes [80]. Release of gentamicin from the lysosomes leads to apoptosis of the tubular epithelial cells involving the mitochondrial activation with release of cytochrome c and caspase-3 activation [81].

2.6.2 Ochratoxin A

Ochratoxin A (OTA) is a mycotoxin produced by *Aspergillus* and *Penicillium* species and is found in a variety of foodstuffs such as cereals, nuts, spices, dried fruits, coffee, beer and wine. Its structure comprises a dihydrocoumarin moiety linked to a molecule of *L*-ß-phenylalanine via an amide bond (Fig. 2.6.2.1). OTA is suspected to cause balkan endemic nephropathy (BEN) in humans, which is characterized by interstitial fibrosis, vascular and glomerular lesions as well as proximal tubule degeneration [82; 83].

In rats, OTA nephrotoxicity is characterized by polyuria and histopathological lesions of the proximal tubule epithelium [84]. Short-term studies showed disorganization of the tubule arrangement, single cell degeneration, nuclear enlargement and polyploidy. Chronic exposure to OTA leads to adenomas and carcinomas of tubule cells, whereby males are more susceptible than females [85; 86].

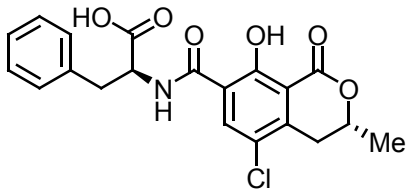

Figure 2.6.2.1: *Chemical structure of the mycotoxin and renal carcinogen ochratoxin A.*

The mechanism of OTA-mediated carcinogenicity is still unclear. There exists little evidence of genotoxicity [83], and a combination of various epigenetic mechanisms is discussed [87]. There is evidence of the involvement of protein synthesis inhibition, oxidative stress, nuclear factor kappa B (NF-κB), as well as disturbance of cell signaling and calcium homeostasis [87].

2.6.3 Aristolochic acid

Aristolochic acid (AA) is a mixture of nitrophenanthrene carboxylic acid derivatives, predominantly AAI and AAII, found primarily in *Aristolochia* species [88]. AA is a potent renal toxin and carcinogen, associated with Chinese herb nephropathy and BEN in humans [89]. The former is caused by exposure to AA-containing plants mistakenly used in traditional Chinese medicine formulations, the latter is suspected to be caused by the ingestion of *aristolochia* contaminated flour [89].

AA is metabolized primarily by CYP1A1 and CYP1A2 to aristolactams via a reactive cyclic nitrenium ion (Fig. 2.6.3.1), and this reactive metabolite binds preferentially to the exocyclic amino groups of purine bases, thereby acting as a genotoxic cancer initiating agent [88]. In rats, oral administration of 10 mg AA/kg bw for three months leads to renal pelvis carcinomas, urinary bladder carcinomas and forestomach carcinomas after nine months [90].

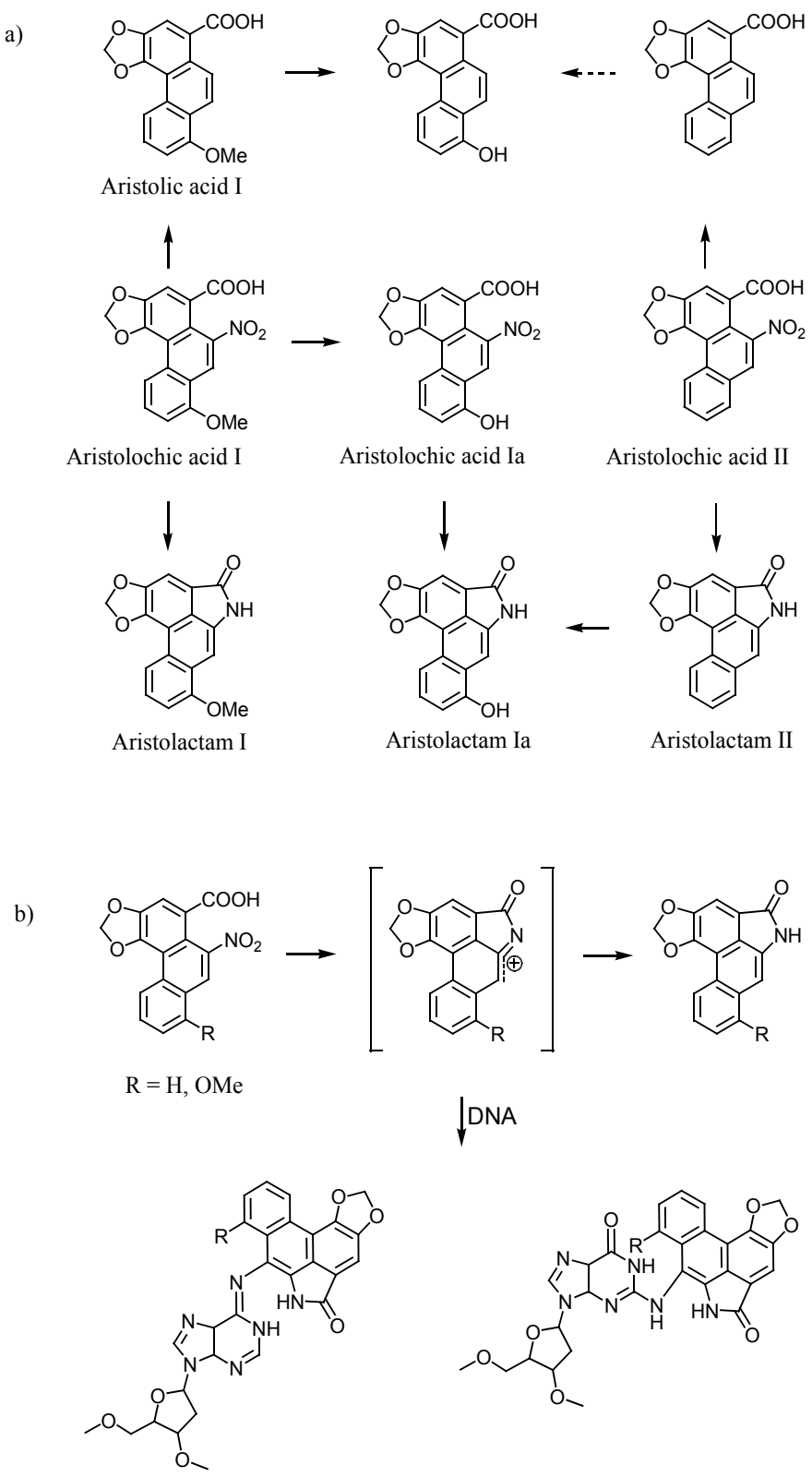

Figure 2.6.3.1*: Chemical structures and CYP450 mediated metabolism of aristolochic acids (a) and the formation of DNA adducts via the cyclic nitrenium ion intermediate (b).*

2.6.4 Furan

Furan is an industrial chemical that serves as an intermediate in the production of polymers. It has been shown to cause liver carcinoma in rodents and is classified as possibly carcinogenic to humans [91]. Concentrations in foodstuffs, especially canned meat products, reach levels that cause an increased tumor incidence in rodents [92].

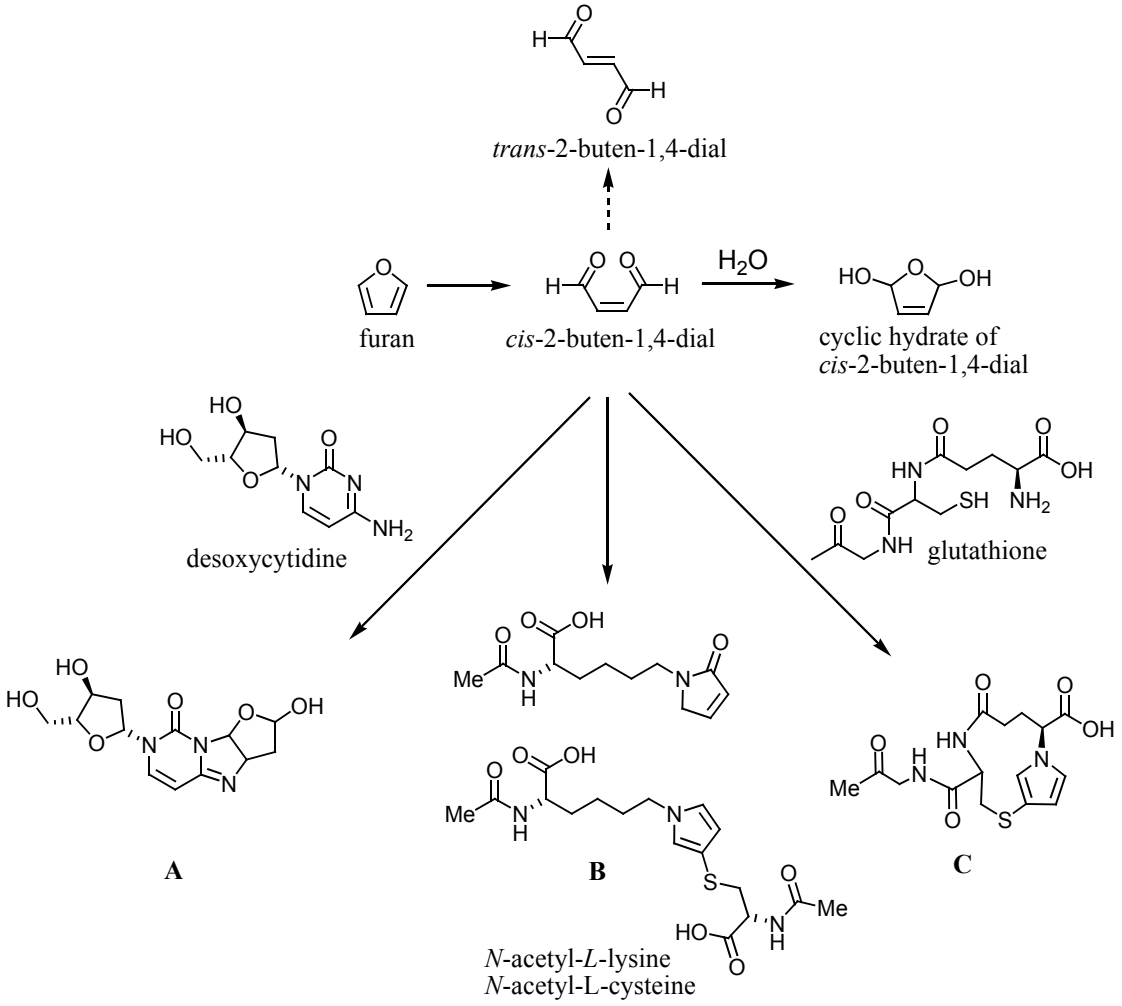

Figure 2.6.4.1*: Metabolism of furan. Furan is metabolized oxidatively by CYP 2E1 to cis-2-butene-1,4-dial. The isomerization to trans-2-butene-1,4-dial is prevented in aqueous solution by the formation of a cyclic hydrate. cis-2-Butene-1,4-dial may react further with nucleosides (A) and amino acids (B) in proteins. Conjugation with glutathione (C) eliminates the reactive metabolite.*

It is readily absorbed and rapidly metabolized by the liver. CYP enzymes open the furan ring, forming the reactive metabolite *cis*-2-butene-1,4-dial (Fig. 2.6.4.1). This reactive metabolite is eliminated by conjugation with glutathione, but a fraction binds irreversibly to proteins, and possibly to DNA as well (Fig. 2.6.4.1). The exact mechanism

of toxicity is still unclear, but the carcinogenicity of furan is probably due to a genotoxic mechanism, combined with secondary cell proliferation and thereby indirectly amplifying tumor growth. [92; 93].

2.6.5 The InnoMed PredTox project

The InnoMed PredTox project is a joint industry and European Commission collaboration aimed at improving drug safety. The consortium is composed of 14 pharmaceutical companies, three academic institutions and two technology providers. The goal of InnoMed PredTox is to assess the value of combining results from omics technologies together with the results from more conventional toxicology methods in more informed decision making in preclinical safety evaluation [74].

The studies conducted and evaluated in the project comprised 16 compounds in total, 14 of those were drug candidates that failed during the preclinical development process in part due to hepato- or nephrotoxicity. Troglitazone and gentamicin were analyzed as reference compounds for hepatotoxicity and nephrotoxicity, respectively. (Fig. 2.6.5.1).

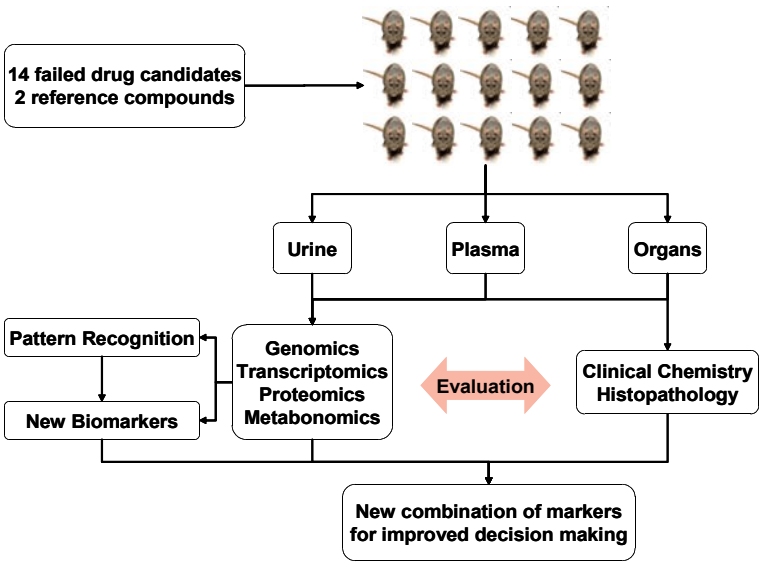

Figure 2.6.5.1*: Work flow scheme of the InnoMed PredTox Project. 16 compounds are administered orally in a standardized study design. Besides histopathology and clinical chemistry data, which are routinely collected in toxicity studies, a panel of various omics technologies is applied to the samples in order to evaluate which benefit can be gained from these techniques.*

Although the number of compounds is rather limited compared to other projects such as COMET [72], InnoMed PredTox is outstanding as it tries to evaluate a large panel of different omics technologies. It has to be kept in mind that the project is designed as a proof-of-concept to serve as a basis for a large follow-up project. The questions the project is designed to answer is which combination of methods and technologies is suited best to deliver predictive results for each compound and for each class of toxicity (hepatotoxicity, nephrotoxicity). Besides, the identification and evaluation of potential new biomarkers from the omics technologies might be achieved [74]. A great value of the project is also the joint effort made by pharmaceutical companies, universities and technology providers for a global perspective of preclinical safety evaluation in the 21st century [94].

3 Objectives

Aim of this thesis was the assessment of metabonomics techniques for early, non-invasive detection of toxicity in animal experiments compared to classical endpoints such as clinical chemistry and histopathology. This required

- Development/establishment of a GC/MS method for metabolite profiling
- Establishment of a peak picking and alignment software for GC/MS data
- Analysis of urine samples from various rodent toxicity studies with GC/MS and ^{1}H NMR
- Identification of potential biomarkers of toxicity and their evaluation in the context of biological pathways and mechanisms of toxicity

The focus thereby lay on ^{1}H NMR and GC/MS analysis of urine samples. Urine samples were obtained from four studies conducted in-house, as well as from the InnoMed PredTox project. ^{1}H NMR analysis is the best-established metabonomics method, high reproducibility and a large number of studies published allow easy comparison with results and fast reproduction of the methods used. Only few toxicological studies have applied GC/MS metabonomics up to date, therefore the development of a GC/MS metabonomics approach offers the possibility of acquiring more comprehensive metabolite profiles and the chance of discovering novel biomarkers.

The focus of this work lies in the measurement and interpretation of data from three rodent studies conducted in-house with various nephrotoxins. Application of gentamicin to rats for seven consecutive days was used as a pilot study, comparing the GC/MS metabonomics method to previously published ^{1}H NMR data [95]. A 90 day subchronic ochratoxin A study that had been conducted in-house previously [96] with full histopathology and clinical chemistry data was reanalyzed and evaluated with metabonomics methods. Aristolochic acid was administered to rats for 12 days at doses causing forestomach, kidney and bladder carcinomas [90; 97]. All three studies were analyzed with ^{1}H NMR and GC/MS for changes in the endogenous metabolite profile. These changes were evaluated with regard to mechanisms of toxicity and whether changes in urinary composition can be used as early, sensitive and specific marker of toxicity as compared to classical histopathology and clinical chemistry analysis.

The second part of the work was the analysis of urine samples from the InnoMed PredTox project, part of the European Union 6th Framework Programme. 14 failed drug candidates from the participating pharmaceutical companies and two reference compounds were evaluated. Here, the focus lay on the evaluation of quantitative ^{1}H NMR data and on a subgroup of four studies with compounds inducing bile duct necrosis. In the course of the project, urinary ^{1}H NMR data was quantitatively analyzed with regard to changes in metabolite excretion. The performance of the GC/MS method in combination with ^{1}H NMR was also tested.

4 Materials and methods

4.1 Chemicals and solvents

All chemicals and reagents were purchased from commercial suppliers. Methoxyamine hydrochloride, *myo*-inositol, dried pyridine, acetone and chloroform were obtained from Sigma Aldrich (St. Louis, MO). Methanol was purchased from Carl Roth GmbH (Karlsruhe, Germany). *N*-methyl-*N*-(trimethylsilyl)-trifluoracetamide (MSTFA) was purchased from AppliChem (Darmstadt, Germany). Gentamicin (GM) was purchased as solution (5 × 50 mg/mL in deionized water, liquid, sterile-filtered, cell culture tested, Sigma Aldrich Lot number 057K2371). Ochratoxin A (OTA) (CAS No. 303-47-9; 99 % purity) was purchased from Axxora, Grüneberg, Germany (batch no. L16528/a). Aristolochic acid (AA) sodium salt was purchased from Sigma Aldrich as a mixture of 65 % AA I and 27 % AA II (lot 054K06551).

4.2 Animal handling

Animals were purchased from commercial suppliers. The animal were housed in groups of five in standard macrolon cages. They had free access to water and standard diet (SSniff, Soest, Germany) and were kept under standard conditions (12 h day/night cycle, temperature 21–23 °C, humidity 45–55 %). All animal experimentation was performed under permit from the appropriate authorities in the approved animal care facility of the department. Treatment was carried out as described below in detail for each study. Animals were sacrificed by CO_2 asphyxation and cervical dislocation. Urine samples were collected for 24 h on ice, aliquoted and stored at −20 °C until further analysis. Blood samples were obtained by punctuation of either the tail vein or the retro-orbital plexus during the study and by cardiac puncture at sacrifice. Livers and kidneys were removed, snap-frozen in liquid nitrogen and stored at −80 °C until further analysis. Aliquots of tissues were fixed in neutral-buffered formalin, embedded in paraffin, cut into 5 µm sections and stained with haematoxilin and eosin for histopathological evaluation. Histopathological evaluation was carried out by two independent pathologists.

4.3 Clinical chemistry

Analysis of clinical chemistry parameters was carried out at the central laboratory of the university hospital of the University of Würzburg on a Vitros 700XR (Ortho-Clinical

Diagnostics, Neckarsgemuend, Germany) using standard protocols for the determination of these parameters according to the manufacturer's instructions. The following parameters were determined in urine: glucose, gamma glutamyl transferase (GGT), total protein, creatinine and osmolarity. The following parameters were determined in plasma: creatinine, urea, total bilirubin, glutamate pyruvate transaminase (GPT) (alanine amino transferase (ALAT)), glutamate oxalacetate transaminase (GOT) (aspartate amino transferase (ASAT)), gamma glutamyl transferase (GGT), alkaline phosphatase (ALP) and total protein.

4.4 Study design

4.4.1 Gentamicin

The study design was based on a previously published study by Lenz *et al.* [95]. Male Wistar rats, 6–8 weeks old, weighing 200 g (Harlan-Winkelmann, Borchen, Germany) were divided into three groups of five animals each. Following one week of acclimatization, animals were adjusted to metabolic cages three days prior to treatment.

Gentamicin (GM) dosing solutions of 10 mg/mL (low dose group) and 20 mg/mL (high dose group) were prepared daily by diluting the stock solution 1 : 5 or 1 : 2.5 with sterile water. Control groups received 0.9 % physiological saline.

Dosing solutions were administered subcutaneously twice a day at an eight hour interval for seven consecutive days. The low dose group received 2 × 30 mg GM/kg bw per day and the high dose group 2 × 60 mg GM/kg bw per day. The control group received an equivalent volume of physiological saline. The animals were housed in individual metabolic cages during the study. Food and water consumption was recorded daily. Urine was collected daily at 24 h intervals. A 250 µL aliquot of urine was used directly for clinical chemistry analyses. The remaining urine was aliquoted (250 µL) and stored at −20 °C. Blood samples were drawn from the retro-orbital plexus under light isoflourane anaesthesia 24 h and 72 h after the first dosing and used for clinical biochemistry and haematology. On the eighth day, the animals were sacrificed by CO_2 asphyxiation and blood was collected by cardiac puncture. A 250 µL aliquot of blood was used for clinical biochemistry analyses. Blood samples were collected in heparinized tubes and centrifuged. Plasma was used for clinical chemistry. The remaining plasma was stored at −20 °C. Organs (liver and kidney) were removed and weighed. The liver was partitioned in lobes and snap-frozen in liquid nitrogen and stored at −80 °C. One part of the left liver lobe was

stored in formalin. The left kidney was partitioned transversely in a ratio of approximately 2 : 1, the larger part was stored in formalin. The remainder and the right kidney were snap-frozen in liquid nitrogen and stored at −80 °C.

4.4.2 Ochratoxin A

Urine samples collected in several fractions were obtained from a previously published study [96]. Shortly, male Fisher F344 rats (205–225 g, n = 5 per group) were dosed with 21, 70 or 210 µg OTA/kg bw by gavage for 14, 28 or 90 days 5 days per week. Controls received corn oil only. Urine samples were collected over a 24 h collecting period pre-dose and after 14, 28 and 90 days of administration. Urine was collected on ice and stored at −20 °C until further analysis. Samples were only thawed once and prepared for metabonomic analysis within six hours.

Histopathology scores were obtained as previously described [96]. Scoring for the following endpoints was integrated in the data analysis: liver glycogen, liver fatty change, liver inflammatory foci, kidney hyaline inclusions, kidney tubular basophilia, kidney tubular vacuolization, kidney tubular cell apoptosis, kidney mononuclear foci, kidney tubular casts, kidney karyomegaly and kidney interstitial fibrosis.

4.4.3 Aristolochic Acid

Male Wistar rats, 6–8 weeks old, weighing 200 g were purchased from Harlan-Winkelmann, Borchen, Germany.

Aristolochic acid (AA) dosing solutions of 26.7 µg/mL (low dose group), 267 µg/mL (mid dose group) and 2.67 mg/mL (high dose group) were prepared daily by dissolving AA in tap water.

Male Wistar rats (n = 20) were randomly divided into four groups with five animals each. Dosing solution was administered daily by gavage, five days per week for two weeks. The low dose group received 0.1 mg AA/kg bw per day, the mid dose group 1.0 mg AA/kg bw per day and the high dose group 10 mg AA/kg bw per day. Control animals received an equivalent volume of tap water. The animals were transferred to individual metabolic cages for urine collection for 24 h after dosing on day one, five and twelve. An aliquot of urine (250 µL) was used directly for clinical chemistry analyses. The remaining urine was aliquoted (250 µL aliquots) and stored at −20 °C. Blood samples were drawn from the retro-orbital plexus under light isoflourane anesthesia 24 h and 120 h after the

first dosing and used for clinical biochemistry and haematology. On the twelfth day, the animals were sacrificed by CO_2 asphyxiation and blood was collected by cardiac puncture. An aliquot of blood (250 µL) was used for clinical biochemistry analyses. Blood samples were collected in heparinized tubes and centrifuged. Plasma was used for clinical chemistry. The remaining plasma was stored at −20 °C. Organs (liver, kidney and bladder) were removed and weighed. The liver was partitioned in lobes and snap-frozen in liquid nitrogen and stored at −80 °C. Part of the left liver lobe was stored in formalin. The left kidney was partitioned transversely in a ratio of approximately 2 : 1, the larger part was stored in formalin. The remainder and the right kidney were snap-frozen in liquid nitrogen and stored at −80 °C. The bladder was stored in formalin.

The following parameters were determined in urine: GGT, total protein, creatinine and osmolarity. Urinalysis was carried out for erythrocytes, leukocytes, nitrite, protein, glucose, ketone bodies, bilirubin, urobilinogen, pH-value and specific gravity. The following parameters were determined in plasma: creatinine, urea, total bilirubin, GOT (ASAT), GPT (ALAT), GGT, alkaline phosphatase and total protein.

4.4.4 Furan

Urine samples were obtained from a study conducted in-house [98]. Male F344/N rats (Harlan-Winkelmann, Borchen, Germany) aged 7–9 weeks were randomly allocated to four groups of 15 animals each. They received furan at doses of 0.0 mg, 0.1 mg, 0.5 mg and 2.0 mg/kg bw by gavage in corn oil. Dosing solutions were prepared directly prior to administration to prevent loss of furan by evaporation. Animals were treated five days per week for four weeks, with an interim sacrifice of five animals after five days. A group of rats was also left for two weeks without treatment after the four week dosing period (recovery group). In the recovery group, only controls (0.0 mg/kg bw) and high dose animals (2.0 mg/kg bw) were included. Urine was collected on ice in metabolic cages 24 h before sacrifice. Animals were fasted during urine collection but had free access to tap water.

4.4.5 InnoMed PredTox

In the course of the InnoMed PredTox project, the toxicity of 16 compounds after single and repeated administration was investigated. The compounds included two reference compounds, troglitazone as a model hepatotoxin and gentamicin as a model

nephrotoxin, and 14 compounds that failed in the drug development pipeline of the participating companies in part due to signs of hepato- or nephrotoxicity. The compounds were administered to rats at two dose levels for 14 consecutive days. The animal experiments were carried out in the animal experimentation units of the participating companies, following a standardized protocol.

Male Wistar rats (SPF quality, acquired from Charles River Laboratories) aged 8–10 weeks were allocated to nine groups of five animals each, i.e. three dose groups (vehicle control, low dose, high dose) and three necropsy time points (one day, three days and twelve days after the first administration). Animals received the test substances orally by gavage. The dose levels were selected on the basis of previous studies so that the low dose was between the no-observed-adverse-effect-level (NOAEL) and the lowest-observed-adverse-effect-level (LOAEL) and the high dose was selected to produce clear signs of toxicity after 14 days of administration observable by clinical chemistry and/or histopathology. Urine was collected on ice for a 24 h interval in metabolic cages. For metabonomic studies, the urine of the study groups sacrificed on the twelfth day was collected throughout the studies, i.e. urine samples of the same animals were collected one, three and twelve days after start of treatment. Blood was collected at necropsy. Urine and serum clinical chemistry data, haematology, clinical observations as well as toxicogenomics of blood samples and proteomics of plasma and urine samples was performed by participating parties.

^{1}H NMR analysis of urine samples was performed by the participating parties according to a standard protocol (for experimental details see below). GC/MS analysis was performed in-house following the experimental procedures described below.

The compounds administered are coded FP001RO, FP002BI, FP003SE, FP004BA, FP005ME, FP006JJ, FP007SE, FP008AL, FP009SF (gentamicin), FP010SG (troglitazone), FP011OR, FP012SV, FP013NO, FP014SC, FP015NN, FP016LY. Structures and doses of the compounds administered are confidential.

Three studies FP004BA, FP005ME and FP007SE inducing bile duct necrosis were analyzed as single studies with ^{1}H NMR- and GC/MS-based metabonomics.

4.5 GC/MS analysis

4.5.1 Sample treatment for GC/MS analysis

Urine samples were thawed overnight at 4 °C. After thawing, the samples were vortexed shortly to remove any inhomogeneity in the solution due to the freezing-thawing process. Proteins were precipitated by addition of 100 µL cold methanol to 50 µL of urine. After centrifugation (2.31 g, 10 min), 50 µL of the supernatant were transferred to a GC autosampler vial with micro insert. The samples were evaporated to dryness at 30 °C in a Centrivac vacuum centrifuge (Heraeus Instruments, Osterode, Germany). After 2 h, 50 µl of acetone were added to each sample to ensure complete drying of the sample. Acetone addition was repeated once. After removal of acetone, the samples were derivatized with 50 µL methoxyamine hydrochloride in pyridine (20 mg/mL) at 40 °C for 90 min. Then, the samples were silylated at 40 °C for 1 h with 100 µL MSTFA and directly used for GC/MS analysis. All samples were randomized for each treatment step.

Additionally, 50 µL of each sample were pooled. After every fourth sample, this pooled urine was worked up in the same manner as the samples and used as quality control. The repeated work-up and analysis of a pooled sample for quality control was proposed by Sangster *et al*. [99] to overcome the problem of monitoring sample preparation and analytical performance in untargeted analysis, where internal standards cannot be implemented easily.

Treatment with urease is often used to remove urea from urine samples [26; 100], because urea is contained in such large quantities that the urea peak is overloading the column and saturates the detector. However, it has been demonstrated that urease treatment drastically alters urinary profiles apart from the removal of urea [101], therefore it has to be applied with care and was not used for the preparation of GC/MS samples throughout this thesis.

4.5.2 GC/MS analysis

Samples were analyzed on a HP6980 gas chromatograph with split/splitless inlet (split ratio 20:1) equipped with a J&W Scintific DB5-MS column (dimensions: 30 m × 0.25 mm × 0.1 µm film) coupled to a HP5973 mass selective detector. Data recording and instrument control was performed by HP ChemStation version D.02.00 (all from Agilent GmbH, Waldbronn, Germany). Samples were introduced by a CombiPal autosampler

(CTC Analytics GmbH, Zwingen, Switzerland). Inlet temperature and transfer line temperature were set to 280 °C. The oven temperature increased from 60 °C to 250 °C at a rate of 9 °C/min and held at 250 °C for 5 min. Helium carrier gas flow was kept constant at 0.8 mL/min. The detector was switched off during the elution of the urea signal from 11.50 min to 16.00 min. The detector operated in the scan mode from 60 m/z to 650 m/z with a sampling rate of 1 leading to 8.69 scans/sec and a threshold of 50 counts. Source temperature and quadrupol temperature was kept at 230 °C and 150 °C, respectively.

4.5.3 Raw data handling and statistical analysis

Chromatograms were inspected visually and those that deviated strongly from the rest due to chromatographic problems were excluded, since these do not carry any relevant information for statistical analysis and interfere with the automatic peak picking and alignment process. The remaining chromatograms were exported in the platform-independent netCDF (*.cdf) format with the ChemStation export function for further analysis.

Automatic peak detection and peak alignment was performed by the freely available software XCMS. R-program version 2.4.0 [102] and XCMS version 1.6.1 [44] were used. Default parameters of XCMS were used except for the following: fwhm = 4.0 sec, profmethod = ”binlinbase”. The results table containing mass spectral features as mass/retention time pairs in a tab-separated text file (*.txt) was imported into Excel work sheets (Microsoft, Unterschleißheim, Germany). Normalization to total ion current (TIC) and further data handling steps such as sorting the data according to retention time was carried out in Excel prior to statistical analysis with SIMCA-P version 11.5+ (Umetrics, Umeå, Sweden).

Variables were mean-centered and pareto-scaled for principle component analysis (PCA) and orthogonal projection to latent structures discriminant analysis (OPLS-DA). The significance of the components was determined by leave-one-out cross validation, the default validation tool in SIMCA P+ 11.5. Only significant components were used for the analysis. If a separation between control and dose groups was observed in the PCA scores plot, OPLS-DA was performed to highlight the differences between the groups.

Potential molecular markers responsible for group separation were identified by looking at the S-plot [41], which plots the covariance (p) against the correlation (pcorr). For a marker, both the contribution to the model expressed in p and the effect and

reliability of this contribution expressed in p(corr) should be high, therefore the potential markers are located on the outer ends of the S-shaped point swarm. To limit the number of potential markers and focus on the most important ones, cut-off values of $p \geq |0.05|$ and $p(corr) \geq |0.5|$ were used. Marker selection was done in a conservative manner so that only markers showing a significant jack-knifed confidence interval of less than half of the variable's covariance p were investigated further. With the mass/retention time pairs, the corresponding peak was identified in the original GC/MS chromatograms. Then, AMDIS deconvolution was run and the peak was compared to the NIST mass spectral database (National Institute of Standards and Technology, Gathersburg, MD) for identification. Confirmation of peak identity was carried out by co-eluting authentic reference compounds if available.

4.6 ^{1}H NMR analysis

4.6.1 Sample treatment for ^{1}H NMR analysis

Urine samples were thawed overnight at 4 °C and precipitated solids were removed by centrifugation (14.000 rpm, 10 min). 630 µL of urine were buffered with 70 µL of a 1 M phosphate buffer in D_2O containing 10 mM d_4-trimethylsilylpropionic acid sodium salt (TSP) as shift lock reagent prior to the transfer into a 5 mm NMR tube (Aldrich Series 30). Samples were randomized for each treatment step.

4.6.2 ^{1}H NMR analysis

^{1}H NMR spectra were recorded on a Bruker DMX 600 spectrometer equipped with a 5 mm DCH cryoprobe using pulsed magnetic field gradients (both by Bruker Biospin GmbH, Rheinstetten, Germany). Water suppression was achieved with the noesygppr1d pulse sequence from the Bruker library. For Fourier transformation, 32 scans with an aquisition time of 2.75 sec and a delay time of 2.00 sec were recorded. Spectral width was 11904 Hz or 19.8 ppm. Each spectrum was manually baseline-corrected and referenced to TSP ($\delta = 0.00$ ppm). Instrument control, data recording and baseline correction was carried out with the Bruker WIN NMR Suite.

4.6.3 Raw data handling and statistical analysis

^{1}H NMR spectra were inspected visually to exclude any outliers due to dilute samples or inadequate water suppression. The spectra were then imported into the Chenomx NMR Suite 4.6 (Chenomx, Edmonton, Canada) and binned into 0.04 ppm wide bins. The bins around the water resonance from 4.40 to 6.20 ppm were excluded from the analysis. Binned ^{1}H NMR data were normalized to total integral and imported into SIMCA-P+ version 11.5. Multivariate data analysis was carried out in the same manner as described for the GC/MS data. The compounds contained in the bins which were found to be altered due to treatment with toxicants were identified using the spectral library of the Chenomx NMR Suite.

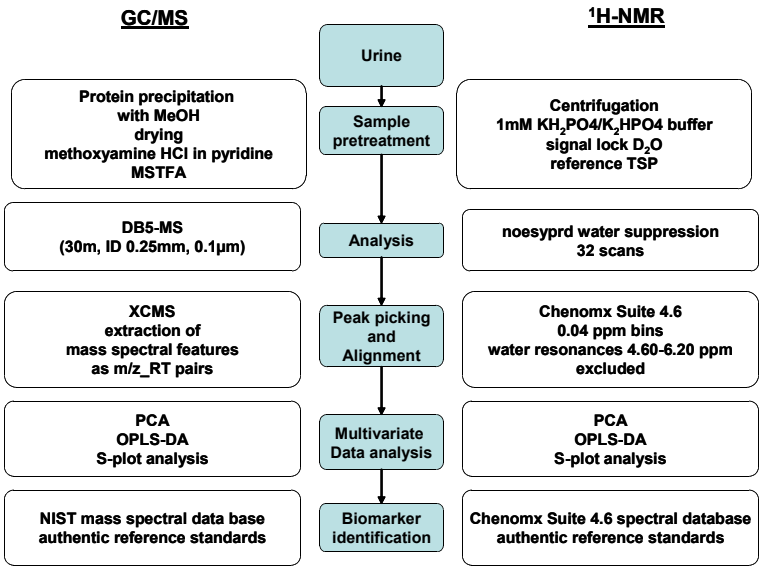

Figure 4.6.2.1*: Workflow for metabonomic analysis with GC/MS and ^{1}H NMR as it was applied in this thesis.*

4.7 LC/MS analysis

4.7.1 Sample treatment for LC/MS analysis

Urine samples were thawed, centrifuged at 14.000 g and 4 °C for 10 min and diluted to an equal osmolality of 154 mosmol/kg for adjustment of salt content (final volume 150 µL, dilution with water). An amount of 10 µL of the adjusted samples was taken to prepare a pooled quality control sample [99]. This sample was analyzed four times at the

beginning of the batch and then after every ten runs of study samples. Samples were randomized for all treatment and analytical steps.

4.7.2 LC/MS analysis

LC/MS analyses were carried out at the analytical laboratory of the Drug Safety Evaluation department, Sanofi Aventis, Frankfurt, Germany. Analyses were run on an UPLC system coupled to a Micromass LCT Premier (ESI-TOF) controlled by MassLynx software version 4.1. The analytical column was an ACQUITY BEH C18 (dimensions: 2.1 × 100 mm, 1.7 µm) and kept at 40 °C (Waters GmbH, Eschborn, Germany). An injection volume of 10 µL was used with a flow rate of 0.500 mL/min. The solvents were water with 0.1 % formic acid (solvent A) and acetonitrile with 0.1 % formic acid (solvent B) with the following gradient: 0 min 100% A, 4.00 min 80% A, 9.00 min 5 % A, 12.00 min 100 % A. The following MS parameters were used: negative ionization mode, survey scan mass range 50–1000 Da, nebulization gas (N_2) 700 L/h at 450 °C, cone gas 15–20 L/h, source temperature 120 °C, capillary voltage 60 V, LCT-W optics mode with 12000 resolution using dynamic range extension (DRE), data acquisition rate 0.1 sec with a 0.01 sec interscan delay; lock spray 2000 counts; lock spray method: leucine/enkephalin 50 fmol/µL, lock mass: m/z = 556.2771, flow rate: 30 µL/min, frequency: 5 sec; data collection was performed in centroid mode averaged over 10 scans.

4.7.3 LC/MS raw data handling and statistical analysis

Raw data files were exported in the platform-independent netCDF (*.cdf) format with the MassLynx export function for further analysis. Automatic peak detection and peak alignment was performed by XCMS. R program version 2.6.2 [102] and XCMS version 1.11.20 [44] were used. The following XCMS parameters were used: xcmsSet function method = centWave, chromfiles ppm = 50, peakwidth c(3, 15); group function bw = 2, minfrac = 0.5, minsamp = 1, mzwid = 0.05, max = 50. The results table containing mass spectral features as mass/retention time pairs in a tab-separated text file (*.txt) was exported to SIMCA P+ version 11.5. Multivariate data analysis was carried out in the same manner as described for the GC/MS data. Mass traces of known compound metabolites were excluded prior to any multivariate data processing steps. Identity proposals for regulated metabolites were made with the METLIN Metabolite Database [44] using the links supplied by XCMS in the results table.

4.7.4 Targeted bile acid screening

A bile acid standard mix was analyzed with the full scan LC/MS method in ESI negative mode described in section 4.7.3.

The peak lists extracted from the urinary LC/MS chromatograms with XCMS where then manually searched for the mass ratio and retention time of the characteristic ions of the bile acid standards. In this way, the data obtained by the full scan LC/MS screening method could be mined for altered bile acid excretion with urine. The mass spectral features corresponding to bile acids found by this approach are given in Table 4.7.4.1.

Table 4.7.4.1: *Bile acids and their masses (m/z) and retention times (RT) used in the targeted bile acid screening (ESI negative mode).*

bile acid	m/z	RT[min]
taurocholic acid (TCA)	514.3	5.89
tauro-β-muricholic acid (TbMCA)	514.3	5.72
u-TbMCA	512.3	5.77
taurodeoxychilic acid (TDCA)	498.3	7.20
glycocholic acid (GCA)	464.3	6.25
cholic acid (CA)	453.3	6.69

5 Method and workflow development

For a functional metabonomics platform, several steps in the analysis procedure have to be optimized and combined to a working unit. Metabonomics requires the following separate procedures: a comprehensive analysis method detecting as many metabolites as possible, a software solution that converts the chromatograms or spectra into a machine-readable format for statistical analysis, a software for the statistical analysis itself and the use of databases and biochemical pathways for the structural elucidation of altered metabolites and their evaluation within the context of toxic mechanisms.

Analytical tools and software solutions are well developed for ^{1}H NMR analysis and can be implemented rapidly. Using the noesypr1d pulse sequence from the Bruker spectral library for water suppression, ^{1}H NMR spectra were recorded in buffered urine. Alignment of the spectra and binning was performed with the Chenomx NMR Suite, which also allows identification and quantitation of metabolites from the original spectra with the spectral data base included in this software package. The statistical calculations for the identification of altered metabolites was carried out with the SIMCA P+11.5 software, using projection-of-variance-based methods such as principal component analysis (PCA) and orthogonal projection to latent structures discriminant analysis (OPLS-DA).

GC/MS analysis required the development of a analysis method and workflow suitable for global metabolite profiling that could be implemented on the HP6980 gas chromatograph and the HP5973 mass selective detector available at our laboratory. Silylation of nucleophilic groups preceded by methoximation of ketogroups was chosen as derivatization method as this approach allows the analysis of a wide range of compound classes such as alcohols, ketones, aldehydes, organic acids, amino acids, sugars etc. A large number of reference spectra of silylated compounds is included in the NIST mass spectral database, allowing the rapid identification of unknown metabolites.

The recording of a global metabolite profile in a urine sample requred adapting and combining a variety of existing GC/MS methods [20, 24; 26; 27]. *Bis*-trimethylsilyl-trifluoroacetamide (BSA) and *N*-methyl-*N*-trimethylsilyl-trifluoroacetamide (MSTFA) were tested derivatization agents, the latter was chosen as it had a higher reproducibility and introduced less variance. Sample pretreatment such as protein precipitation and drying, sample volume, derivatization times and temperatures had to be adapted for our method. Furthermore, GC and MS parameters such as temperature gradient, carrier gas flow and

injection volume as well as scan range and sampling rate had to be optimized to allow the recording of a global metabolite profile. These parameters had to be chosen in such a way that across the whole runtime, the chromatographic peaks were baseline-separated and of gaussian peak shape. These requirements were necessary for the proper functioning of the peak picking and alignment software.

In order to use multivariate statistics on GC/MS data, sophisticated peak picking and alignment of GC/MS chromatograms is necessary. Three publicly available software packages for peak picking and alignment, MetAlign [42], mzMine [43] and XCMS [44], were tested and XCMS was found to perform best regarding data quality, run time and user friendliness. A result that was later confirmed by Lange *et al.* [46]. As XCMS was originally developed for LC/MS analysis, a variety of software parameters regarding peak shapes and intensities had to be optimized for the routine handling of GC/MS data.

With the converted chromatograms from the XCMS package, the multivariate statistics could be performed with the SIMCA P+11.5 program. The scaling and normalization of the data had to be tested. With the peak identity of the altered metabolites supplied by the multivariate data analysis, the original chromatograms were compared to the NIST mass spectral data base and authentic reference standards.

For both ^{1}H NMR and GC/MS based metabonomic analysis, a large part of the work consisted in the evaluation of the altered metabolites within the biochemical pathways and toxic mechanisms, requiring extensive literature research.

6 Gentamicin

Metabonomic changes in a rat model of gentamicin nephrotoxicity

6.1 Introduction

Gentamicin (GM) is an aminoglycoside antibiotic used against life threatening gram negative bacterial infections, but its use is limited due to its nephrotoxic potential. GM selectively damages the S1 and S2 segments of the proximal tubuli and was thus selected as a model substance for nephrotoxicity. After binding to membrane components, GM is taken up to a certain extent into the epithelial cells by phagocytosis and stored in lysosomes [103]. After reaching a threshold, these lysosomes burst and release their contents, including reactive oxygen species, into the cells, and thereby inducing cell death.

The overall study design and choice of the model compound were deliberately based on the report by Lenz *et al.* [95], but a lower dose and quantitative assessment of the major urinary metabolites detected by ^{1}H NMR were included. The study was planned as a proof-of-concept study to test the GC/MS metabonomics approach for the early non-invasive detection of drug-induced nephrotoxicity.

Male Wistar rats received 0 mg (control), 60 mg (low dose) or 120 mg (high dose) GM/kg bw per day by subcutaneous (s.c.) injection twice daily for seven consecutive days. The injection of two doses per day was chosen to achieve a higher basal plasma level of GM, as the damage to the proximal tubuli induced by GM correlates with the basal plasma level and not with the peak plasma levels. As GM enters the cells by phagocytosis this route becomes saturated at high plasma levels. Therefore, permanently high basal plasma levels result in greater GM-induced kidney damage than high peak levels. For clinical antibiotic therapy therefore, dosing is once daily to reduce risk of kidney injury. Urine was collected in 24 h intervals throughout the study and plasma was collected one, three and seven days after the start of treatment.

***Table 6.2.1**: Clinical chemistry data of the gentamicin study. Values are given as mean ± SD; significance levels were determined with ANOVA and Dunnett's post hoc test (* p<0.05, ** p<0.01, *** p<0.001).*

Urine clinical chemistry

		volume [mL]	osmolarity [mosmol/kg]	creatinine [mg/24h]	glucose [mg/24h]	GGT [U/24h]	total protein [mg/24h]
	C[1]	11.8 ± 4.5	1348 ± 476	4.88 ± 0.17	2.31 ± 0.24	150.7 ± 42.8	8.27 ± 3.79
day 0	L[2]	8.2 ± 2.5	1140 ± 258	4.82 ± 0.69	1.84 ± 0.44	113 ± 17.1	7.51 ± 3.63
	H[3]	7.8 ± 1.6	1525 ± 361	4.96 ± 0.29	1.93 ± 0.27	126.5 ± 38.1	7.74 ± 1.97
	C	11.4 ± 2.4	1457 ± 385	5.63 ± 0.75	2.86 ± 0.36	93.7 ± 23.9	11.29 ± 4.86
day 1	L	8.2 ± 2.2*	1477 ± 147	5.64 ± 0.73	2.82 ± 0.34	151.3 ± 27.7	11.96 ± 3.81
	H	8.0 ± 1.2*	1728 ± 370	5.85 ± 0.49	6.21 ± 2.37**	153.4 ± 52.7	14.44 ± 3.12
	C	10.0 ± 1.6	1568 ± 411	5.35 ± 0.51	2.54 ± 0.26	127.4 ± 18.6	10.68 ± 4.10
day 2	L	6.6 ± 1.1	1615 ± 327	4.85 ± 0.89	3.51 ± 0.59	194 ± 38.5	9.93 ± 4.24
	H	7.5 ± 3.8	1563 ± 717	5.19 ± 0.31	5.11 ± 0.99***	244.2 ± 58.5*	12.61 ± 3.21
	C	10.6 ± 2.9	1551 ± 347	5.72 ± 0.83	2.43 ± 0.32	145.2 ± 34.4	10.36 ± 3.41
day 3	L	8.8 ± 1.7	1472 ± 165	5.03 ± 0.65	3.07 ± 0.52	163.3 ± 43.3	9.51 ± 0.67
	H	10.4 ± 3.4	1216 ± 500	5.54 ± 0.85	4.00 ± 1.05**	175.7 ± 52.3	13.62 ± 4.74
	C	9.4 ± 3.0	1883 ± 765	5.62 ± 0.87	2.48 ± 0.51	157.5 ± 46.9	9.41 ± 3.42
day 4	L	8.8 ± 3.1	1392 ± 318	4.51 ± 1.27	3.50 ± 1.27	203.4 ± 67.9	11.91 ± 3.18
	H	14.0 ± 5.8	1365 ± 840	7.10 ± 3.23	4.89 ± 2.27	256.4 ± 75.1	28.78 ± 17.07*
	C	8.8 ± 2.1	1933 ± 338	6.10 ± 0.46	2.57 ± 0.27	197.5 ± 40.9	110.60 ± 1.89
day 5	L	12.2 ± 4.8	1380 ± 594	5.62 ± 0.57	3.76 ± 1.41	234.3 ± 70.3	16.24 ± 5.81
	H	17.4 ± 9.3	436 ± 104***	4.03 ± 1.49*	24.4 ± 21.9	285.7 ± 143.8	40.59 ± 16.28**
	C	9.6 ± 3.3	1959 ± 614	6.10 ± 0.97	3.07 ± 0.97	153.6 ± 36.9	12.71 ± 5.25
day 6	L	14.4 ± 4.2	1171 ± 434*	6.21 ± 0.47	19.5 ± 30.8	201.6 ± 47.6	24.56 ± 7.53
	H	12.0 ± 6.2	377 ± 61***	2.71 ± 1.10***	26.3 ± 24.5	62.2 ± 52.8**	28.18 ± 16.19
	C	9.6 ± 4.7	1550 ± 352	6.46 ± 1.32	3.39 ± 1.21	161.2 ± 52.8	14.06 ± 5.34
day 7	L	15.8 ± 2.5	1023 ± 312*	6.32 ± 0.95	31.2 ± 49.3	211.9 ± 66.7	28.96 ± 6.20
	H	8.3 ± 7.8	384 ± 53***	1.62 ± 1.26***	14.8 ± 15.5	9.7 ± 11.0**	15.62 ± 12.61*

Plasma clinical chemistry

		creatinine [mg/dL]	urea [mg/dL]	GGT [U/L]	GOT(ASAT) [U/L]	GPT(ALAT) [U/L]	ALP [U/L]	total protein [g/dL]
	C	0.2 ± 0.0	37.5 ± 3.8	0.1 ± 0.0	133.5 ± 78.8	48.7 ± 9.2	249.8 ± 32.7	5.8 ± 0.1
day 1	L	0.2 ± 0.0	43.7 ± 1.5	0.1 ± 0.0	136.7 ± 28.1	43.3 ± 4.6	230.2 ± 30.7	5.8 ± 0.3
	H	0.2 ± 0.0	46.0 ± 9.3	0.2 ± 0.3	134.6 ± 38.0	47.4 ± 3.5	227.6 ± 24.1	5.8 ± 0.2
	C	0.2 ± 0.0	38.1 ± 6.8	0.1 ± 0.0	88.0 ± 13.7	45.9 ± 2.4	233.8 ± 24.6	5.7 ± 0.2
day 3	L	0.2 ± 0.0	42.4 ± 4.9	0.1 ± 0.0	161.1 ± 44.9*	53.3 ± 5.3	199.4 ± 19.5*	5.6 ± 0.3
	H	0.3 ± 0.1*	50.2 ± 5.5*	0.1 ± 0.0	139.3 ± 42.2	42.9 ± 7.2	194 ± 13.4*	5.7 ± 0.2
	C	0.2 ± 0.0	39.2 ± 4.1	0.4 ± 0.6	129.5 ± 60.9	83.8 ± 36.6	266.2 ± 27.6	6.5 ± 0.1
day 7	L	0.6 ± 0.6	89.6 ± 54.6	0.9 ± 1.0	174.3 ± 55.1	62.2 ± 11.6	218.4 ± 34.5	6.1 ± 0.2*
	H	5.0 ± 1.6***	496.3 ± 145.5***	49.1 ± 60.6	277.7 ± 76.6**	49.3 ± 9.5	160.0 ± 26.0***	5.3 ± 0.2***

Organ and animal weights

				rel. kidney weight		
		animal wt [g]	rel. liver wt [g/kg bw]	left [g/kg bw]	right [g/kg bw]	total [g/kg bw]
	C	253.0 ± 6.0	4.5 ± 0.2	0.41 ± 0.04	0.40 ± 0.03	0.81 ± 0.07
day 7	L	241.4 ± 24.6	4.0 ± 0.5	0.47 ± 0.03	0.46 ± 0.04*	0.93 ± 0.06
	H	203.8 ± 12.1***	3.6 ± 0.9	0.49 ± 0.07*	0.48 ± 0.05**	0.97 ± 0.11*

[1]C, control group, 0 mg/kg bw/day; [2]L, low dose group, 60 mg/kg bw/day; [3]H, high dose group, 120 mg/kg bw/day

6.2 Results

Clinical chemistry analyses showed a significant increase in urinary glucose excretion in the high dose group from the first day onwards. A two- to threefold increase could be observed in the first three days, then the individual urinary glucose levels vary strongly with up to 50-fold increase as compared to controls. The low dose group showed an increase in glucose excretion from day five onwards. (Tab. 6.2.1). Urinary osmolarity decreased significantly from day five onwards in the high dose and from day six onwards in the low dose group while urinary volume was not changed. A parallel decrease in urinary creatinine and an increase in protein excretion was observed in the high dose group. As the creatinine excretion was not constant due to the induced kidney damage, clinical chemistry parameters were not normalized to creatinine, but are given as 24 h excretion rates. Plasma parameters showed an increase in creatinine and urea starting on day three. An increase in plasma GGT, a parameter used for the diagnosis of kidney failure in clinical chemistry, could only be observed in the high dose group as late as day seven (Tab. 6.2.1). The high dose animals showed decreased body weight gain on day seven, and two high dose animals were removed from the study on day six due to overt signs of toxicity. After necropsy on day seven, relative kidney weight of the high dose group was increased and kidneys of both treated groups appeared pale and discolored. Histopathological inspection showed marked epithelial necrosis, predominantly involving proximal convoluted tubules of the cortex, with increasing severity related to dose.

Urine samples collected on day one, two, three and six after start of GM treatment were subjected to ^{1}H NMR and GC/MS analysis. Visual inspection of ^{1}H NMR spectra and GC/MS chromatograms revealed differences in urinary composition between controls and treated animals, most prominently an increase in glucose excretion in urine of treated animals. (Fig. 6.2.1). To further investigate these differences, principal component analysis (PCA) models were constructed using ^{1}H NMR and GC/MS data respectively. The ^{1}H NMR model shows a clear dose-dependent separation of controls and treated animals along the first principal component (PC) t[1] from day one onwards (Fig. 6.2.2a). From the first day after start of treatment onwards, low and high dose animals can be separated from control animals by unsupervised multivariate data analysis. The shift of the high dose day six animals and one low dose day six individual to the lower left corner of the plot along the second PC t[2] shows that at this time point the samples deviate strongly from all other

samples, which correlates with the onset of marked alterations in urine and plasma clinical chemistry on day six.

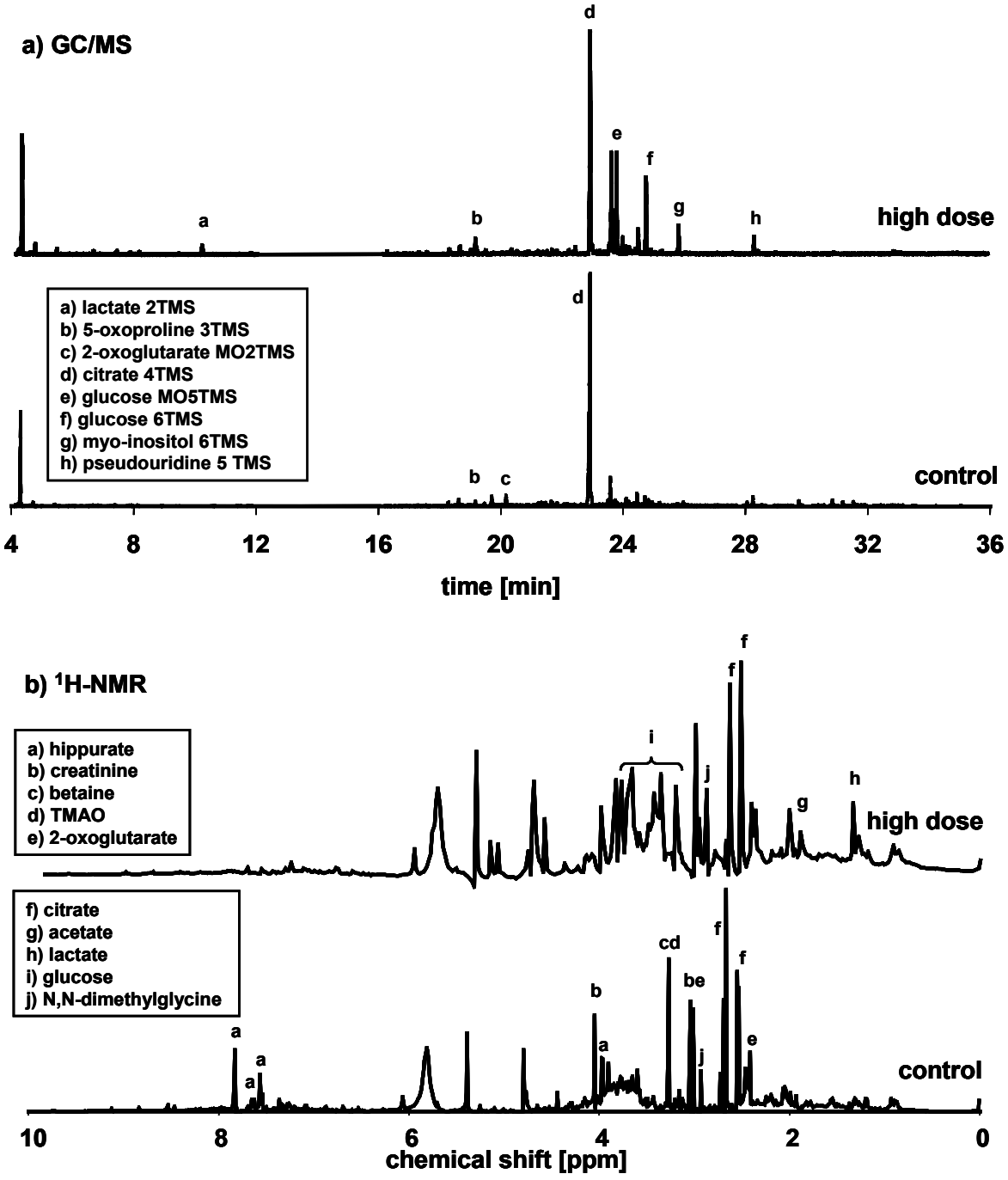

Figure 6.2.1*: GC/MS chromatograms (a) and [1]H NMR spectra (b) of representative day 6 control and high dose urine samples of the gentamicin study. Prominent signals are labeled, an increase in glucose excretion upon GM treatment can be observed. TMS, trimethylsilyl; MO, methoxyamine.*

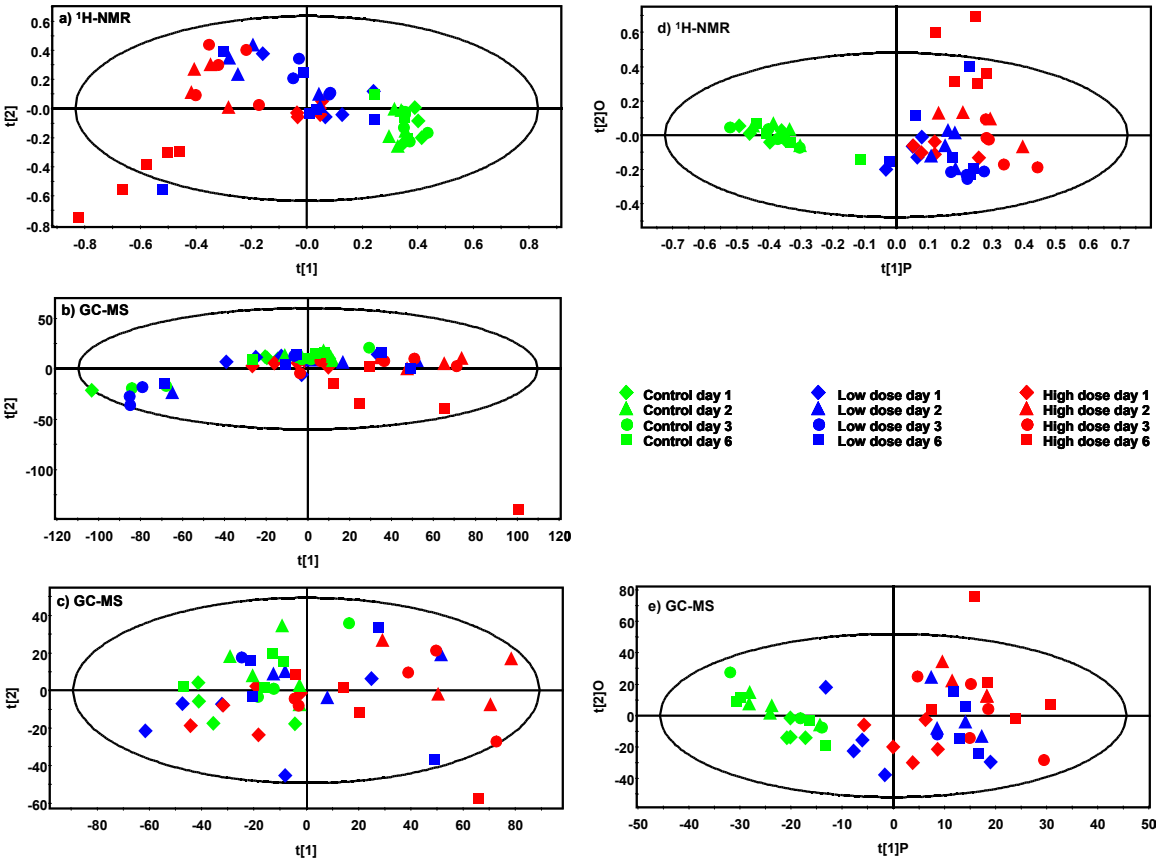

Figure 6.2.2: *Scores plots of multivariate models of urinary gentamicin ^{1}H NMR and GC/MS data. (a) PCA of ^{1}H NMR data, all time points. (b) PCA of GC/MS data, all time points. Note the outlier in the bottom right corner. (c) PCA of GC/MS data, with outlier excluded. (d) OPLS-DA of ^{1}H NMR data, all time points. (e) OPLS-DA of GC/MS data, all time points, with outlier excluded. Model characteristics are (a) $R^2X(cum) = 0.84$, $Q^2(cum) = 0.64$, 6 significant components; (b) $R^2X(cum) = 0.90$, $Q^2(cum) = 0.72$, 8 significant components; (c) $R^2X(cum) = 0.82$ $Q^2(cum) = 0.68$, 5 significant components; (d) $R^2X(cum) = 0.70$, $R^2Y(cum) = 0.88$ $Q^2(cum) = 0.83$, 1 + 2 significant components; (e) $R^2X(cum) = 0.60$, $R^2Y(cum) = 0.75$, $Q^2(cum) = 0.62$, 1 + 2 significant components.*

PCA of GC/MS data resulted in a model dominated by a strong outlier due to high glucose concentrations in a high dose animal on day six and a cluster of control and low dose animals moving away from the main body of samples (Fig 6.2.2b). Analysis of the original chromatograms revealed that a large signal of 2-oxoglutarate 3TMS was responsible for the deviation of these samples in the scores plot. To obtain a homogeneous data set for subsequent supervised multivariate data analysis and marker identification, these samples were excluded from the following analyses, since no analytical or biological cause could be found for this deviation. The high dose day six outlier was also excluded to

obtain a more homogeneous data structure. The resulting PCA is shown in Fig. 6.2.2c. GC/MS analysis is also able to discriminate treated animals from controls, however, a large variance probably introduced by the necessary sample work-up and derivatization procedure is dominating the plot. To analyze the metabolic changes in more detail, a supervised multivariate data analysis was used. Orthogonal projection to latent structures discriminant analysis (OPLS-DA) models were constructed with both ^{1}H NMR and GC/MS data respectively (Fig. 5.2.2d and e). In OPLS-DA models, a classifier, in this case control, Y = 0, and dose, Y = 1 is given to each sample, and the data is modeled in such a way that the discriminating information contributing to group separation is forced onto the first PC t[1]P, while the orthogonal information not contributing to the separation is modeled in the following components.

Table 6.2.2: *^{1}H NMR spectral bins and the corresponding putative metabolite IDs found to be altered significantly upon gentamicin treatment in urine. Changes in excretion levels are marked with arrows, (↑) up and (↓) down. Metabolites that could only be assigned speculatively are marked with (?).*

δ [ppm]	Change	Identification	δ [ppm]	Change	Identification
8.80 - 8.84	↓	trigonelline	3.48 - 3.52	↑	glucose (?)
7.76 - 7.84	↓	hippurate	3.40 - 3.44	↑	glucose (?)
7.64 - 7.68	↓	3-indoxylsulfate	3.32 - 3.36	↑	glucose (?)
7.60 - 7.64	↓	hippurate	3.16 - 3.20	↓	?
7.52 - 7.56	↓	hippurate	3.08 - 3.12	↓	creatinine
7.48 - 7.52	↓	3-indoxylsulfate	2.88 - 2.92	↑	N,N-dimethylglycine
7.44 - 7.48	↓	?	2.68 - 2.76	↑	dimethylamine
7.24 - 7.32	↓	?	2.60 - 2.68	↓	citrate
7.04 - 7.12	↓	?	2.48 - 2.52	↓	?
6.72 - 6.76	↓	?	2.16 - 2.20	↓	?
4.16 - 4.24	↑	?	2.00 - 2.04	↑	N-acetyl groups
4.04 - 4.08	↑	lactate (?)	1.92 - 1.96	↑	acetate
3.96 - 4.04	↓	creatinine	1.84 - 1.88	↑	?
3.92 -3.96	↓	hippurate	1.52 - 1.56	↓	?
3.76 - 3.80	↑	?	1.28 - 1.40	↑	lactate
3.56 - 3.64	↓	?	1.12 - 1.16	↓	?

Both ^{1}H NMR model (Fig. 6.1.2d) and GC/MS model (Fig. 6.2.2e) show a clear separation of controls from dosed animals from the first day onwards along the discriminating component t[1]P. Compared to the control groups, the dosed groups show a much larger orthogonal variance on the second orthogonal component t[2]O. Especially the high dose animals at the late time points shift to the upper part of the plot, which mainly stems from an increased urinary glucose excretion.

The S-plot was applied for marker identification in OPLS-DA models as proposed by Wiklund *et al*. [104]. Following GM treatment, citrate, hippurate, trigonelline and 3-indoxylsulfate were found to be decreased in a dose-dependent manner using ^{1}H NMR. Lactate, acetate, *N*,*N*-dimethylglycine and glucose increased in a dose-dependent manner. Several other spectral regions were also altered compared to controls, but no metabolite assignment could be made for those (Tab. 6.2.2). In agreement with ^{1}H NMR analysis, the GC/MS model showed decreased citrate and increased lactate. Additionally, decreased 2-oxoglutarate and increased 5-oxoproline was observed as well as alterations in aromatic gut microflora metabolites such as phenyllactate and hydroxyphenylpropionate (Tab. 6.2.3).

Table 6.2.3: *Mass spectral features and the corresponding putative metabolite IDs found to be altered significantly upon gentamicin treatment in urine. Mass fragments and retention time in the GC/MS chromatogram are given. Changes in excretion levels are marked with arrows, (↑) up and (↓) down. Metabolites that could only be assigned speculatively are marked with (?).*

main fragments [m/z]	RT [s]	Change	Metabolite ID
117	399	↑	Lactate 2TMS
156	1123	↑	5-Oxoproline 2TMS
113, 147, 318, 347	1211	↓	2-Oxoglutarate 3TMS
193	1234	↑	Phenyllactic acid 2TMS (?)
177, 192, 205, 310	1302	↓	3-Hydroxyphenylpropionate 2TMS (?)
174	1304	↑	Putrescine 4TMS (?)
179	1326	↑	(?)
273, 347, 363, 465	1374	↓	Citrate 4TMS
192, 209	1422	↑	(?)
179	1455	↑	4-Hydroxyphenylpropionate 2TMS (?)
169, 257, 375	1785	↓	(?)
191	1892	↓	(?)

Quantitative analysis of ^{1}H NMR spectra with the Chenomx NMR Suite spectral data base (Tab. 6.2.4) generally confirmed results found by multivariate data analysis (Tab. 6.2.2). The data shown here is the metabolite excretion over 24 h. A decrease in Krebs cycle intermediates could be observed, especially malonate excretion was decreased significantly in both dose groups from the second day onwards, while citrate was only decreased significantly on day six in the high dose group. A decrease in renal osmolytes, prominently trimethylamine-*N*-oxide (TMAO), could be observed from the second day onwards. The most sensitive alterations were the increase in lactate and alanine excretion, which occurred in the high dose group already on day 1 and in both dose groups after 2-3 days. Although still quite variable, these levels returned to control levels on day 6.

Aromatic gut flora metabolites were also found to be altered significantly, especially hippurate was decreased highly significantly from the first day onwards (Tab. 6.2.4).

6.3 Discussion

Unsupervised PCA of ^{1}H NMR data is able to discriminate treated from control animals from the first day post treatment, and GC/MS is able to completely separate high dose samples from the first day and low dose samples from the second day onwards from untreated controls with supervised OPLS-DA. This demonstrates that multivariate pattern recognition methods are able to detect GM-induced changes in renal function earlier than classical clinical chemistry approaches.

The PCA and OPLS-DA scores plots show that the toxic insult produced by the GM administered in this study is very variable, leading to a large scattering of the treated samples in the scores plot for both ^{1}H NMR and GC/MS. This is especially evident for the GC/MS analysis, where there are several outliers and even with those outliers excluded from the model the treated animal scatter widely across the plot. However, a deviation of the 120 mg/kg bw/day day 6 samples is obvious in both GC/MS and LC/MS analysis and can be attributed mainly to a marked glucosuria.

Markers found by analysis of the S-plot of the OPLS-models of both ^{1}H NMR and GC/MS confirmed increased glucose excretion upon GM dosing. Metabolites found to be altered upon GM treatment with ^{1}H NMR in this study confirm the results of Lenz *et al.* [95], who reported increased lactate, glucose and decreased hippurate, TMAO and betaine excretion. Lenz *et al*. reported an increase in citrate excretion [95], while in this study multivariate data analysis of both ^{1}H NMR and GC/MS samples indicated decreased citrate excretion upon GM dosing. Quantitative analysis of the ^{1}H NMR spectra confirmed citrate to be significantly decreased in the 60 mg/kg bw/day and 120 mg/kg bw/day group on day 6. How these differences in urinary citrate levels between the two studies may be explained is unclear.

GC/MS analysis found several aromatic compounds such as phenyllactic acid and hydroxyphenylpropionate altered upon GM dosing. Together with the decrease in hippurate excretion observed with ^{1}H NMR, this shows the alteration of the gut microflora induced by the pharmacologic antibiotic effect of GM as already observed [95].

Increased urinary 5-oxoproline excretion as observed with GC/MS metabonomics and decreased excretion of the antioxidant trigonelline as observed with ^{1}H NMR are evidence for an involvement of oxidative stress in gentamicin toxicity [105]. 5-oxoproline is accumulated in the γ-glutamyl cycle upon glutathione (GSH) depletion. 5-oxoprolinuria has been observed after treatment of compounds leading to oxidative stress, such as bromobenzene [52].

Decreased excretion of guanidoacetic acid, which has been observed as a sensitive indicator of gentamicin toxicity with LC/MS [106] could not be observed in ^{1}H NMR. Due to the inherent insensitivity of the ^{1}H NMR method, guanidoacetate is almost lost in the baseline of the ^{1}H NMR spectrum and thus could not be quantified.

In a recent study, where quantitative ^{1}H NMR metabolite data were used, Xu *et al.* [107] found an increase in the urinary excretion of acetoacetate, glucose, lactate, 3-hydroxybutyrate, creatine and various amino acids together with a decrease in hippurate, *N*-acetyl-tryptophan, taurine and trigonelline upon daily administration of 0, 20, 80 and 240 mg/kg bw for 3, 9 or 15 days. In this study, transcriptomics revealed the participation of transporters in gentamicin toxicity [107].

Significant alterations in the composition of urinary profiles were detected before marked changes in clinical chemistry parameters were evident, supporting the use of metabolite profiles as non-invasive sensitive endpoints of kidney injury. However, the dominating metabolites responsible for group separation for this study were increased urinary glucose, a well known marker of kidney damage; and changes in metabolites such as hippurate, which are widely attributed to alterations in the gut microflora [68; 69], a pharmacological effect to be expected from an antibiotic. These results demonstrate that any group separation observed by pattern recognition methods has to be investigated closely. Mechanistic understanding is necessary to separate toxic effects from pharmacological or adaptive changes.

Table 6.2.4: *24h excretion rate of urinary metabolites after gentamicin administration quantified with Chenomx NMR Suite; values are given as mean ± SD in [µmol/24h]; significance levels were determined with ANOVA and Dunnett's post hoc test, * p<0.05, ** p<0.01, ***p<0.001. Arrows indicate whether metabolite excretion is primarily increased (↑) or decreased (↓) compared to controls.*

		Krebs cycle intermediates					Renal Osmolytes					
	Dose [mg/kg bw]	Citrate	2OG[1]	Malonate ↓	Succinate ↓	cis-Aconitate ↓	TMAO[2] ↓	Betaine ↓	Methylamine	DMG[3]	DMA[4]	Formate ↓
	0	719 ± 145	305 ± 72	23.9 ± 4.9	35.0 ± 6.2	25.9 ± 4.2	18.3 ± 5.2	18.8 ± 21.6	0.0 ± 0.0	11.8 ± 6.3	15.7 ± 1.6	12.2 ± 2.2
day 1	**60**	589 ± 226	279 ± 165	19.2 ± 4.1	23.3 ± 8.2	23.2 ± 6.9	13.7 ± 8.4	20.2 ± 17.6	0.6 ± 1.4	23.7 ± 9.5*	14.9 ± 6.0	9.8 ± 2.4
	120	548 ± 112	296 ± 64	19.1 ± 4.6	28.4 ± 7.8	24.7 ± 4.3	16.8 ± 6.9	13.6 ± 2.9	2.9 ± 3.4	30.8 ± 3.2**	18.0 ± 2.6	9.8 ± 2.7
	0	585 ± 104	243 ± 58	23.1 ± 5.8	49.2 ± 12.1	24.4 ± 2.2	17.1 ± 2.4	13.3 ± 13.9	3.5 ± 2.0	10.5 ± 4.9	17.2 ± 1.4	11.6 ± 2.0
day 2	**60**	501 ± 152	216 ± 118	11.2 ± 4.0**	27.2 ± 13.2*	18.9 ± 4.5*	5.2 ± 2.9***	11.6 ± 6.7	1.4 ± 1.4	14.6 ± 6.1	11.3 ± 4.3*	8.1 ± 2.7
	120	385 ± 26*	198 ± 36	131 ± 3.3*	30.2 ± 10.9	18.7 ± 2.8	5.1 ± 1.9***	8.9 ± 1.5	0.7 ± 0.6*	11.7 ± 6.8	11.7 ± 2.2*	7.1 ± 2.1*
	0	583 ± 70	245 ± 35	19.0 ± 3.9	33.2 ± 5.5	25.3 ± 3.2	19.2 ± 4.2	15.2 ± 17.4	0.8 ± 1.8	10.1 ± 6.7	16.8 ± 2.6	10.9 ± 2.2
day 3	**60**	559 ± 110	299 ± 59	8.0 ± 2.8***	25.8 ± 3.7	20.5 ± 2.6	5.5 ± 2.5***	19.4 ± 15.7	0.5 ± 0.6	20.0 ± 10.6	11.7 ± 2.6*	8.3 ± 1.6
	120	501 ± 121	284 ± 97	10.5 ± 2.7*	23.0 ± 4.9*	16.0 ± 4.3**	2.9 ± 2.4***	9.2 ± 5.6	1.3 ± 0.8	17.1 ± 11.4	12.7 ± 2.7	6.6 ± 2.4*
	0	537 ± 71	226 ± 55	19.0 ± 6.5	40.6 ± 10.2	25.8 ± 4.3	19.4 ± 4.1	14.1 ± 14.1	2.2 ± 1.0	10.0 ± 6.3	16.5 ± 3.3	11.1 ± 2.9
day 4	**60**	678 ± 334	353 ± 185	9.9 ± 9.8	34.4 ± 16.5	24.6 ± 10.6	12.5 ± 7.1	17.4 ± 13.4	1.3 ± 0.4	19.3 ± 14.1	11.7 ± 5.4	10.7 ± 5.3
	120	627 ± 90	281 ± 54	4.4 ± 4.7*	26.6 ± 5.8	9.5 ± 9.1*	5.5 ± 3.2**	8.0 ± 3.5	1.1 ± 0.7	16.9 ± 2.3	17.1 ± 2.4	8.3 ± 2.7
	0	613 ± 63	231 ± 21	19.1 ± 4.5	36.0 ± 4.7	27.8 ± 3.1	19.7 ± 2.0	7.7 ± 2.9	1.4 ± 1.3	7.3 ± 3.7	17.7 ± 1.3	11.3 ± 1.6
day 5	**60**	765 ± 169	345 ± 120	6.1 ± 6.5**	34.4 ± 8.0	19.0 ± 11.5	17.9 ± 11.3	24.1 ± 19.9	1.1 ± 0.8	26.6 ± 13.9*	18.3 ± 6.1	12.4 ± 4.9
	120	452 ± 259	171 ± 87	0.0 ± 0.0***	20.9 ± 10.2	0.0 ± 0.0***	7.0 ± 4.3*	8.6 ± 5.8	0.0 ± 0.0	13.7 ± 3.7	13.6 ± 4.3	6.3 ± 3.1
	0	650 ± 163	274 ± 55	17.9 ± 12.8	39.9 ± 6.9	31.3 ± 7.9	21.5 ± 5.9	16.8 ± 16.4	3.1 ± 2.4	9.9 ± 6.9	17.6 ± 2.6	12.0 ± 3.1
day 6	**60**	881 ± 163	361 ± 110	7.3 ± 13.7	36.1 ± 5.4	21.3 ± 7.5	15.4 ± 9.3	19.8 ± 18.3	0.3 ± 0.7*	18.4 ± 13.6	14.7 ± 3.9	12.0 ± 3.2
	120	274 ± 185**	71 ± 51**	0.0 ± 0.0*	11.2 ± 8.3***	4.5 ± 4.8***	4.2 ± 6.1**	6.7 ± 11.9	0.3 ± 0.5*	20.3 ± 11.9	9.5 ± 4.2**	3.8 ± 2.6**
	0	618 ± 82	266 ± 45	20.3 ± 9.0	36.4 ± 7.6	28.0 ± 4.3	19.2 ± 7.6	13.9 ± 12.7	1.4 ± 2.1	9.0 ± 5.7	17.3 ± 3.2	11.29 ± 2.78
day 7	**60**	851 ± 227	373 ± 228	8.2 ± 5.1*	30.5 ± 8.7	23.2 ± 9.2	22.7 ± 4.4	23.6 ± 16.0	0.3 ± 0.6	24.9 ± 10.3*	15.2 ± 3.0	10.73 ± 3.36
	120	146 ± 65*	30 ± 15	0.0 ± 0.0*	4.7 ± 0.9**	6.7 ± 4.1**	2.2 ± 0.1*	7.5 ± 6.5	0.0 ± 0.0	12.3 ± 3.2	7.5 ± 0.2**	3.70 ± 0.42*

[1]2OG, 2-oxoglutarate; [2]TMAO, trimethylamine-N-oxide; [3]DMG, N,N-dimethylglycine; [4]DMA, dimethylamine;

Table 6.1.4 (continued): *24h excretion rate of urinary metabolites after gentamicin administration quantified with Chenomx NMR Suite; values are given as mean ± SD in [µmol/24h]; significance levels were determined with ANOVA and Dunnett's post hoc test, * p<0.05, ** p<0.01, ***p<0.001. Arrows indicate whether metabolite excretion is primarily increased (↑) or decreased (↓) compared to controls.*

		Gut microflora metabolites											
	Dose [mg/kg bw]	Hippurate ↓	4HPA[1]	PAG[2]	Lactate ↑	MNA[3]	Acetate	TRIG[4] ↓	3IS[5] ↓	Alanine ↑	Creatine ↑	Creatinine	Glucose ↑
	0	142 ± 24	6.6 ± 2.9	10.6 ± 1.3	6.2 ± 1.9	2.8 ± 1.2	7.9 ± 1.1	13.7 ± 2.0	13.9 ± 3.0	3.0 ± 0.7	0.0 ± 0.0	92 ± 10	44.0 ± 6.5
day 1	**60**	65 ± 37**	9.5 ± 3.1	18.0 ± 6.7	7.2 ± 1.5	2.8 ± 1.1	5.5 ± 0.9*	11.7 ± 3.4	15.1 ± 3.6	3.3 ± 0.8	0.0 ± 0.0	95 ± 13	39.0 ± 6.5
	120	65 ± 21**	9.3 ± 1.3	14.1 ± 7.6	18.8 ± 5.9***	2.7 ± 0.9	6.7 ± 1.8	11.9 ± 2.7	11.6 ± 7.7	7.9 ± 2.7**	0.0 ± 0.0	103 ± 10	77.8 ± 25.9*
	0	101 ± 27	10 ± 1.0	9.3 ± 1.9	5.5 ± 1.5	2.5 ± 1.1	13.7 ± 8.7	12.5 ± 1.8	14.6 ± 2.3	2.7 ± 0.5	0.0 ± 0.0	98 ± 14	49.2 ± 10.2
day 2	**60**	9.4 ± 3.0 ***	12.9 ± 2.9	11.3 ± 0.9	9.9 ± 1.7**	2.4 ± 0.8	6.4 ± 1.3	9.7 ± 4.8	10.2 ± 0.7	4.8 ± 1.2**	2.5 ± 2.3*	93 ± 23	49.2 ± 11.9
	120	7.8 ± 1.4***	13.8 ± 1.0*	12.90± 2.9*	12.1 ± 1.9***	2.5 ± 1.1	6.1 ± 1.2	7.6 ± 1.8	4.3 ± 5.1***	7.2 ± 1.0***	4.9 ± 0.5***	100 ± 10	70.3 ± 16.5
	0	105 ± 17	6.8 ± 4.5	7.9 ± 4.7	4.7 ± 0.9	2.0 ± 0.5	8.4 ± 3.6	13.3 ± 2.0	16.3 ± 2.2	2.4 ± 0.7	0.0 ± 0.0	96 ± 13	36.1 ± 6.8
day 3	**60**	7.6 ± 2.2 ***	11.2 ± 10.0	12.2 ± 3.5	9.4 ± 0.7*	2.6 ± 1.9	4.7 ± 0.9	9.9 ± 2.0	14.7 ± 2.7	3.9 ± 0.2*	0.4 ± 0.7	85 ± 11	38.4 ± 5.4
	120	6.6 ± 1.8***	7.9 ± 4.6	13.6 ± 4.0	10.1 ± 3.4**	1.9 ± 0.8	5.4 ± 2.3	7.7 ± 3.1**	8.7 ± 5.5*	4.8 ± 1.2**	5.9 ± 4.7*	102 ± 25	49.8 ± 16.9
	0	118 ± 37	9.2 ± 2.7	9.6 ± 1.6	4.8 ± 1.2	1.8 ± 0.6	9.5 ± 2.6	12.2 ± 1.8	15.2 ± 3.4	2.6 ± 0.6	0.0 ± 0.0	98 ± 18	40.8 ± 9.5
day 4	**60**	9.3 ± 3.5***	20.6 ± 8.0*	11.2 ± 5.2	9.6 ± 4.4	2.7 ± 2.2	8.4 ± 3.9	11.0 ± 4.8	12.9 ± 9.5	4.3 ± 2.2	1.1 ± 1.6	107 ± 44	57.2 ± 36.5
	120	7.2 ± 0.8***	10.3 ± 7.0	13.4 ± 3.6	10.9 ± 3.0*	1.9 ± 0.5	8.3 ± 0.4	8.3 ± 2.2	8.2 ± 6.4	4.8 ± 3.1	20.3 ± 24.1	115 ± 21	72.7 ± 29.7
	0	108 ± 24.1	10.2 ± 3.0	11.1 ± 0.2	4.9 ± 0.6	1.9 ± 0.4	9.4 ± 2.0	12.6 ± 1.5	17.1 ± 3.5	3.0 ± 0.6	0.0 ± 0.0	107 ± 7	47.4 ± 7.6
day 5	**60**	10.1 ± 3.4***	22.6 ± 4.8**	18.3 ± 3.4*	13.4 ± 6.6	2.7 ± 1.4	9.0 ± 2.4	13.5 ± 5.2	15.8 ± 10.0	5.6 ± 3.8	4.0 ± 5.8	122 ± 33	71.2 ± 52.7
	120	6.3 ± 1.8***	9.8 ± 4.9	14.0 ± 4.4	19.9 ± 19.2	1.1 ± 0.7	15.1 ± 5.8	4.7 ± 2.6*	3.1 ± 4.2*	5.8 ± 2.9	50.1 ± 62.8	89 ± 27	365 ± 365
	0	117 ± 68	10.0 ± 2.1	11.7 ± 2.2	4.9 ± 1.1	2.0 ± 0.6	11.2 ± 3.8	14.7 ± 4.0	19.3 ± 5.5	2.7 ± 0.6	0.0 ± 0.0	115± 20	45.5 ± 10.7
day 6	**60**	10.9 ± 3.5**	16.8 ± 7.5	15.0 ± 3.7	12.8 ± 2.4	2.4 ± 1.8	11.7 ± 4.0	13.1 ± 8.8	12.7 ± 9.3	4.0 ± 2.8	4.6 ± 6.3	122 ± 23	243 ± 369
	120	5.1 ± 2.2**	4.7 ± 3.4	13.0 ± 4.3	21.5 ± 25.0	0.1 ± 0.2*	15.7 ± 10.2	3.1 ± 2.1*	0.3 ± 0.8***	4.1 ± 2.9	57.8 ± 42.2**	73 ± 38	382 ± 311
	0	101 ± 63	5.5 ± 4.9	10.0 ± 1.9	5.6 ± 1.2	1.7 ± 0.3	8.8 ± 2.0	13.4 ± 2.7	15.7 ± 3.6	3.5 ± 0.8	0.0 ± 0.0	106 ± 17	51.2 ± 19.1
day 7	**60**	8.9 ± 1.7*	14.0 ± 7.1	15.6 ± 4.3*	12.1 ± 2.9*	1.9 ± 1.5	9.8 ± 3.6	13.0 ± 4.2	15.9 ± 8.1	4.3 ± 0.5	6.1 ± 13.6	110 ± 13	323 ± 495
	120	4.0 ± 0.7*	2.6 ± 1.0	6.9 ± 1.1	21.8 ± 6.0***	0.0 ± 0.0	30.9 ± 29.3	2.8 ± 0.5**	0.0 ± 0.0*	5.3 ± 3.1	30.7 ± 22.1*	56 ± 9**	350± 75

[1]4HPA, 4-hydroxyphenylacetate; [2]PAG, phenylacetylglycine; [3]MNA, 1-methylnicotinamide; [4]TRIG, trigonelline; [5]3IS, 3-indoxylsulfate;

7 Ochratoxin A

7.1 Introduction

Ochratoxin A (OTA) is a mycotoxin produced by various species of the *Aspergillus* and *Penicillium* genus. It is found in a variety of food stuffs and beverages such as cereals, spices, nuts, dried fruits, coffee, beer and wine [82] and as a consequence, the human population is continuously exposed to OTA. Since OTA is a nephrotoxin and a potent renal carcinogen in rodents [85; 86], it is of concern to the public health, even more so as its mode of action is not fully understood [87].

In routine toxicity testing, histopathology is still the "gold standard" for detection of chemically induced pathologic lesions. Histopathology data is acquired together with urine and plasma samples for clinical chemistry analysis. For metabonomic analysis however, only the body fluid samples are used, and the changes in urinary or plasma composition are correlated to the dose of the compound examined in the study. The first aim of this study was to test the metabonomics approach for the assessment of toxicity in comparison to the "gold standard" histopathology. The second aim was to demonstrate the use of metabonomics as a tool for biomarker discovery and for the elucidation of toxic mechanisms. Since histopathology is the phenotypic anchoring of toxic lesions, information which is generally not included in the metabonomic analysis, an approach was developed which allows the inclusion of histopathology data in metabonomics studies.

To demonstrate how metabonomics may be used for toxicity assessment and biomarker identification, GC/MS-, ^{1}H NMR- and LC/MS-based techniques were applied to investigate metabolic changes in urine caused by OTA. Full histopathology and clinical chemistry of a 13 week subchronic study on OTA have been reported [96]. Rats (n = 5 per group) were treated with 0, 21, 70 or 210 µg/kg bw by gavage 5 days per week for 90 days. Urine samples were collected over night after 14, 28 and 90 days of treatment. The suitability of different metabonomic techniques and their power to detect changes in the molecular composition of urine indicative of toxicities and its mechanisms were assessed. Chemometric analyses of urine samples separated treated animals from controls in a dose-dependent manner and a series of molecular markers of OTA toxicity was identified.

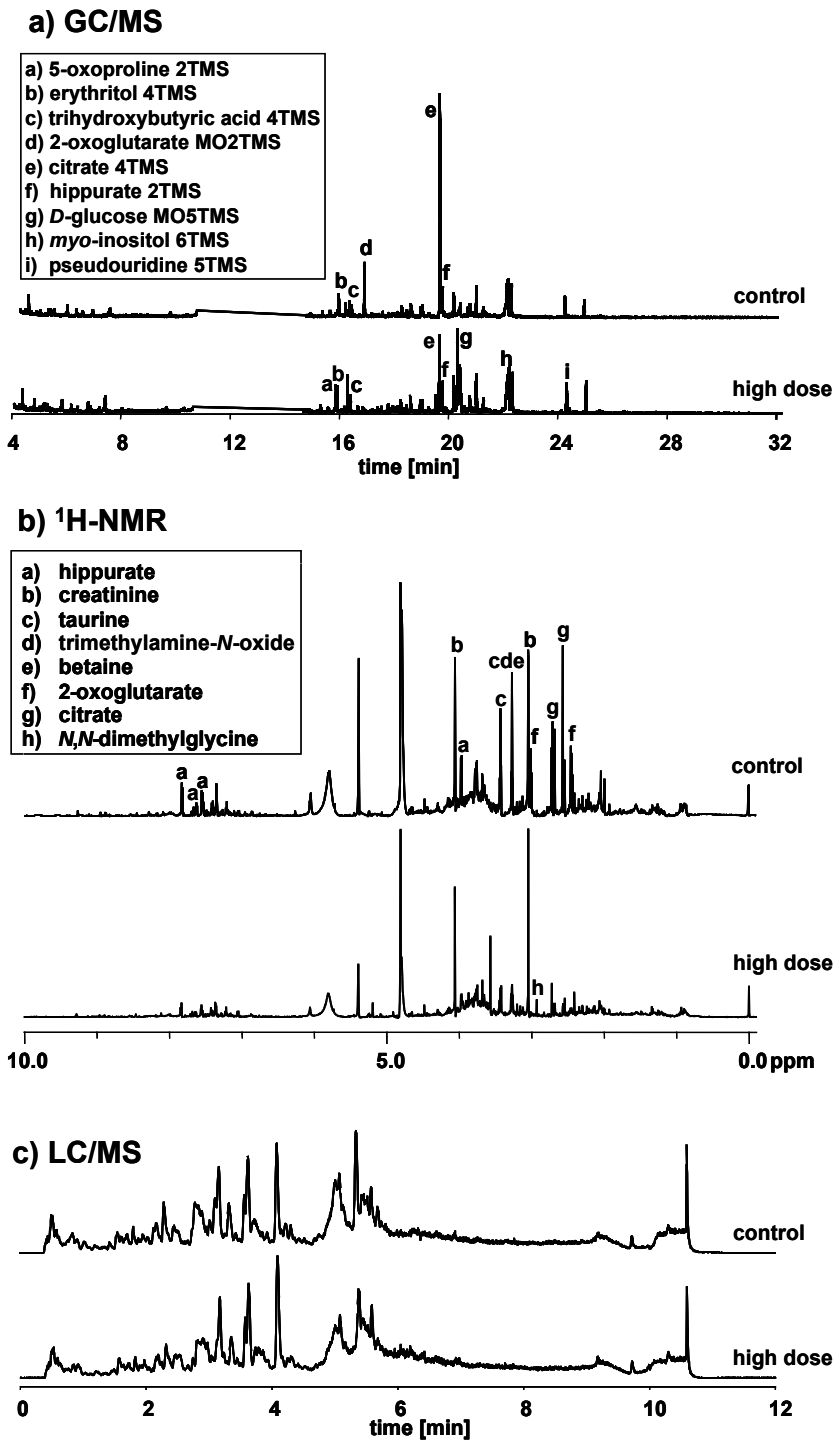

***Figure 7.2.1**: GC/MS chromatograms (a), ^{1}H NMR spectra (b) and LC/MS chromatograms (c) of a representative control group and high dose group animals respectively after 13 weeks of OTA administration showing subtle changes in urinary composition. The GC/MS analytes are given as the derivatized compounds, MO = methoxime, TMS = trimethylsilyl.*

7.2 Results

Visual inspection of GC/MS chromatograms and ^{1}H NMR spectra showed differences between control group and high dose group animals respectively (Fig. 7.2.1a and b). The LC/MS total ion current (TIC) chromatograms of control group and high dose group animals could not be distinguished. (Fig. 7.2.1c). PCA models constructed with GC/MS and ^{1}H NMR data respectively separated control animals from high dose animals (210 µg/kg bw) after 4 weeks of OTA treatment along the first and second principal component (PC) t[1] and t[2] (Fig. 7.2.2a and b). GC/MS also showed a trend to separate animals of the mid dose group (70 µg/kg bw) from controls from the fourth week onwards, however, the plot was dominated by a large variance, presumably introduced by the necessary sample work-up (Fig. 7.2.2a). With ^{1}H NMR, individual animals from the high dose group separated from controls as soon as two weeks after the start of treatment (Fig. 7.2.2b). The LC/MS model discriminated only sampling time points along the first two PCs t[1] and t[2] (Fig. 7.2.1c and 7.2.2c), dose-dependent information was only evident on the fourth PC (data not shown).

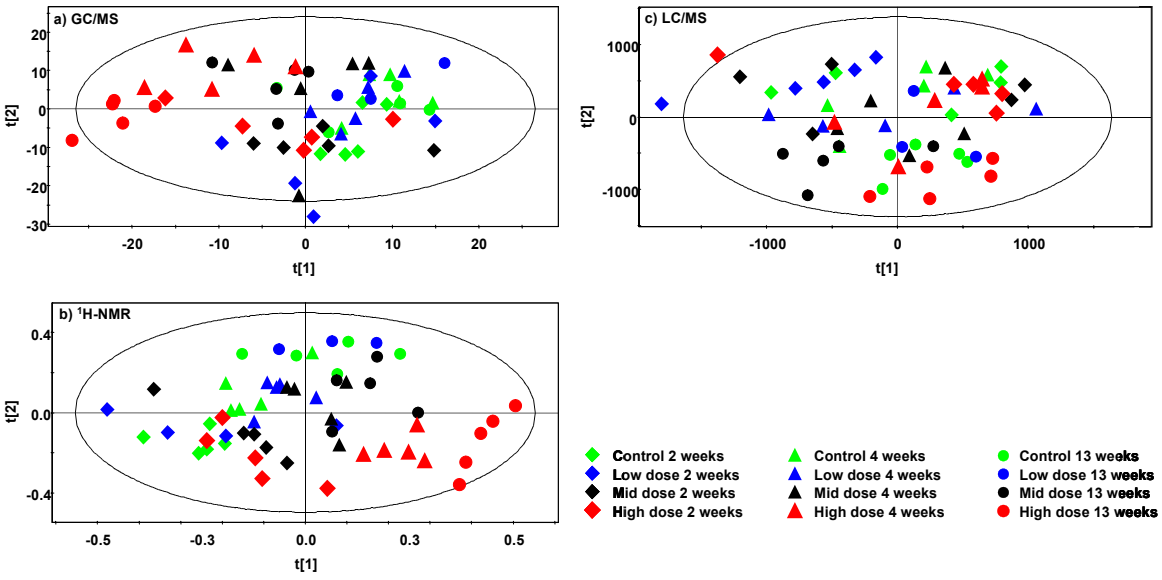

***Figure 7.2.2**: PCA scores plots of GC/MS (a), ^{1}H NMR (b) and LC/MS (c) data. Models include all time points, variables are mean-centered and pareto-scaled. PCA model characteristics are the following: (a) $R^2X(cum) = 0.74$, $Q^2(cum) = 0.41$, 7 significant PCs, (b) $R^2X(cum) = 0.87$, $Q^2(cum) = 0.59$, 9 significant PCs and (c) $R^2X(cum) = 0.68$, $Q^2(cum) = 0.38$, 8 significant PCs.*

In order to identify discriminating markers between control and dose groups, OPLS-DA models were constructed. In contrast to the unsupervised PCA models, where discrimination originates only from the projection of variance, the class identity in OPLS-DA is given in a Y-matrix to which the spectral data is then correlated. Discriminating information is forced to the first PC, while the following components contain orthogonal information, i.e. information not contributing to class separation. In the OPLS-DA models, the control group and low dose group animals (vehicle and 21 µg OTA/ kg bw) were combined into a new control group as 21 µg OTA/kg bw was established as no-observed-effect-level (NOEL) with regard to the classical clinical chemistry and histopathological endpoints [96]. They were analyzed against the combined mid and high dose animals (given 70 and 210 µg OTA/kg bw) as a new dose group. A Y-Matrix containing the values Y = 0 for the control group and Y = 1 for the dose group was used. This approach was chosen since model quality improves with the number of observations and equal group sizes [37]. Mean centering and pareto-scaling were applied to the data when constructing the models. This scaling procedure is a compromise between unit variance scaling, which tends to overestimate noise, and no scaling, which causes the model to be dominated by the few high-intensity signals in the chromatograms or ^{1}H NMR spectra [37]. Characteristics of the dose-based OPLS-DA models (Fig. 7.2.3a-c) are summarized in Table 7.2.2.

The OPLS-DA models constructed with data from all three analytical methods separate control groups from dose groups in a dose-dependent manner along the discriminating component t[1]P. Control groups and high dose groups are located on the outer edges of the plot, while the low and mid dose groups are situated inbetween. A time trend can be recognized in the dose groups. In the GC/MS and ^{1}H NMR models, the high dose samples are clearly separated from the rest from the four week time point onwards (Fig 7.2.3a, b). The LC/MS model separates high dose samples already after two weeks of administration. The orthogonal component t[2]O, which models information that is not contributing to the group separation, contains information on the sampling time point. This can be observed especially in the ^{1}H NMR model (Fig. 7.2.3b), where the 13 weeks samples are located in the upper region of the plot.

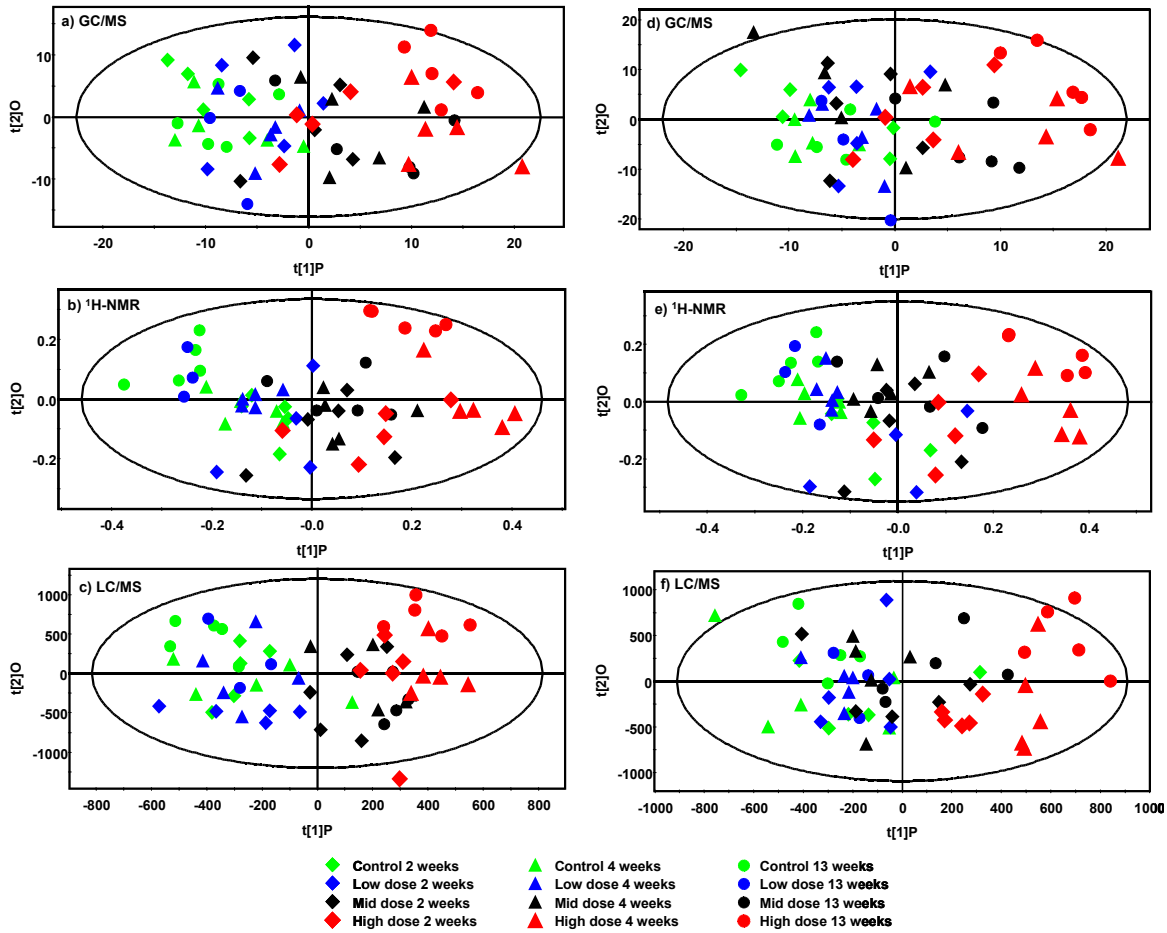

Figure: 7.2.3: *Scores plots of OPLS-DA models. As discriminating Y-Matrix, either the dose (control and low dose animals versus mid and high dose animals, plots a, b and c) or the histopathology scores of kidney tubular basophilia (plots d, e, and f) were used.*

In order to further enhance the power of the multivariate statistics models, a data analysis approach was chosen in which information regarding the severity of histopathological changes caused by OTA treatment, i.e. histopathology scores, was included. The histopathology scores of all animals at all time points and all findings examined and were used to construct a separate PCA model (Fig. 7.2.4). The resulting scores plot shows a time- and dose-dependent separation of OTA-dosed animals from controls along PC1 and PC2 from the top left to the bottom right side of the plot. In the loadings plot, five kidney findings, i.e. karyomegaly, interstitial fibrosis, tubular vacuolization, tubular basophilia and tubular cell apoptosis are responsible for the dose-dependent separation of samples in the scores plot. From these five findings, correlating with the administration of OTA, the tubular basophilia histopathology score was selected as Y-matrix for the construction of OPLS-DA models as it showed the strongest correlation with dose and was diagnosed in a large number of animals. Model

characteristics of the OPLS-DA models constructed with histopathology scores as discriminators (Fig. 7.2.3d-f) are compared to those of models constructed with dose in Table 7.2.2.

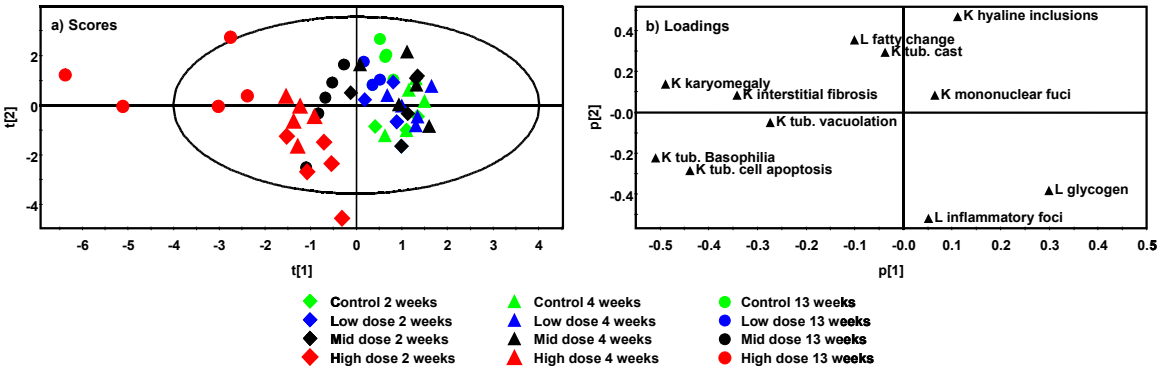

Figure 6.2.4: *Scores plot (a) and the corresponding loadings plot (b) of a PCA model using histopathology scores as variables. The dose- and time-dependent separation of dose group animals from control group animals is best reflected by the finding of kidney tubular basophilia, thus this parameter was chosen as Y-matrix for OPLS-DA models. K = kidney findings, L = liver findings.*

Construction of supervised OPLS-DA models with histopathology scores as classifier (Fig. 7.2.3d-f) yielded three models with similar qualities to those constructed with dose as classifier (Fig. 7.2.3a-c). A clear dose-dependent separation along the discriminating component t[1]P can be observed with all three analytical methods (Fig. 7.2.3d-f) with the control and high dose groups on either side of the plot and the mid dose group clustering inbetween.

Even though they do not differ when inspected visually, the histopathology-based OPLS-models (Fig 7.2.3d-f) better reflect the data structure described by the model characteristics in Table 7.2.2. With all three analytical models, the variance modeled with first component $R^2Y(P1)$ increased when using histopathology scores instead of dose as classifiers. This parameter is indicative of how much of the information of the data that is modeled into the discriminating component t[1]P of the model can be correlated with the discriminating Y-matrix. The predictive power in leave-one-out cross validation $Q^2(P1)$ of the discriminating component also increased with all three analytical methods when using histopathology scores instead of dose as classifiers. In general, it can be stated that model quality improved when histopathology scores were used as classifiers instead of dose.

***Table 7.2.1**: Summary of histopathological observations in kidneys of male F344/N rats treated with 0, 21, 70 or 210 µg OTA/kg bw for 14, 28 or 90 days. - lesion not observed, +, minimal, ++ mild, +++ moderate and ++++high severity of lesion.*

Histopathological change	Interval [days]	Ochratoxin A [µg/kg bw]			
		0	21	70	210
Tubular basophilia	14	+(3/5)	+(4/5)	+(2/5)	++(5/5)
	28	+(1/5)	+(2/5)	+(2/5)	+++(5/5)
	90	+(2/5)	+(5/5)	++(5/5)	+++(5/5)
Tubular degeneration	14	-	-	-+(1/5)	++(5/5)
	28	-	-	+(5/5)	+++(5/5)
	90	-	-	++(+)(5/5)	++++(5/5)
Nuclear enlargement	14	-	-	-	+(5/5)
	28	-	-	+(5/5)	+++(5/5)
	90	-	-	++(5/5)	++++(5/5)
Cell proliferation	14	-	-	-	+(5/5)
	28	-	-	+(5/5)	+++(5/5)
	90	-	-	+++(5/5)	++++(5/5)

The S-plots of the OPLS-DA models were used for identification of potential markers of group separation as proposed by Wiklund *et al*. [41]. The variables responsible for group separation are presented in Tables 7.2.3-7.2.5. For all three analytical methods, there was substantial overlap between the variables found with either dose or histopathology scores as Y-Matrix.

For marker identification, the original GC/MS chromatograms and ^{1}H NMR spectra were used. For the identification of GC/MS markers, AMDIS-deconvoluted peaks or peaks from the original HP ChemStation chromatograms were compared to the NIST mass spectral library and subsequently to chromatograms of authentic reference compounds, if available. ^{1}H NMR peaks were identified by comparison to the spectral library of the Chenomx NMR Suite. LC/MS signals were compared to the contents of the METLIN Metabolite Database using the queries supplied by the XCMS program [44]. However, due to the limited size of the METLIN Metabolite Database and the large mass tolerance used in the queries, the identities given for LC/MS-based markers require further elucidation and should be considered only as tentative assignments.

***Table 7.2.2**: Characteristics for OPLS-DA models constructed with either dose or histopathology scores (histo) as Y-Matrix.*

	Y-Matrix	R^2X(cum)	R^2Y(P1)	R^2Y(cum)	Q^2(P1)	Q^2(cum)	Significant Components
GC/MS	dose	0.33	0.42	0.58	0.32	0.29	1+0
	histo	0.33	0.51	0.67	0.43	0.51	1+1
LC/MS	dose	0.32	0.52	0.78	0.15	0.36	1+2
	histo	0.18	0.54	0.71	0.26	0.47	1+0
NMR	dose	0.38	0.49	0.59	0.39	0.33	1+0
	histo	0.39	0.53	0.61	0.45	0.43	1+0

Putative markers of OTA toxicity were found by analyzing either the dose-based (0 and 21 versus 70 and 210 µg/kg bw) or histopathology-based OPLS-DA models for each analytical technique. There was substantial overlap for both analytical strategies. GC/MS analysis showed that excretion of the following metabolites was increased in OTA-treated animals exhibiting histopathological changes in the kidney (Tab. 7.2.3): 5-oxoproline, a C_4-polyol, presumably erythritol, 2,3,4-trihydroxybutyric acid, *D*-glucose, *myo*-inositol, pseudouridine, and 5-hydroxy-1*H*-indole. 2-Oxoglutarate and citrate were decreased using the dose-based model.

***Table 7.2.3:** Main fragments and chromatographic retention time (RT) of metabolic changes upon ochratoxin A administration identified using GC/MS. Metabolites are given as the actual analyte, i.e. the methoxime (MO) and trimethylsilyl (TMS) derivate. Metabolite identification was carried out by comparison to the NIST mass spectral database.*

Main fragments [m/z]	RT [s]	↑↓[1]	Identification
156, 157, 258	1046	↑	5-oxoproline 2TMS
205, 217	1049	↑	C4-polyol 4TMS (erythritol 4TMS)[2]
100, 115, 143, 329	1075	↑	creatinine enol 3TMS[3]
292	1082	↑	tetroric acid 4TMS
277, 278	1207	↑	(5-hydroxy-1-H-indole 2TMS)[2, 4]
103, 117, 133, 205	1354	↑	*D*-glucose MO5TMS
191, 204	1412	↑	*D*-glucose 5TMS
305	1472	↑	*myo* -inositol 6TMS
217, 218, 357	1619	↑	pseudouridine 5TMS
112, 156, 229, 304	1113	↓	2-oxoglutarate MO2TMS
273, 347, 363, 465	1303	↓	citrate 4TMS

[1]↑ Indicates increased excretion in exposed groups compared to the control group, ↓ indicates decreased excretion in exposed groups. [2]Metabolites in brackets are only putatively assigned. [3]Observed in histopathology based model only.[4]Observed in dose based model only.

^{1}H NMR analysis showed increases in the excretion of *N,N*-dimethylglycine, taurine and creatinine. Excretion levels of acetate, 2-oxoglutarate and citrate were decreased. Bins 23 (1.32–1.36 ppm) and 26 (1.44–1.48 ppm) were also increased. These bins are known to contain the resonances of lactate and alanine, respectively. However, due to

overlaying signals, a definite identification of the signals responsible for this increase could not be performed (Tab. 7.2.4). A number of other bins for which no metabolite assignment could be made were also changed.

Table 7.2.4: *Bins and chemical shifts of the metabolites altered upon OTA administration identified using ^1H NMR analysis. Metabolite identification was carried out by comparison to the Chenomx NMR Suite database.*

Bin dose	Bin histo	∂ [ppm]	↑↓[1]	Identification
20	20	1.20 – 1.24	↑	(lactate)[2]
---	22	1.32 – 1.36	↑	
23	23	1.36 – 1.40	↓	
26	---	1.44 – 1.48	↑	(alanine)[2]
39	39	1.96 – 2.00	↓	acetate
43	43	2.12 – 2.16	↓	
50, 51	50, 51	2.40 – 2.48	↓	2-oxoglutarate
53	53	2.52 – 2.56	↓	citrate
56, 57	56, 57	2.64 – 2.72	↓	citrate
62	62	2.88 – 2.92	↑	*N,N* -dimethylglycine
64	64	2.96 – 3.00	↓	2-oxoglutarate
---	69	3.16— 3.20	↑	(glucose)[2]
---	73	3.32— 3.36	↑	(glucose)[2]
74	74	3.36 – 3-40	↑	(glucose)[2]
76	76	3.44 – 3.48	↑	
78	78	3.52 – 3.56	↑	taurine
79	79	3.56 – 3.60	↑	
81 – 88	81 – 88	3.64 – 3.94	↑	(glucose)[2]
89	---	3.96 – 4.00	↑	creatinine

[1]↑ Indicates increased excretion in exposed groups compared to the control group, ↓ indicates decreased excretion in exposed groups. [2]Signals were not strong enough for unambiguous identification and are only putatively assigned.

LC/MS analysis showed a number of variables to be changed due to OTA treatment. Based on the spectral information, these metabolites may represent citrate and oxoglutarate, as well as aldose phosphates and steroid hormones. However, due to insufficient information obtained from the spectra, further structure elucidation was not possible (Tab. 7.2.5), and these alterations are not discussed any further.

7.3 Discussion

In this study, three complementary analytical techniques were used to correlate metabonomic findings with histopathology endpoints from a 90 day toxicity study with OTA. In the study, histopathologic analysis gave a NOEL of 21 µg OTA/kg bw, minimal to mild changes in kidney histopathology and clinical chemistry at doses of 70 µg/kg bw, visible as early as four weeks after continuous OTA administration and minimal to mild changes in histopathology as early as two weeks at doses of 210 µg OTA/kg bw. After 90 days, the 210 µg/kg bw group showed degeneration of tubular lining cells and nuclear variability implying increased nuclear size and mitotic figures [96]. Applying metabonomic analysis, alterations in the composition of urine samples were indicated in

urine samples collected after four weeks in the 70 µg/kg bw and 210 µg/kg bw dose groups and after two weeks in individual animals of the 210 µg/kg bw dose group with both GC/MS and ^{1}H NMR using unsupervised PCA, and with all three analytical approaches using supervised OPLS-DA metabonomics.

Table 7.2.5: *Mass-retention time pairs of the metabolic alterations upon OTA administration identified using LC/MS. Mass traces of OTA and its metabolites were excluded in the analysis.*

Variable ID dose [M(m/z)T(RT)]	Variable ID histo [M(m/z)T(RT)]	↑↓[1]	Identity proposal[2]
M145T40	M145T40	↓	2-oxoglutarate, adipate, lysine
M145T46	M145T64	↓	2-oxoglutarate, adipate, lysine
---	M181T153	↓	
M191T51	M191T51	↓	citrate
---	M191T62	↓	
M192T51	M192T51	↓	citrate (isotope peak)
---	M201T303	↓	
M206T260	M206T260	↑	acetylphenylalanine, phenylpropinylglycine
---	M217T281	↓	
M231T141	M231T141	↑	
M231T79	M231T79	↓	melatonine
M232T143	---	↑	
M237T339	---	↑	
M244T117	M244T117	↓	aldose phosphates
---	M249T234	↑	
M251T32	M251T32	↑	aldose phosphates
---	M252T260	↑	
---	M259T102	↓	
M259T306	---	↓	aldose phosphates
M259T325	M259T325	↓	aldose phosphates
M260T325	M260T325	↓	aldose phosphates (isotope peak)
---	M260T90	↑	
M261T113	M261T113	↓	
---	M261T138	↓	
---	M262T138	↓	
---	M269T344	↑	
---	M273T283	↑	
---	M275T174	↓	
M287T367	---	↑	
M301T309	---	↓	steroid hormone
M302T131	---	↓	steroid hormone
M303T248	---	↓	steroid hormone
M303T260	M303T260	↓	
M317T253	M317T253	↓	
M318T253	M318T253	↓	
---	M323T284	↓	
---	M337T313	↓	
M350T135	M350T135	↑	
M372T111	---	↓	
M402T419	---	↑	
---	M409T372	↑	
M411T194	M411T194	↑	
---	M412T194	↑	
M417T299	---	↑	
---	M421T211	↑	
---	M445T248	↑	
M461T167	---	↑	
M473T318	M473T318	↑	
---	M474T318	↑	
---	M523T138	↓	

[1]↑ indicates increased excretion in exposed groups compared to the control group, ↓. indicates decreased excretion in exposed groups. [2]Identity proposals are made by the METLIN Metabolite Database using the linking function in XCMS.

Predictivity of the OPLS-DA models increased when using histopathology scores as Y-matrix instead of dose, while yielding the same metabolites to be responsible for separating controls from dosed animals. This approach allows the inclusion of the information gained by histopathology, which is otherwise not used for metabonomic analysis. Moreover, it helps to overcome the problem of heterogeneous response of dosed animals to toxic insults which is often observed in toxicity studies, since the actual effect that is used for the diagnosis of toxicity, i.e. the histopathological findings, is correlated to the changes in the metabolism.

In our studies, both GC/MS and ^{1}H NMR were able to differentiate between controls and exposed groups and complemented each other with regard to marker identification due to the availability of databases, as well as sensitivity and metabolite coverage. However, GC/MS analysis may be further improved with the use of sampling robots to minimize variance introduced by the derivatization procedure and the introduction of two-dimensional GC coupled to time-of-flight detectors (GC×GC/TOF-MS) [26; 108]. LC/MS analysis contained more noise and structural elucidation of putative markers requires substantial effort due to lack of characteristic mass spectral features and spectral data bases. Thus, LC/MS appears to be more suited for targeted analysis of specific compound classes [109].

The combined GC/MS and ^{1}H NMR based metabonomic analysis of urine samples from rats administered OTA showed a decrease in the urinary excretion of the Krebs cycle intermediates citrate and oxoglutarate, as well as an increased excretion of glucose, creatinine, pseudouridine, alanine, *N,N*-dimethylglycine and renal osmolytes such as taurine and *myo*-inositol.

These changes may be rationalized based on the well described OTA-toxicity and general considerations on kidney toxicity. In histopathology, OTA toxicity is characterized by damage to the S3 segment of the proximal tubule of the kidney with accompanying impairment of renal excretory function resulting in alteration of osmolyte excretion as an early toxic effect [84; 86; 96]. Whether the altered osmolyte excretion is due to impaired excretory function or just due to damaged cells remains unclear. On the cellular level, impairment of mitochondrial function, oxidative stress and inhibition of protein synthesis have been described as toxic effects [110–113] and these can be associated with altered levels of Krebs cycle intermediates, increased 5-oxoproline and amino acid excretion as described below.

Increased excretion of glucose in urine as observed in some of the high dose group animals is associated with impairment of renal function. Although no significant changes in urinary glucose and creatinine excretion were found by clinical chemistry analysis from the study an increase in serum creatinine after 13 weeks was observed in the 210 µg/kg bw group [96], suggesting impaired renal function at this dose and time-point. Such changes in the excretion levels of a number of metabolites contribute to group separation in multivariate data analysis, even if these alterations are not statistically significant when considered isolated for each single metabolite. Thus, multivariate data analysis may be more sensitive than classical clinical chemistry regarding small and variable changes of effect markers.

A decrease in citrate and 2-oxoglutarate excretion is widely attributed to a disturbance of mitochondrial energy production. Impaired energy metabolism results in a depletion of ATP in the cells. ATP depletion is a consequence of mitochondrial toxicity as a prominent feature of OTA-induced renal toxicity in rodents [110]. However, impairment of the Krebs cycle is described in many metabonomic studies [15] and may rather be an effect of stress response and general toxicity than of specific kidney toxicity or OTA effects.

5-Oxoproline is involved in the γ-glutamyl-cycle, which is responsible for GSH synthesis [114]. Accumulation can either occur by inhibition of the enzyme 5-oxoprolinase or by ATP-depletion. ATP-depletion would also result in the accumulation of cysteine and glycine (Fig. 7.3.1). This would also explain the increase in taurine excretion observed by ^{1}H NMR, since excess cysteine is converted to taurine to prevent its accumulation. Alternatively, glutathione may act as a feedback-inhibitor for the production of 5-oxoproline [115]. Excessive GSH depletion in the kidney due to oxidative stress may lead to induction of the γ-glutamyl cycle. The consequence is increased 5-oxoproline production, exceeding the capacity of the 5-oxoprolinase, leading to accumulation of 5-oxoproline. Oxoprolinuria in rats is induced by several agents which induce GSH depletion [116; 117]. The observation of increased secretion of 5-oxoproline is consistent with a reduction of detoxifying capacity via inhibition of Nrf2-dependent gene expression and reduced glutathione concentrations observed after OTA-treatment [118]. The increase of *N,N*-dimethylglycine observed with ^{1}H NMR is probably also related to oxidative stress and increased glutathione synthesis. There is evidence that glycine needed for GSH synthesis may also be supplied by dietary choline, which is transferred to glycine via

betaine, dimethylglycine and sarcosine [119]. Induction of this pathway may explain the observed increase in *N,N*-dimethylglycine excretion. Thus, increased urinary 5-oxoproline and *N,N*-dimethylglycine excretion is further evidence for the involvement of oxidative stress in OTA toxicity [120].

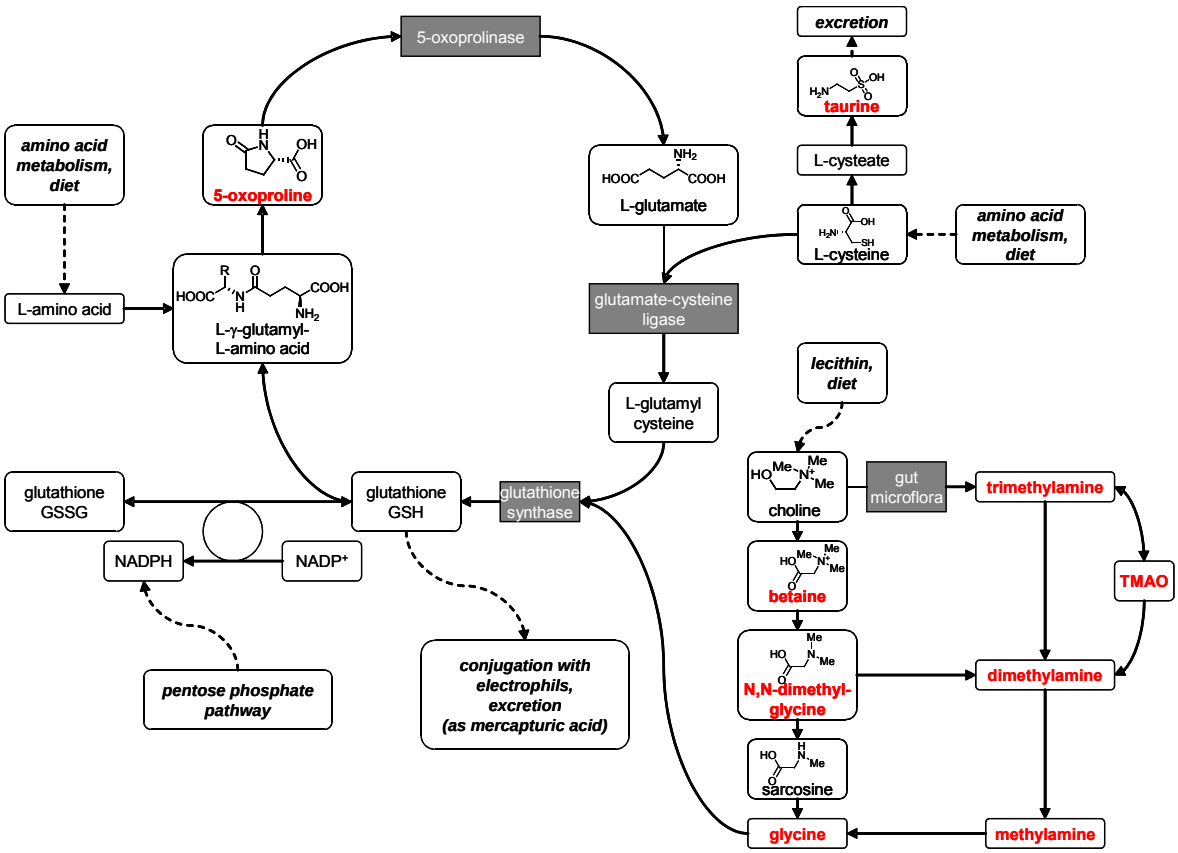

Fig 7.3.1: *The γ-glutamyl cycle is responsible for the production of glutathione. Metabolites accessible by the GC/MS or 1H NMR analysis methods described are marked in red.*

Kidney injury and impaired renal function may result in changes in osmolyte excretion, either by leakage from damaged cells or by disturbances of osmolyte transporters, and the metabonomic analysis identified increased excretion of several osmolytes in OTA-treated animals. Taurine is a renal osmolyte whose excretion and re-uptake is regulated by sodium-dependent transporters [121]. An increase in taurine excretion may occur due to inhibition of the taurine re-uptake or by leakage from damaged renal cells. Increased taurine excretion is also discussed as a marker of impaired liver function. However, no histopathology in the liver was observed in the study providing the samples for this analysis, and the link to OTA toxicity remains unclear.

myo-Inositol, which regulates the osmotic pressure in renal cells, is the osmolyte with the highest concentration in proximal tubule cells [122] and its cellular concentration is regulated by transporters, two sodium-dependent transporters SMIT1 and SMIT2 and a sodium-independent transporter HMIT [123; 124]. Increase in *myo*-inositol excretion as observed after OTA treatment may occur as a response to hypotonicity of the urine or from a decreased reabsorption due to a disturbance of the transporters [125].

Several other markers identified by the metabonomic analysis may be related to stimulation of cell proliferation in the kidney induced by OTA as observed by 5-bromo-2'-deoxyuridine (BrdU) staining [96]. Pseudouridine is a modified nucleoside in sRNA and tRNA. When RNA is degraded to nucleosides and bases, pseudouridine cannot be reused for *de novo* nucleotide synthesis and is excreted into the urine. Pseudouridine excretion with urine is therefore indicative of increased RNA turnover and has been postulated as a cancer marker [126]. An increase in RNA turnover is consistent with increased DNA synthesis as a result of the stimulation of renal cell proliferation observed in the study [96]. 5-Hydroxyindole is a product of tryptophan metabolism. Increased excretion of various tryptophan metabolites was associated with tumor growth [127], since tryptophan metabolites play a role in various regulatory and signaling pathways. A targeted screening method for tryptophan metabolites [128] may reveal alterations in tryptophan metabolite excretion that yield insights into these pathways.

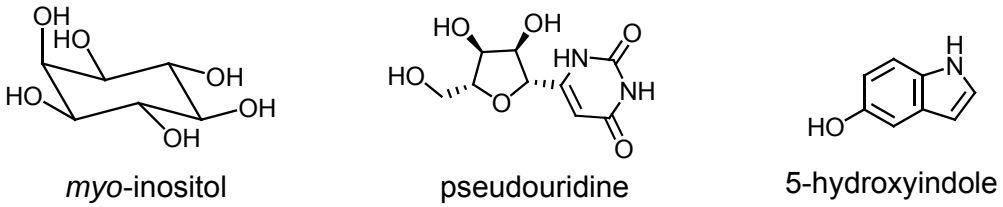

myo-inositol pseudouridine 5-hydroxyindole

Figure 7.3.2: *The renal osmolyte myo-inositol, the modified nucleoside pseudouridine and the tryptophan metabolite 5-hydroxyindole were found to be increased in urine upon OTA treatment.*

After application of OTA at higher doses and a shorter period of observation, Mally *et al.* observed increased excretion of the renal osmolyte trimethylamine-*N*-oxide (TMAO) as dominating molecular marker by ^{1}H NMR metabonomics [84]. GC/MS analysis of these samples also yielded a nine-fold increase of *myo*-inositol excretion in dosed animals (unpublished results). Since there was no alteration of TMAO excretion observed in this

study, *myo*-inositol seems to be a more sensitive indicator of disturbed renal osmolyte handling in OTA toxicity than TMAO.

Although the biochemical perturbations observed in this study reflect rather general alterations and none of the metabolites observed in this study is predictive on its own, they correlate well with observations made in other studies on OTA toxicity. With metabonomics, the onset of toxic lesions could be observed at the same time points as with histopathology. It must be noted however, that the mechanistic hypotheses postulated for the OTA-induced alterations in urinary profiles are only speculative. However, for compounds with unknown toxic mechanisms, such hypotheses allow specific confirmatory experiments.

The integrated multi-platform metabonomics approach with GC/MS, ^{1}H NMR and LC/MS shows promise for the investigation of changes in urinary metabolite pattern, since good correlation exists between metabonomics group discrimination and histopathological findings, especially since the histopathological changes were rather subtle [96]. The alterations in urinary metabolite profile observed for OTA toxicity are rather a pattern of various metabolites than one specific marker. However, they correlate with the observations made on OTA toxicity. The data show that an inclusion of histopathology scores in a metabonomic analysis improves model quality and allows greater confidence in discriminating markers found by metabonomics. The data analysis strategy presented here can be used for the analysis of existing toxicology studies to gain mechanistic insight of observed toxicities.

Table 7.2.5: *Excretion levels of urinary metabolites after OTA administration quantified with the Chenomx NMR Suite; values are given as mean ± SD in [µmol/µmol Crea]; significance levels were determined with ANOVA and Dunnett's post hoc test* p<0.05, ** p<0.01, ***p<0.001. Arrows indicate whether metabolite excretion is primarily increased (↑) or decreased (↓) compared to controls.*

		Krebs cycle intermediates			Renal Osmolytes						
		Citrate ↓	**2OG[1] ↓**	**Malonate**	**Betaine**	**myo-Inositol**	**DMG[2] ↑**	**Taurine**	**Acetoacetate**	**5-Oxoproline**	**Glycolate ↑**
week2	**C[6]**	9.45 ± 4.93	6.06 ± 3.00	0.50 ± 0.36	0.35 ± 0.13	0.38 ± 0.20	0.11 ± 0.04	3.64 ± 2.94	0.48 ± 0.42	0.54 ± 0.44	0.50 ± 0.19
	L[7]	5.86 ± 4.62	2.85 ± 2.16	0.13 ± 0.07*	0.32 ± 0.22	0.38 ± 0.21	0.06 ± 0.04	2.94 ± 1.85	0.21 ± 0.20	0.54 ± 0.53	0.35 ± 0.14
	M[8]	7.03 ± 4.09	3.69 ± 1.97	0.18 ± 0.04	0.33 ± 0.21	0.26 ± 0.09	0.11 ± 0.05	3.77 ± 1.68	0.30 ± 0.14	0.54 ± 0.36	0.48 ± 0.14
	H[9]	6.56 ± 2.72	3.34 ± 1.63	0.33 ± 0.22	0.58 ± 0.36	0.50 ± 0.27	0.26 ± 0.17*	3.16 ± 2.09	0.63 ± 0.48	0.41 ± 0.17	0.64 ± 0.24
week4	**C**	13.11 ± 6.57	9.54 ± 4.22	0.55 ± 0.38	0.62 ± 0.64	0.42 ± 0.22	0.16 ± 0.09	10.91 ± 7.17	0.59 ± 0.45	0.46 ± 0.25	0.59 ± 0.15
	L	9.63 ± 5.16	7.11 ± 4.09	0.48 ± 0.37	0.41 ± 0.21	0.40 ± 0.32	0.11 ± 0.05	8.86 ± 4.82	0.45 ± 0.40	0.67 ± 0.64	0.63 ± 0.22
	M	7.38 ± 3.37*	5.60 ± 2.52*	0.71 ± 0.53	0.48 ± 0.31	0.52 ± 0.36	0.26 ± 0.21	8.56 ± 4.07	054 ± 0.53	0.78 ± 1.08	0.72 ± 0.36
	H	5.70 ± 1.95**	2.28 ± 0.78***	0.70 ± 0.34	0.44 ± 0.18	0.33 ± 0.09	0.61 ± 0.16***	9.48 ± 3.68	0.24 ± 0.08	0.58 ± 0.16	1.06 ± 0.15***
week13	**C**	9.47 ± 3.55	6.74 ± 2.33	0.48 ± 0.34	0.40 ± 0.19	0.41 ± 0.14	0.06 ± 0.02	12.16 ± 6.36	0.47 ± 0.26	0.61 ± 0.27	0.62 ± 0.23
	L	17.66 ± 10.76	12.42 ± 7.35	0.87 ± 0.34	0.58 ± 0.10	1.04 ± 0.21	0.10 ± 0.02	18.99 ± 0.80	0.97 ± 0.09	1.55 ± 0.24	1.00 ± 0.22
	M	8.45 ± 4.28	3.73 ± 2.50**	0.80 ± 0.49	0.55 ± 0.47	0.70 ± 0.69	0.18 ± 0.06*	10.35 ± 3.34	0.32 ± 0.22	0.84 ± 0.85	0.78 ± 0.26
	H	3.06 ± 1.14**	0.78 ± 0.26***	0.68 ± 0.53	0.47 ± 0.21	0.44 ± 0.33	0.43 ± 0.07***	10.97 ± 6.51	0.43 ± 0.48	1.74 ± 3.06	0.97 ± 0.33**

		Gut microflora metabolites									
		Hippurate ↓	**4HPA[3]**	**PAG[4]**	**Lactate ↑**	**MNA[5]**	**Acetate**	**Choline ↑**	**Glycine ↑**	**Alanine ↑**	**Creatine**
week2	**C**	3.61 ± 1.70	0.37 ± 0.22	3.72 ± 1.84	0.37 ± 0.15	0.72 ± 0.29	0.86 ± 0.31	0.14 ± 0.07	0.77 ± 0.33	0.34 ± 0.14	0.18 ± 0.14
	L	2.81 ± 1.18	0.18 ± 0.06	1.40 ± 0.89	0.28 ± 0.12	0.31 ± 0.29	0.87 ± 0.34	0.09 ± 0.03	0.53 ± 0.22	0.26 ± 0.14	0.27 ± 0.25
	M	3.36 ± 1.70	0.32 ± 0.07	2.27 ± 0.54	0.28 ± 0.09	0.44 ± 0.13	0.67 ± 0.41	0.12 ± 0.04	0.63 ± 0.20	0.27 ± 0.09	0.16 ± 0.13
	H	4.04 ± 1.50	0.38 ± 0.23	3.93 ± 2.70	0.43 ± 0.18	0.70 ± 0.41	1.04 ± 0.31	0.15 ± 0.05	1.08 ± 0.49*	0.41 ± 0.19*	0.17 ± 0.19
week4	**C**	6.21 ± 2.77	0.57 ± 0.29	4.41 ± 2.42	0.52 ± 0.30	1.23 ± 0.70	0.58 ± 0.35	0.20 ± 0.09	1.04 ± 0.61	0.50 ± 0.28	0.33 ± 0.40
	L	4.84 ± 2.19	0.42 ± 0.16	3.69 ± 1.56	0.37 ± 0.20	0.91 ± 0.43	0.75 ± 0.39	0.17 ± 0.07	0.95 ± 0.37	0.35 ± 0.18	0.30 ± 0.20
	M	6.07 ± 2.86	0.61 ± 0.39	4.75 ± 3.90	0.59 ± 0.43	1.20 ± 0.68	0.77 ± 0.52	0.22 ± 0.15	1.34 ± 0.90	0.54 ± 0.42	0.44 ± 0.52
	H	5.41 ± 1.59	0.58 ± 0.21	3.32 ± 0.99	0.91 ± 0.22***	1.08 ± 0.20	0.82 ± 0.14	0.22 ± 0.05*	6.17 ± 1.49***	0.71 ± 0.22**	0.21 ± 0.12
week13	**C**	3.80 ± 1.24	0.37 ± 0.11	2.45 ± 0.58	0.34 ± 0.11	0.86 ± 0.31	0.44 ± 0.10	0.14 ± 0.04	0.81 ± 0.38	0.31 ± 0.09	0.42 ± 0.29
	L	7.81 ± 2.87	0.55 ± 0.06	3.73 ± 0.44	0.56 ± 0.08	1.51 ± 0.21	1.83 ± 1.54	0.22 ± 0.06	1.14 ± 0.26	0.62 ± 0.12	0.53 ± 0.33
	M	6.01 ± 2.34	0.67 ± 0.26	3.72 ± 1.72	0.59 ± 0.22	1.21 ± 0.46	0.94 ± 0.62	0.19 ± 0.08	1.62 ± 0.58	0.53 ± 0.23	0.48 ± 0.40
	H	2.85 ± 1.02*	0.42 ± 0.20	2.85 ± 0.73	1.09 ± 0.23***	0.67 ± 0.27	0.78 ± 0.38	0.23 ± 0.07***	5.02 ± 0.70***	0.49 ± 0.20*	3.10 ± 6.38

[1]2OG, 2-oxoglutarate; [2]DMG, *N,N*-dimethylglycine; [3]4HPA, 4-hydroxyphenylacetate; [4]PAG, phenylacetylglycine; [5]MNA, 1-methylnicotinamide; [6]C, control group, 0 µg OTA/kg bw; [7]L, low dose group, 21 µg OTA /kg bw; [8]M, mid dose group, 70 µg OTA/kg bw; [9]H, high dose group, 210 µg OTA/kg bw;

8 Aristolochic Acid

8.1 Introduction

Aristolochic acid (AA) occurs in plants of the genus *aristolochia* and is a mixture of structurally related nitrophenanthrene carboxylic acid derivatives, mainly aristolochic acids I and II (AAI and AAII) [88]. AA shows nephrotoxic potential in rodents with a clear site-specificity in the proximal tubuli [90; 129; 130]. The mechanism of action is not fully understood, but DNA adducts of reactive AA-metabolites correlate with bladder carcinoma induced by AA administration [131]. Its relevance for human health is based on the occurrence of Chinese herb nephropathy (CHN) and Balkan endemic nephropathy (BEN), which, although occurring in completely different populations, show the same symptoms and are presumably caused by chronic exposure to AA [89]. Traditional Chinese medicine (TCM) uses herbs of *aristolochia sp.* and related plants for various medications [88]. Exposure to nephrotoxic concentrations of AA occurs when herbs in TCM preparations are accidentally substituted with leafs from *aristolochia sp*. with high AA contents. The cause of BEN is postulated to be the uptake of AA-contaminated flour. The contamination occurs when A*ristolochia clematitis* growing on the wheat fields is harvested with the grain and processed [89].

A number of studies have been already published applying various metabonomics techniques to analyze changes induced by AA administration in rats. LC/MS analysis of urine [132; 133] and plasma [134] as well as GC/MS [135] and ^{1}H NMR [136] analysis of urine have been used to identify various putative biomarkers of AA nephrotoxicity.

This study was designed to detect early signs of nephrotoxicity after AA-administration. The dose levels were based on a previous four week oral gavage study, were 0.2 mg/kg bw was established as NOAEL concerning clinical chemistry and histopathology and mild renal lesions were observed at 1.0 mg/kg bw [129]. In our study, male Wistar rats received 0, 0.1, 1.0 and 10.0 mg AA/kg bw dissolved in water daily by oral gavage for 12 consecutive days. Urine and blood were collected on days 1, 5 and 12 and necropsy occurred on day 12 of the study. Routine clinical chemistry, histopathological assessment of liver and kidney as well as metabonomic analysis of urine with GC/MS and ^{1}H NMR was carried out.

***Table 8.2.1**: Clinical chemistry data of the aristolochic acid study. Values are given as mean ± SD; significance levels were determined with ANOVA and Dunnett's post hoc test. (* p<0.05, ** p<0.01, *** p<0.001).*

Urine clinical chemistry

		volume [mL]	osmolarity [mosmol/kg]	creatinine [mg/24h]	GGT [U/mg Crea]	total protein [mg/g Crea]
day 1	C[1]	29.4 ± 11.7	339.8 ± 158.7	21.6 ± 8.3	0.34 ± 0.07	759 ± 374
	L[2]	24.4 ± 13.0	434.0 ± 181.2	27.6 ± 12.1	0.30 ± 0.07	841 ± 414
	M[3]	18.8 ± 7.2	583.4 ± 194.7	32.5 ± 10.9	0.32 ± 0.09	524 ± 151
	H[4]	17.0 ± 5.8	504.6 ± 159.8	34.4 ± 12.0	0.32 ± 0.07	692 ± 360
day 5	C	30.5 ± 7.6	295.5 ± 115.8	21.9 ± 7.1	0.43 ± 0.08	722 ± 419
	L	23.8 ± 8.1	394.4 ± 154.4	29.7 ± 12.8	0.41 ± 0.06	857 ± 269
	M	18.8 ± 9.0	387.8 ± 184.2	30.2 ± 14.5	0.42 ± 0.08	666 ± 161
	H	20.3 ± 10.9	414.8 ± 266.9	33.1 ± 23.6	0.36 ± 0.06	584 ± 416
day 12	C	27.8 ± 14.1	552.8 ± 351.5	36.4 ± 20.7	0.30 ± 0.06	1452 ± 154
	L	30.6 ± 9.9	410.8 ± 121.0	28.1 ± 7.1	0.35 ± 0.09	1179 ± 200
	M	20.8 ± 12.8	687.4 ± 317.8	47.7 ± 22.2	0.29 ± 0.05	1137 ± 335
	H	27.2 ± 9.9	489.4 ± 278.8	33.5 ± 17.3	0.22 ± 0.04	1301 ± 357

Plasma clinical chemistry

		glucose [mg/dL]	creatinine [mg/dL]	urea [mg/dL]	total protein [g/dL]
day 1	C	148 ± 14.1	0.24 ± 0.05	35.1 ± 1.76	5.86 ± 0.17
	L	74.6 ± 13.0***	0.24 ± 0.05	27.8 ± 4.70*	5.92 ± 0.23
	M	82.0 ± 7.31***	0.03 ± 0.00	29.6 ± 2.45	5.88 ± 0.11
	H	74.2 ± 8.41***	0.28 ± 0.04	29.0 ± 5.07	5.90 ± 0.14
day 5	C	118 ± 21.7	0.30 ± 0.00	44.0 ± 4.05	6.34 ± 0.23
	L	88.2 ± 48.2	0.24 ± 0.05***	29.5 ± 5.39**	6.42 ± 0.22
	M	132 ± 15.2	0.28 ± 0.04	36.1 ± 7.80	6.08 ± 0.23
	H	114 ± 19.2	0.30 ± 0.00	43.8 ± 7.04	5.84 ± 0.27*
day 12	C	115 ± 18.4	0.26 ± 0.05	32.4 ± 4.33	6.12 ± 0.22
	L	105 ± 18.5	0.26 ± 0.05	29.8 ± 4.19	6.12 ± 0.16
	M	114 ± 10.2	0.30 ± 0.00	37.0 ± 5.58	6.04 ± 0.21
	H	125 ± 17.6	0.28 ± 0.04	37.3 ± 6.15	5.90 ± 0.02

		GOT(ASAT) [U/L]	GPT(ALAT) [U/L]	GGT [U/L]	ALP [U/L]
day 1	C	91.4 ± 6.55	31.4 ± 9.0	0.48 ± 0.47	267 ± 51.4
	L	97.5 ± 7.73	27.9 ± 4.2	0.40 ± 0.37	237 ± 19.8
	M	101.0 ± 26.8	27.1 ± 4.7	0.24 ± 0.32	267 ± 54.8
	H	91.1 ± 25.7	25.3 ± 4.6	0.10 ± 0.00	239 ± 23.2
day 5	C	101.7 ± 40.8	33.4 ± 5.90	0.28 ± 0.40	247 ± 61.7
	L	94.1 ± 9.17	32.2 ± 6.1	0.08 ± 0.04	237 ± 28.8
	M	88.0 ± 13.2	25.5 ± 4.8	0.12 ± 0.04	262 ± 48.0
	H	89.3 ± 11.2	21.4 ± 1.2***	0.16 ± 0.13	211 ± 27.0
day 12	C	75.4 ± 8.24	30.5 ± 2.4	0.10 ± 0.00	211 ± 44.4
	L	86.0 ± 15.5	35.1 ± 6.1	0.10 ± 0.00	185 ± 20.8
	M	92.0 ± 23.6	31.0 ± 10	0.10 ± 0.00	209 ± 40.1
	H	81.5 ± 1.45	29.7 ± 3.2	0.10 ± 0.00	164 ± 32.9

Organ weights

	animal bw gain [g]			relative organ weights [g/kg bw]		
	day 1	day 5	day 12	liver	kidney	bladder
C	35.2 ± 3.03	50.4 ± 10.3	88.6 ± 15.5	3.01 ± 0.23	0.68 ± 0.06	0.07 ± 0.02
L	38.4 ± 6.19	50.0 ± 11.2	89.6 ± 18.1	3.23 ± 0.16	0.66 ± 0.06	0.05 ± 0.02*
M	41.4 ± 3.05	54.8 ± 5.22	92.6 ± 13.1	3.12 ± 0.12	0.67 ± 0.05	0.07 ± 0.02
H	41.8 ± 2.17*	46.4 ± 2.07	71.2 ± 7.66	3.33 ± 0.08*	0.65 ± 0.04	0.06 ± 0.01

[1]C, control group, 0 mg/kg bw; [2]L, low dose group, 0.1 mg/kg bw; [3]M, mid dose group, 1.0 mg/kg bw; [4]H, high dose group, 10 mg/kg bw

8.2 Results

During the course of the study, animals showed no clinical signs of toxicity, except for the high dose group and some individuals of the mid dose group, where introduction of the tube for gavage was difficult due to a swollen esophagus. Irritation of the gastric tract 24 h after oral administration of 10 mg AA/kg bw has been reported in a previous study [97]. Individual animals of the high dose group also showed hair loss on neck and chest, probably due to excessive cleaning.

Clinical chemistry analysis of urine and plasma (Tab. 8.2.1) did not show any signs of toxicity except a highly significant decrease in plasma glucose levels on day one, which may be attributed to decreased feeding. The oral administration of AA causes an irritation of the esophagus, which causes the animals to reduce their food uptake, and the reduced plasma glucose levels would thus reflect fasting. During the course of the study, the animals seemed to adapt, since no differences in plasma glucose levels were observed on day five and day twelve. Other significantly altered clinical chemistry parameters did not show any dose dependency and were not considered to be toxicity-related.

Although body weight gain showed a tendency to decrease in the high dose group on day twelve, this decrease was not significant, and organ weights after necropsy on day twelve were unchanged except for an increase in liver weight in the high dose group (Tab. 8.2.1). Histopathological assessment of tissue sections from liver and kidney did not show any changes upon AA administration.

In total, no changes related to systemic toxicity could be detected by clinical chemistry analyses. This is in concordance with a previous study, where the same doses of 0.1, 1.0 and 10.0 mg AA/kg bw were administered orally for up to twelve months and no changes in clinical chemistry parameters could be observed during the first three months of the study. The same study showed atypical cells with giant nuclei in the tubular epithelium after three months. No earlier time points were recorded [90].

Urine samples collected for all dose groups on day one, five and twelve after start of treatment were subjected to GC/MS and ^{1}H NMR analysis. Unsupervised and supervised multivariate data analysis was performed on the data (Fig. 8.2.1). Principal component analysis (PCA) of GC/MS samples of all time points revealed a tendency to separate samples along the first PC t[1] in a dose-dependent manner, however, the dose groups are not well separated and only the controls and the high dose samples form distinguishable

clusters (Fig. 8.2.1a). PCA of ^{1}H NMR data revealed clear separation of day five and day twelve high dose samples from the rest of the samples. High dose samples from day one however clustered with the controls (Fig. 8.2.1b). In summary, the unsupervised PCA showed effects only for the 10 mg/kg bw high dose group and only from day five onwards.

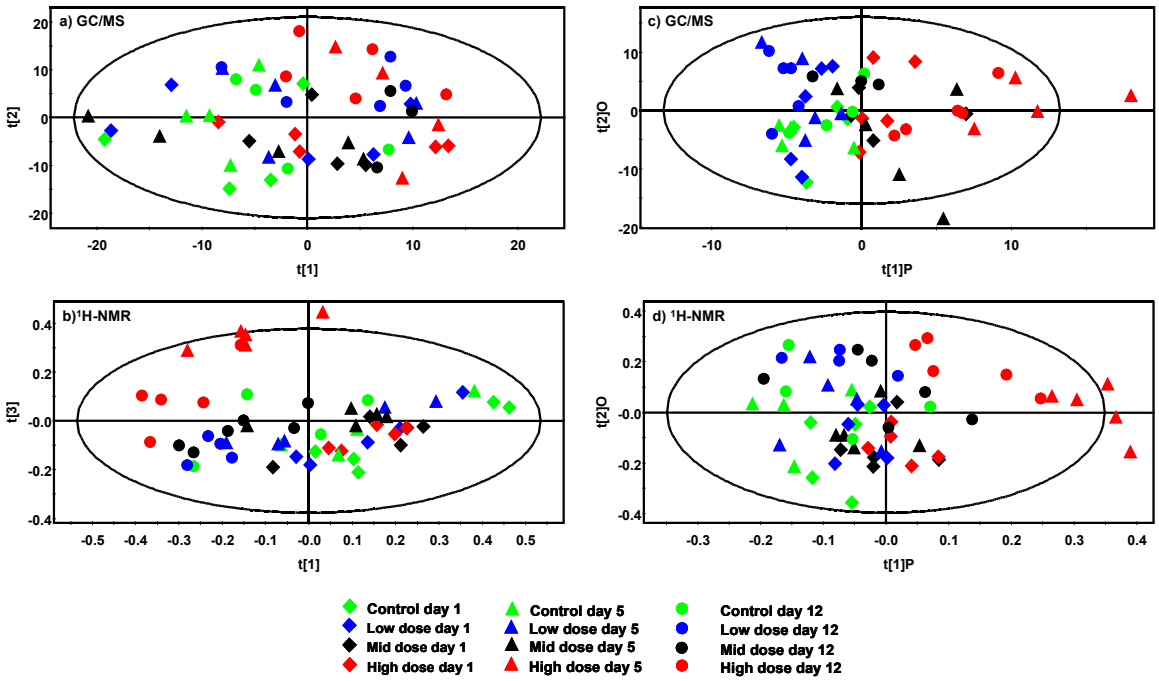

Figure 8.2.1*: Scores plots of multivariate models of urinary aristolochic acid ^{1}H NMR and GC/MS data. (a) PCA of GC/MS data, all time points. (b) PCA of ^{1}H NMR data, all time points. (c) OPLS-DA of GC/MS data, all time points. (d) OPLS-DA of ^{1}H NMR data, all time points. Model characteristics are (a) $R^2X(cum) = 0.63$, $Q^2(cum) = 0.37$, 6 significant components; (b) $R^2X(cum) = 0.81$, $Q^2(cum) = 0.55$, 7 significant components; (c) $R^2X(cum) = 0.26$, $R^2Y(P) = 0.29$, $R^2Y(cum) = 0.51$, $Q^2(cum) = 0.05$, 1 significant component; (d) $R^2X(cum) = 0.37$, $R^2Y(P) = 0.22$, $R^2Y(cum) = 0.33$ $Q^2(cum) = 0.09$, 1 significant component.*

To further analyze these changes and to extract the metabolites responsible for the differences in urinary composition, supervised orthogonal projection to latent structures discriminant analysis (OPLS-DA) models were constructed with GC/MS and ^{1}H NMR data (Fig. 8.2.1c and d). These models show that only the high dose samples can be discriminated from the rest of the study along the discriminating component t[1]P. Controls, low dose and mid dose samples form a tight cluster on the left hand side of the plot, while high dose samples are located on the right hand side of the plot. The orthogonal component t[2]O does not contain any relevant dose- or time-related information, neither for GC/MS nor for ^{1}H NMR data.

S-plot analysis of the discriminating component [41] of the GC/MS-based OPLS-DA model (Fig. 8.2.1c) found decreased urinary concentrations of 2-oxoglutarate and hippurate and increased concentrations of 5-oxoproline, pseudouridine, gluconate, ribitol, gluconate, hydrocinnamic acid, uric acid, and 3- and 4-hydroxyphenylacetate (Tab. 8.2.2). In concordance with the GC/MS-based model, the ^{1}H NMR OPLS-DA model (Fig. 8.2.1d) found resonances of 2-oxoglutarate, hippurate, citrate and creatinine to be decreased and glucose, *N,N*-dimethylglycine and 4-hydroxyphenylacetate to be increased (Tab. 8.2.3). Additionally both GC/MS and ^{1}H NMR models found various spectral features altered, to which no metabolite could be assigned.

8.3 Discussion

AA toxicity in rats has already been investigated by metabonomics approaches using GC/MS, ^{1}H NMR and LC/MS techniques. One study, which was analyzed with all three analytical methods, only administered a single oral dose of 50 mg/kg bw, which induced weight loss, increased BUN and reduced urinary volume [132; 135]. Observed alterations in urinary metabolite profiles include increased amino acid excretion, alterations in aromatic gutflora-derived metabolites and decreased excretion of Krebs cycle intermediates and various fatty acids and phospholipids. Chan *et al*. used LC/MS to study AA nephrotoxicity after administering oral doses of 2, 10 and 30 mg/kg bw for three consecutive days [133; 134]. Increased urinary volume and decreased body weight gain together with increased hippurate and decreased kynurenate and citrate excretion were observed, as well a two unidentified metabolites increasing with dose [133; 134]. A ^{1}H NMR-based study which investigated AA toxicity in relation to various known kidney toxins used 10 mg/kg bw AA intraperitoneally (i.p.) for 5 consecutive days. Increased urinary *N,N*-dimethylglycine, TMAO, glucose, amino acids and taurine together with decreased creatinine and citrate levels in urine were observed [136].

In our study, the alterations observed in metabolite excretion were mainly a decrease in the urinary excretion of the Krebs cycle intermediates (2-oxoglutarate and citrate) and an alteration of gut microflora derived metabolites (hippurate, 3- and 4-hydroxyphenyl-acetate). Citrate and 2-oxoglutarate excretion is quite variable and alterations in the excretion of Krebs cycle intermediates are observed in almost any metabonomics study [15]. The changes in aromatic gut flora metabolites are also described as common reaction upon administration of toxins and thus are probably not directly related to the AA-induced

kidney injury. The alterations of pseudouridine, 5-oxoproline and uric acid however can be linked to AA kidney toxicity. Pseudouridine substitutes uridine in mRNA and is excreted upon degradation of the mRNA. It is a marker of increased DNA synthesis and thus of cell proliferation [137; 138]. However, this is more probably a reflection of the irritated gastrointestinal tract than of the renal impairment. Necrosis of the mucosa of the forestomache after two days and onset of regenerative hyperplasia after four days was reported for daily oral gavage of 10 mg AA/kg bw [97] and this regeneration, involving cell proliferation and consequently increased mRNA turnover, may be responsible for increased pseudouridine excretion. In our study, no evidence of tubular cell proliferation could be found by histopathological examination.

***Table 8.2.2**: GC/MS mass spectral features and the corresponding putative metabolite IDs found to be significantly altered upon aristolochic acid treatment in urine. Mass fragments and retention time in the GC/MS chromatogram is given. Changes in excretion levels are marked with arrows, (↑) up and (↓) down. Metabolites that could only be assigned speculatively are marked with (?).*

main fragments [m/z]	RT [s]	Change	Identification
292	1084	↑	5-oxoproline 2TMS
74	1115	↓	2-oxoglutarate MO2TMS
164, 179, 252	1123	↑	4-hydroxyphenylacetate 2TMS
217	1222	↑	ribitol 5TMS
177, 192, 205, 310	1232	↑	3-hydroxyphenylacetate 2TMS
179, 192, 310	1255	↑	hydrocynnamic acid 2TMS
77, 105, 206	1315	↓	hippurate 2TMS
333	1380	↑	gluconate 6TMS
441, 442, 457	1486	↑	uric acid 4TMS
217	1621	↑	pseudouridine 5TMS
169, 257, 375	1628	↑	(?)

Increased 5-oxoproline excretion is associated with increased GSH production and thus with oxidative stress [114]. In the γ-glutamyl cycle responsible for GSH production, GSH may act as a feedback-inhibitor for the production of 5-oxoproline [115]. Excessive GSH depletion in the kidney due to oxidative stress may lead to induction of the γ-glutamyl cycle. The consequence is increased 5-oxoproline production, exceeding the capacity of the 5-oxoprolinase, leading to accumulation of 5-oxoproline. Oxoprolinuria in rats is induced by several agents which induce GSH depletion [116; 117]. Oxidative stress was evident in Wistar rats after daily subcutaneous administration of 10 mg AA/kg bw, as reflected by an increase in the urinary excretion of nitric oxide metabolites and a decrease in antioxidative enzyme activity [139]. Increased urinary uric acid excretion is associated with renal failure [140; 141], thus the detection of an increased uric acid excretion in dosed animals with GC/MS may be an early marker of AA-induced renal failure.

Table 8.2.3: *^{1}H NMR spectral bins and the corresponding putative metabolite IDs found to be significantly altered upon aristolochic acid treatment in urine. Changes in excretion levels are marked with arrows, (↑) up and (↓) down. Metabolites that could only be assigned speculatively are marked with (?).*

d [ppm]	Cange	Identification	d [ppm]	Change	Identification
8.68 - 8.72	↑	?	3.92 - 3.96	↓	hippurate
7.80 - 7.84	↓	hippurate	3.48 - 3.52	↑	glucose
7.60 - 7.64	↓	hippurate	2.96 - 3.00	↓	2-oxoglutarate
7.52 - 7.56	↓	hippurate	2.88 - 2.92	↑	N,N-dimethylglycine
7.00 - 7.08	↓	?	2.76 - 2.80	↑	4-hydroxyphenylacetate
6.88 - 6.92	↑	?	2.64 - 2.68	↓	citrate
6.32 - 6.36	↑	?	2.60 - 2.64	↓	citrate
6.24 - 6.28	↓	?	2.40 - 2.44	↓	2-oxoglutarate
3.96 - 4.04	↓	creatinine	2.28 - 2.32		?

A comparison to previous metabonomic studies of AA toxicity has to be carried out carefully, since study design and administered doses are different and not directly comparable. The study of Chen *et al.* [132; 135] revealed alterations of amino acid metabolism and phospholipid handling, which were not evident in our study. However, a very high single dose of 50 mg AA/kg bw was administered, leading to clear signs of renal toxicity in clinical chemistry parameters and histopathology which were not observed in our study. Chan *et al.* did not report any clinical chemistry parameters or histopathology scores. Although their multivariate models separated controls from dosed animals, they only identified decreased citrate and kynurenic acid as well as increased hippurate as markers of AA toxicity, as well as some unidentified mass spectral peaks [133; 134]. Changes in serum and urine clinical chemistry parameters after i.p. administration of 10 mg AA/kg bw were found to be related to increased resonances of lactate, dimethylamine, *N*,*N*-dimethylglycine, TMAO, glucose and hippurate as well as decreased resonances of Krebs cycle intermediates and creatinine [136]. This is generally in concordance with our observations of increased urinary excretion of *N*,*N*-dimethylglycine and decreased excretion of Krebs cycle intermediates and creatinine. The other metabolites observed by Zhang *et al.* probably occur only with the onset of the alterations in clinical chemistry parameters. The alterations in hippurate and other aromatic gut flora metabolites, which are inconsistently up- or down-regulated across all studies, may be explained by a different composition of the microbial gut flora population in different laboratories. Such variations have been described even for different rooms of the same animal house [142].

The AA study demonstrates very well the problems associated with metabonomics studies. In our study, it was not possible to attribute the observed alterations to early onset

of kidney damage since it cannot be excluded that they may arise from the local irritation of the gastrointestinal tract. A way to deal with this problem is i.p. administration, which induces only kidney damage [139; 143]. However, i.p. administration does not follow the normal exposure route by ingestion. Cross study comparison is difficult due to different doses, duration of application and route of administration. Care has to be taken with the postulation of biomarkers: alterations in metabolites found in a single compound study are not necessarily specific for any toxicity or compound, but only discriminate treated animals from controls in the respective study. Mechanistic insight is necessary to evaluate these markers.

The weak response to AA toxicity may be explained with the different toxic potentials of AAI and AAII. AAII was found to be a much more potent renal toxicant in female Wistar rats than AAI after p.o. administration of 10 mg/kg bw of either AA, AAI or AAII [144] Therefore changes in the composition of the natural product AA may have effects on the toxicity of a formulation used in a study. The AA composition in our study was 27 % AAII and 65 % AAI; Mengs and Stolzem used material with a content of 21 % AAII and 77 % AAI [129]. Contrary to the results in rats, a study in mice receiving 2.5 mg/ kg bw AAI or AAII i.p for 9 consecutive days showed that AAI was solely responsible for nephrotoxicity, while both AAI and AAII formed DNA adducts [145].

These findings show that care has to be taken when associating alterations in metabolite profiles with observed toxicity, especially when a mixture of natural products is examined and the mechanism of toxicity is not yet fully elucidated.

9 Furan

9.1 Introduction

Furan is a product of the Maillard reaction that occurs during the heating and browning of foodstuffs [146]. It is found in high concentrations in canned foods [92] and has been shown to be carcinogenic in rodents [91]. The objective of this study, conducted within the 6th Framework Programme of the European Union, was to assess furan toxicity after repeated oral administration of furan at doses close to human exposure. Urine was collected during a 28 day study in which male Fischer F344/N rats were treated with furan at doses of 0, 0.1, 0.5 and 2 mg/kg bw by oral gavage for up to four weeks (five days per week) [98].

9.2 Results and discussion

Treatment with furan had no effect on body weight and no clinical signs of toxicity were evident throughout the study. Routine clinical chemistry analysis of urine and serum of furan treated animals did not reveal any signs of hepatotoxicity, other than a mild, dose-dependent increase in serum cholesterol after 28 days treatment with furan [98], possibly indicating impaired hepatobiliary transport [147]. The liver and kidneys of treated animals were unaltered as compared to controls upon histopathological examination.

Urine analysis was carried out by both GC/MS and ^{1}H NMR, followed by unsupervised and supervised multivariate data analysis, i.e. principal component analysis (PCA) and orthogonal least squares discriminant analysis (OPLS-DA). Visual inspection of GC/MS chromatograms and ^{1}H NMR spectra did not reveal any differences in urine composition of controls versus treated animals (Fig. 9.2.1).

PCA models using pareto-scaled data (Fig. 9.2.2 and 9.2.3) or unit-variance-scaled data (data not shown) of both GC/MS, ^{1}H NMR and LC/MS analysis could not separate controls from treated animals. Likewise, OPLS-DA models constructed with GC/MS and ^{1}H NMR data did not yield any significant components and thus could not discriminate between controls and treated animals (data not shown).

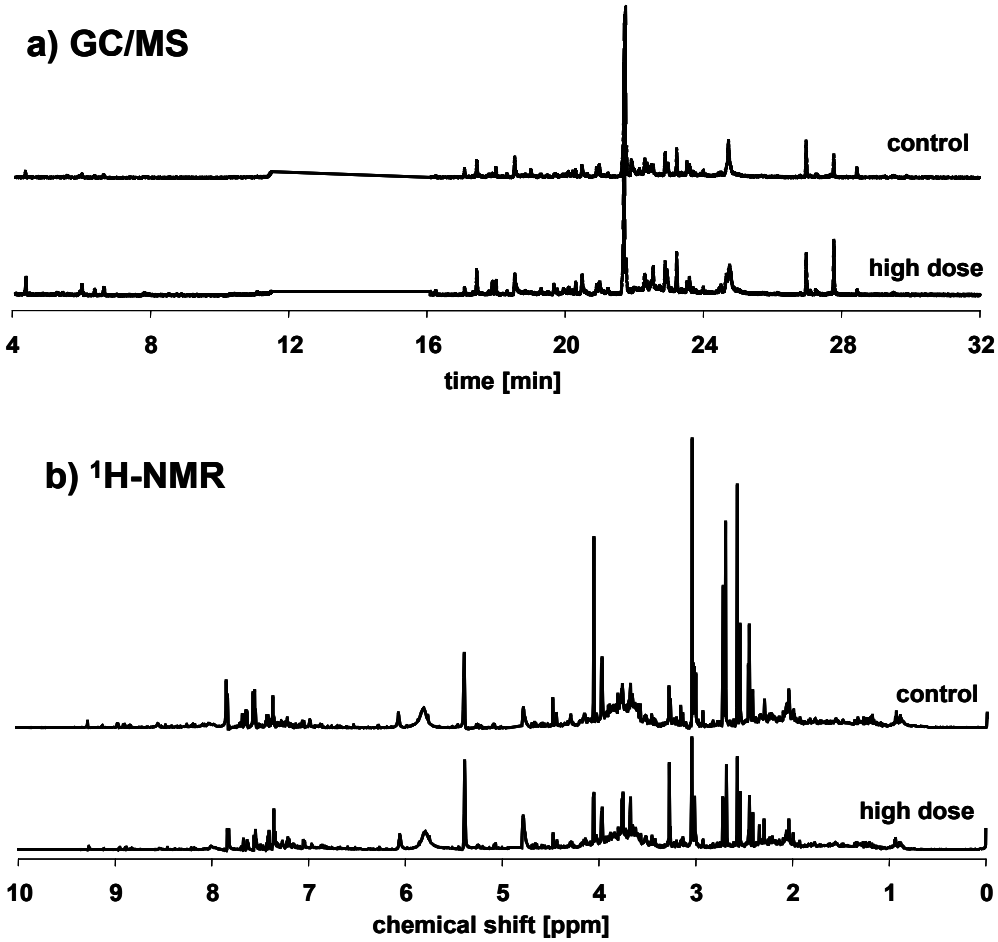

***Figure 9.2.1**: GC/MS chromatograms (a) and ^{1}H NMR spectra (b) of representative control and high dose urine samples collected on day 28 of the furan study. No differences in urinary composition can be observed.*

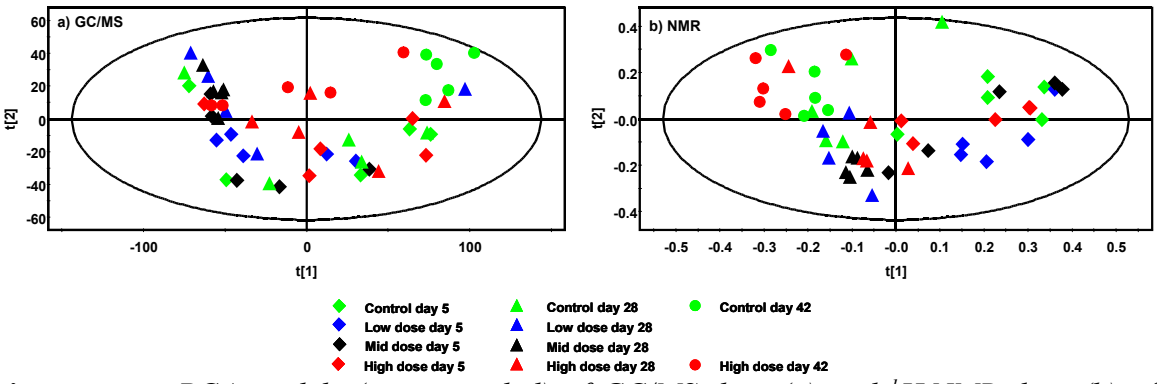

***Figure 9.2.2:** PCA models (pareto-scaled) of GC/MS data (a) and ^{1}H NMR data (b) of urine samples of all time-points and all dose groups did not reveal any differences between controls and treated animals upon furan administration.*

Thus, 28 day treatment with furan did not induce changes in the biochemical composition of urine that are indicative of liver toxicity, consistent with the absence of significant effects on clinical chemistry parameters and histopathology.

The results of the metabonomic analysis show that comprehensive screening methods such as GC/MS or ^{1}H NMR analysis are too limited in sensitivity to detect any minor changes in urinary composition induced by furan treatment in the doses administered in this study. An alteration in hepatobiliary transport after treatment with 2 mg/kg bw furan for 28 days was indicated by a mild, dose-dependent increase in serum cholesterol as well as a small increase in unconjugated bile acids in serum detected by LC/MS analysis [98].

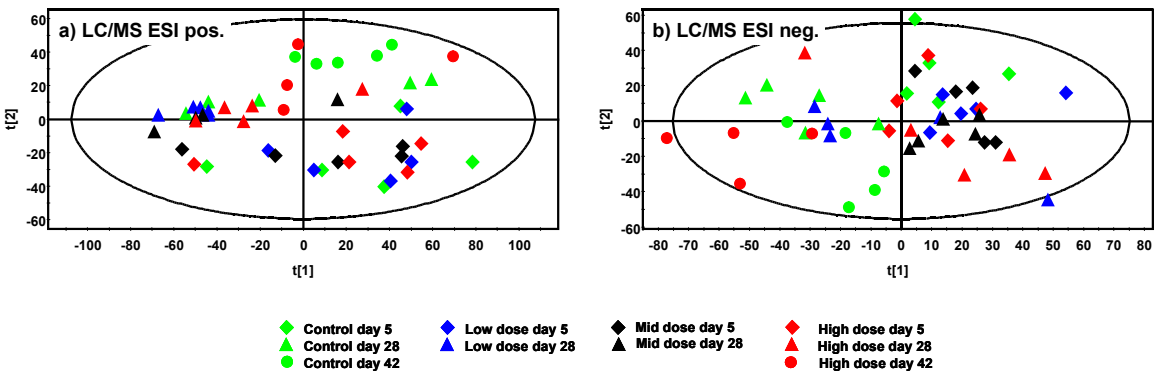

***Figure 9.2.3**: PCA models (pareto-scaled) of LC/MS data using full scan positive (a) or negative (b) electrospray ionization (ESI). Analysis of urine samples of all time points and all dose groups did not reveal any differences between controls and treated animal upon furan administration. Positive ESI only revealed time dependent differences between samples.*

A targeted bile acid screening approach in urine was developed using full scan LC/MS data. A bile acid standard mix was analyzed with the same full scan LC/MS method applied to all urine samples. Mass ratio and retention time of the characteristic ions of the bile acid standards were then manually searched for in the peak lists extracted from the urinary LC/MS chromatograms with the XCMS software. In this way, the data obtained by the full scan LC/MS screening method could be mined for altered bile acid excretion with urine. However, ions with the mass ratio/retention time characteristics of bile acid standards could not be found in the XCMS generated peak lists obtained from urinary LC/MS data of the furan study, thus indicating no alterations in urinary bile acid profile.

10 Innomed PredTox

The InnoMed PredTox project is part of the European Union 6th Framework Programme. It is a joint Industry and European Commission collaboration to improve drug safety. The consortium is composed of 14 pharmaceutical companies, three academic institutions and two technology providers. The project was designed to assess new methods in toxicology such as genomics, proteomics and metabonomics in comparison to the traditional clinical chemistry and histopathology approaches with regard to early detection of toxic lesions and better a predictivity, especially regarding preclinical safety testing of new drug candidates. The work contributed to this project within the scope of this thesis included the following:

- Analysis of urinary ^{1}H NMR data of the studies FP004BA, FP005ME and FP007SE showing bile duct necrosis
- Analysis of the BDN group urine samples with GC/MS
- Quantitation of putative urinary biomarkers of toxicity found by statistical analysis across all studies

The work contributed to the InnoMed PredTox project here is focused on the metabonomic analysis of urine samples with ^{1}H NMR, analyzing the spectral data supplied by the industrial partners. Additionally, in-house GC/MS experiments have been performed. Single study metabonomic analysis was carried out with ^{1}H NMR and GC/MS for the studies FP004BA, FP005ME and FP007SE. These three studies showing bile duct necrosis as common histopathological finding. Furthermore, quantitative ^{1}H NMR analysis was carried out for these studies. A panel of around 20 metabolites included in the Chenomx NMR Suite database has been assigned and quantified.

The 16 studies (14 proprietary compounds + 2 reference compounds) were grouped into three groups according to their histopathology: bile duct necrosis (BDN), hepatocellular cell death (HCD) and hepatocellular hypertrophy (HCH). For confidentiality reasons, structures and indications of the 14 proprietary compounds may not be disclosed, therefore the internal abbreviations are used throughout the text.

In cooperation with Genedata (Genedata, Basel, Switzerland), a cross-study analysis was carried out with urinary ^{1}H NMR data, to extract markers specific for these histopathological endpoints. Two different multivariate statistics models were employed to

obtain a list of ^{1}H NMR bins characteristic for the histopathological endpoints of bile duct necrosis (BDN), hepatocellular cell death (HCD), and hepatocellular hypertrophy (HCH). Requirements for a potential marker of a specific histopathological endpoint were the following: the bins should be altered in all studies showing the respective histopathological endpoint, and they should remain unchanged in the other studies. The cross study analysis required a subtraction of the mean of each bucket of the control group of each study, so that the variable levels of metabolites across the different studies could be leveled out. Subsequently, either a t-test approach corrected for multiple variables or a OPLS-DA model was used for the identification of bins containing putative molecular markers of the respective toxicology. These bins were annotated with the Chenomx NMR Suite and the metabolites identified in the ^{1}H NMR spectra were quantified whenever possible.

10.1 Single study analysis with ^{1}H NMR

10.1.1 FP004BA

Initially, principle component analysis (PCA) was performed on all observations to determine time- and dose-dependent separation of treated animals from untreated controls (Fig. 10.1.1a). While low dose group samples only slightly separated from the controls, day 13 high dose group samples could be completely separated from the controls. The three days high dose samples deviated strongly from the plot and thus required further analysis (see below). In a subsequent PCA analysis, the day 3 high dose samples were removed from the model to obtain a more homogeneous data set for supervised multivariate analysis (Fig. 10.1.1b). No clear separation of control animals from treated animals could be observed in this model, although treated animals, especially the high dose group and at the day 13 time point cluster to the left. To further analyze the high dose day 3 samples, a separate PCA model using only high dose day 3 and high dose day 13 samples was constructed (Fig. 10.1.1c).

To identify altered metabolites in urine samples, an orthogonal partial least squares discriminant analysis (OPLS-DA) model was constructed using control and predose versus low and high dose animals (Fig. 10.1.1d). The score plot shows that the day 3 high dose samples deviate strongly from the rest of the treated animals along the second orthogonal component t[2]O, thus requiring further analysis. To overcome this problem, an OPLS-DA model excluding the outliers (all high dose day 3 samples) was constructed (Fig. 10.1.1e). The model shows a clear dose-dependent separation of controls from treated animal along

the first discriminating component t[1]P with controls and high dose animal on both sides and the low dose animals clustering inbetween. This model was used for marker analysis with the S-plot [41].

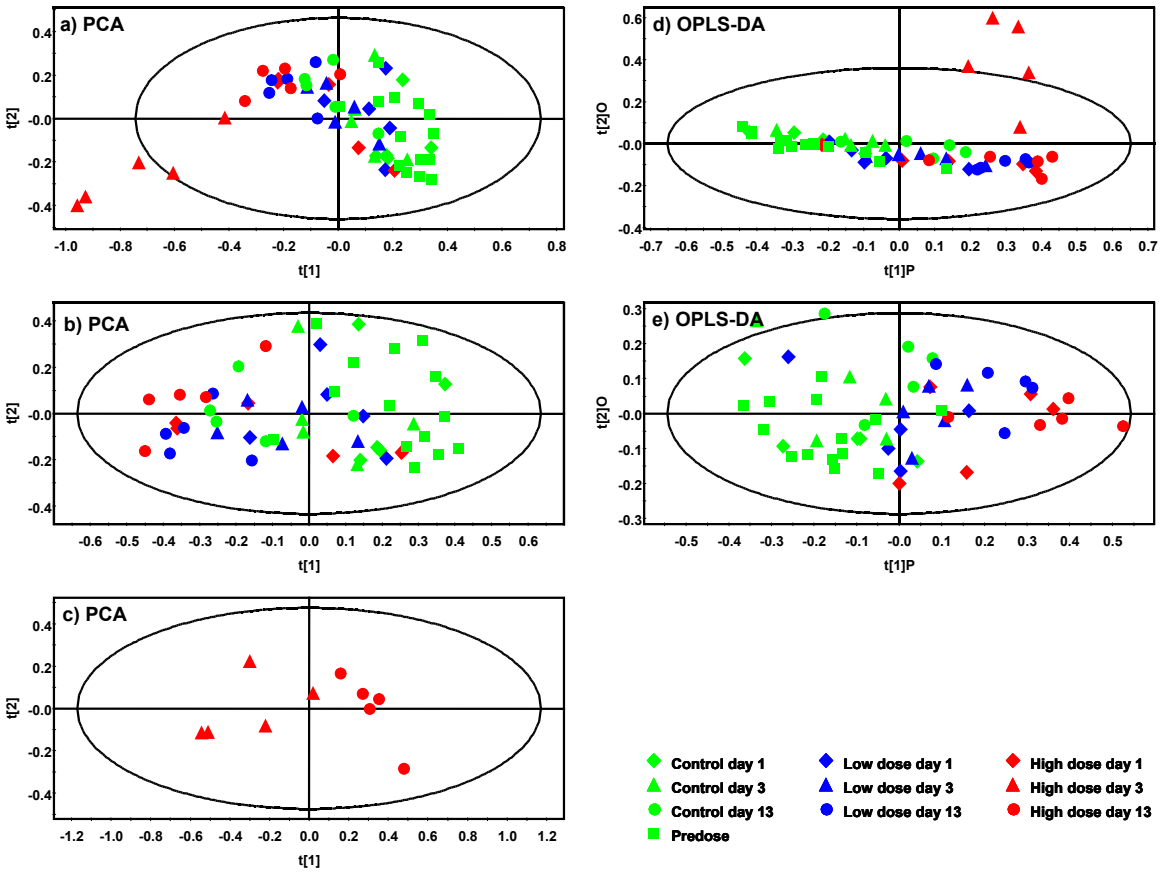

***Figure 10.1.1**: Scores plots of FP004BA ^{1}H NMR data. PCA of all time points (a), showing high dose day 3 samples to differ substantially from the rest. PCA with high dose day 3 samples excluded from the analysis, and PCA of high dose day 3 samples and high dose day 13 samples (c) to find out how they differ from the rest. OPLS-DA of all samples (d) and with high dose day 3 samples excluded (e). Model characteristics are (a) $R^2X(cum) = 0.92$, $Q^2(cum) = 0.73$, 9 significant components; (b) $R^2X(cum) = 0.92$, $Q^2(cum) = 0.72$, 9 significant components; (c) $R^2X(cum) = 0.11$ $Q^2(cum) = 0.63$, 1 significant component; (d) $R^2X(cum) = 0.23$, $R^2Y(cum) = 0.09$ $Q^2(cum) = 0.23$, 1 significant component; (e) $R^2X(cum) = 0.55$, $R^2Y(cum) = 0.50$ $Q^2(cum) = 0.39$, 1 significant component.*

Qualitative S-plot analysis of the OPLS-DA model (Fig. 10.1.1e) revealed a decrease in citrate and 2-oxoglutarate excretion in dosed animals at all time points. Increased excretion of compounds with resonances in the aromatic region of the ^{1}H NMR spectrum (around 7.0 – 8.0 ppm), which may represent drug metabolites, aromatic amino acids or

polyphenol degradation products originating from altered gut microflora, was observed. Furthermore, resonances of CH_2 and CH_3 groups of aliphatic amino acids and short chain fatty acids (around 1.0 – 2.3 ppm) were increased.

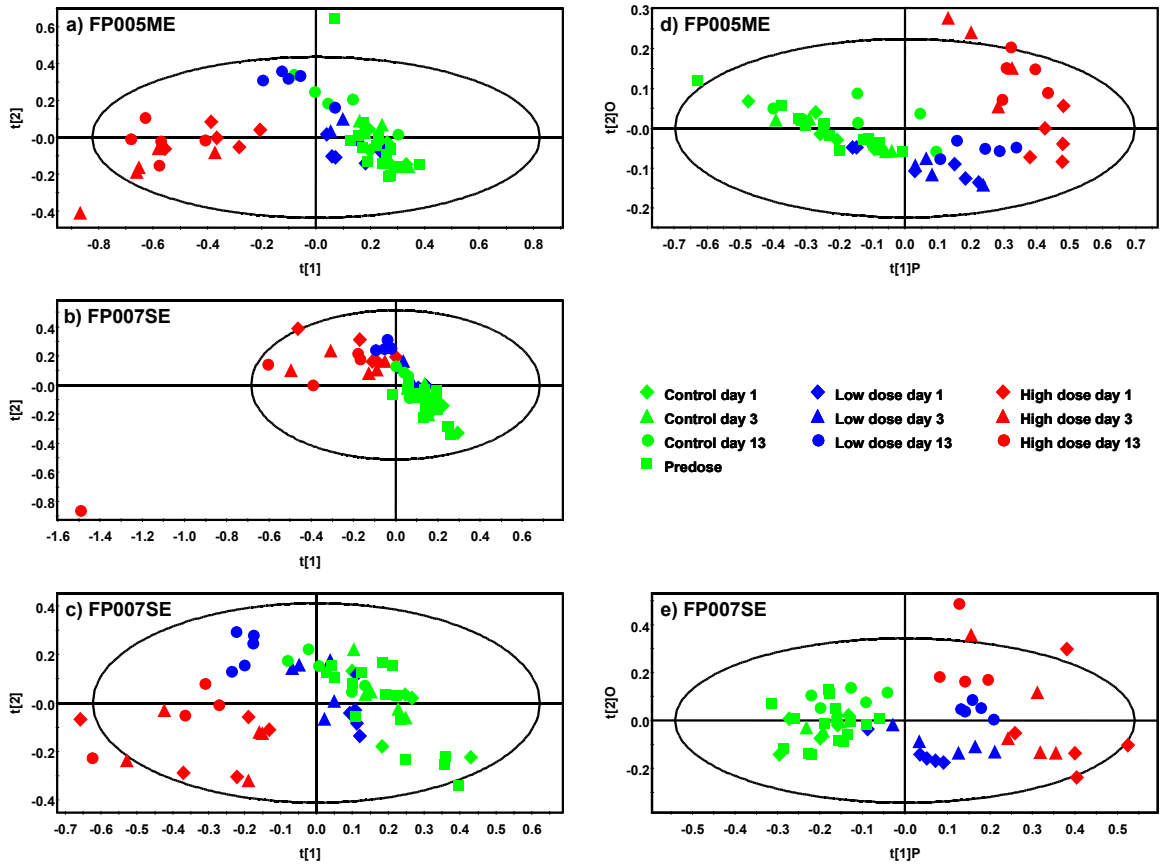

***Figure 10.1.2**: Scores plots of multivariate models of PF005ME and FP007SE ^{1}H NMR data. (a) PCA of FP005ME, all time points. (b) PCA of FP007SE, all time points. The outlier 41-4 showed renal inflammation. (c) PCA of FP007SE, all time points, outlier 41-4 excluded. (d) OPLS-DA of FP005ME, all time points with outliers 43-1 and 45-3 excluded. (e) OPLS-DA of FP007SE, all time points with outlier 41-4 excluded. Model characteristics are (a) $R^2X(cum) = 0.57$, $Q^2(cum) = 0.76$, 2 significant components; (b) $R^2X(cum) = 0.86$, $Q^2(cum) = 0.43$, 8 significant components; (c) $R^2X(cum) = 0.83$ $Q^2(cum) = 0.43$, 8 significant components; (d) $R^2X(cum) = 0.54$, $R^2Y(cum) = 0.61$ $Q^2(cum) = 0.41$, 2 significant components; (e) $R^2X(cum) = 0.41$, $R^2Y(cum) = 0.72$ $Q^2(cum) = 0.66$, 1 + 1 significant components.*

To gain further insight into the effects leading to the differentiation of the high dose day 3 samples as outliers when modeling all samples, a separate OPLS-DA model was constructed comparing only high dose day 3 with high dose day 12 samples (data not shown). Analysis revealed an increase in bile acid and amino acid resonances (0.8 – 2.3 ppm) while citrate, oxoglutarate, betaine, taurine and hippurate excretion

decreased in high dose day 3 samples. The increase in bile acid excretion correlates well with the bile duct necrosis observed with histopathology and was confirmed by a targeted bile acid analysis with LC/MS [148].

Besides these qualitative data, the Chenomx NMR Suite data base with more than 250 endogenous compounds was used to quantify the major urinary metabolites based on integration of ^{1}H NMR signals. Table 10.1.1 summarizes the concentrations of 22 urinary metabolites normalized to urinary creatinine in samples obtained from control, low and high dose animals at all time points. Consistent with the qualitative data analysis, a decrease in urinary concentrations of 2-oxoglutarate and citrate was observed in treated animals on day 1 and day 3, but not on day 12. 4-Hydroxyphenylacetate and phenylacetylglycine (PAG) were increased on day 3 and day 12. Both metabolites may derive from altered gut microflora, although PAG has previously been suggested as a marker of phospholipidosis [65; 149]. Taurine, a putative marker of liver toxicity, was significantly increased in high dose animals on day 12, so was trimethylamine-*N*-oxide (TMAO). Lactate was also increased in high dose animals on day 3 and day 12.

10.1.2 FP005ME

Multivariate data analysis of the urine ^{1}H NMR data of FP005ME shows a clear separation of high dose animals from controls at all time points in the PCA model (Fig. 9.1.2a). While low dose animals on day 1 are indistinguishable from controls, individual low dose day 3 animal start to separate from controls and only on day 12 the complete low dose group clearly separates from controls. In subsequent OPLS-DA, the outliers of the PCA model (one control A43-1 at the top center and one high dose animal A45-4 at the lower left corner) were excluded from the model. In the OPLS-DA model, low dose and high dose animals separated from controls at all time points in a dose-dependent manner along the discriminating component t[1]p (Fig. 10.1.2d). Additionally, a strong contribution to the orthogonal component t[2]O separates the high dose animal from the low dose animals. Inspection of the original ^{1}H NMR spectra revealed that the former were recorded badly and had an extremely high baseline. This may be the reason for this orthogonal contribution, but the bad quality of the spectra did not allow any further investigation.

Qualitative analysis of the alterations with the S-plot [41] revealed a decrease in citrate and 2-oxoglutarate and an increase in the excretion of TMAO, betaine and

creatinine at all time points. An increased excretion of compounds with resonances in the aromatic region (around 7.0 – 8.0 ppm), which may represent drug metabolites, aromatic amino acids or polyphenol degradation products originating from altered gut microflora, was also observed. Resonances that may belong to CH_2 and CH_3 groups of aliphatic amino acids and short chain fatty acids (around 1.3 – 2.3 ppm) were found to be increased as well.

With the spectral database of the Chenomx NMR Suite, 16 major urinary metabolites were quantified in the ^{1}H NMR spectra. Table 10.1.1 summarizes concentrations of 16 urinary metabolites normalized to urinary creatinine in samples obtained from control and low dose animals at all time points and high dose animals on day 12. ^{1}H NMR spectra of high dose animals of day 1 and day 3 could not be quantified as the spectral baseline was extremely high. Consistent with the qualitative data analysis, a decrease in urinary concentrations of the Krebs cycle intermediates 2-oxoglutarate and citrate was observed in treated animals, although these changes were not always statistically significant due to large variability among individual animals. Phenylacetylglycine was significantly increased on day 12. Methylamine, formate, 1-methylnicotinamide and TMAO were significantly increased in high dose animals on day 12. 1-Methylnicotinamide is a metabolite of nicotinamide. It is derived from tryptophan-metabolism, which is responsible for NAD^+ production. An increase was previously observed with PPAR-α agonists [150].

10.1.3 FP007SE

In the PCA model of FP007SE ^{1}H NMR spectra (Fig. 10.1.2b), a separation of high dose animals from controls is visible, but the plot is dominated by an extreme outlier from the high dose day 12 group. In a subsequent PCA, the outlier (A41-4) was removed from the model to obtain a more homogeneous dataset. In this model, a dose-dependent separation of treated animals from controls along the first two principal components is visible, with the high dose animals in the lower left corner of the plot and the controls in the upper right corner with the low dose samples inbetween. (Fig. 10.1.2c). The OPLS-DA model, which was constructed with control and predose animals (control group) versus low and high dose animals (treated group) with the outlier A41-4 excluded, separated controls from treated animals in a dose-dependent manner along the discriminating component t[1]P (Fig. 10.1.2e).

Qualitative S-plot analysis of the OPLS-DA model [41] revealed decreased citrate and 2-oxoglutarate excretion in treated animals and potential changes in the excretion of

TMAO, betaine and creatinine at all time points. Upregulated bins include aromatic regions of the ^{1}H NMR spectrum (around 6 – 8 ppm) which may represent drug metabolites, aromatic amino acids or polyphenol degradation products originating from altered gut microflora, as well as spectral regions containing resonances of CH_2 and CH_3 groups of aliphatic amino acids and short chain fatty acids (around 1.3 – 2.5 ppm).

20 major urinary metabolites were quantified with the spectral database of the Chenomx NMR Suite. Table 10.1.1 summarizes the concentrations of these metabolites normalized to urinary creatinine in samples obtained from control, low and high dose animals at all time points. Consistent with the qualitative data analysis, a decrease in urinary concentrations of 2-oxoglutarate and citrate was observed in treated animals, although these changes were not always statistically significant due to large variability among individual animals. In addition, malonate, which is also a Krebs cycle intermediate, was decreased. 4-Hydroxyphenylacetate and phenylacetylglycine were significantly increased on day 1. Both metabolites may derive from altered gut microflora [67–69; 142], although phenylacetylglycine has previously been suggested as a marker of phospho-lipidosis [65; 149]. Taurine, a putative marker of liver toxicity, was significantly increased in low and high dose animals on day 12. In contrast to the qualitative data analysis, no significant changes in the excretion of TMAO were observed, which may be due to the different normalization methods applied for multivariate (normalized to total integral) and quantitative (normalized to creatinine) analysis. A prominent feature was the highly significant increase of 3-indoxyl sulfate (3-IS) observed on day 1 and day 13 in both dose groups, but not on day 3. 3-IS is formed in the liver from indole, which in turn is produced by the gut microflora as a tryptophan metabolite. It is an uremic toxin and may be associated with the induction of oxidative stress [151].

Separate analysis of the ^{1}H NMR spectrum of the outlier A41 day12, which showed acute renal inflammation grade 4 in histopathological assessment, revealed a strong increase in the excretion of alanine, glycine, lysine, 5-oxoproline, glutamate and creatine, and a decrease in Krebs cycle intermediates.

***Table 10.1.1**: Urinary metabolites [µg/mg creatinine] of the BDN studies FP004BA, FP005ME and FP007SE quantified with the Chenomx NMR Suite. Values are given in mean ± SD, statistically significantly altered (ANOVA + Dunnett's post hoc test) metabolites are marked with * (*, p<0.05; **, p< 0.01; ***, p<0.001).*

			Krebs cycle intermediates									
			Citrate	2-OG[1]	Succinate	Malonate	Glucose	Alanine	Formate	Lactate	1-MNA[2]	3-IS[3]
		C	2.94 ± 0.55	1.91 ± 0.42	0.20 ± 0.05		0.44 ± 0.10	0.05 ± 0.01	0.07 ± 0.02	0.07 ± 0.02	0.007 ± 0.003	0.13 ± 0.05
	day 1	L	2.32 ± 0.43	1.30 ± 0.25	0.21 ± 0.04	n.d.[4]	0.26 ± 0.04*	0.04 ± 0.01	0.07 ± 0.01	0.07 ± 0.01	0.011 ± 0.007	0.12 ± 0.01
		H	1.94 ± 0.50*	0.87 ± 0.67*	0.17 ± 0.06		0.34 ± 0.10	0.06 ± 0.01	0.07 ± 0.01	0.08 ± 0.02	0.009 ± 0.004	0.14 ± 0.03
		C	2.26 ± 0.29	1.47 ± 0.43	0.19 ± 0.02		0.29 ± 0.10	0.05 ± 0.01	0.06 ± 0.01	0.07 ± 0.01	0.005 ± 0.002	0.11 ± 0.02
FP004BA	day 3	L	2.25 ± 0.63	1.19 ± 0.34	0.23 ± 0.07	n.d.	0.31 ± 0.09	0.05 ± 0.01	007 ± 0.03	0.07 ± 0.02	0.011 ± 0.006	0.15 ± 0.05
		H	0.99 ± 0.58**	0.11 ± 0.10***	0.09 ± 0.06*		0.30 ± 0.30	0.06 ± 0.01	0.08 ± 0.02	0.11 ± 0.02***	0.004 ± 0.004	0.11 ± 0.04
		C	1.64 ± 0.16	0.85 ± 0.31	0.14 ± 0.02		0.23 ± 0.06	0.04 ± 0.01	0.05 ± 0.01	0.05 ± 0.01	0.003 ± 0.001	0.11 ± 0.03
	day 14	L	1.28 ± 0.27	0.55 ± 0.11	0.15 ± 0.05	n.d.	0.23 ± 0.05	0.04 ± 0.01	0.07 ± 0.03	0.06 ±0.01	0.007 ± 0.004*	0.11 ± 0.02
		H	1.81 ± 0.31	080 ± 0.21	0.13 ± 0.02		0.26 ± 0.05	0.06 ± 0.02**	0.09 ± 0.02*	0.11 ± 0.02***	0.001 ± 0.003	0.17 ± 0.02**
		C	6.46 ± 0.53	4.12 ± 0.72	0.21 ± 0.04				0.07 ± 0.01		0.02 ± 0.01	0.17 ± 0.04
	day 1	L	5.81 ± 0.56	2.72 ± 0.66	0.18 ± 0.03	n.d.	n.d.	n.d.	0.09 ± 0.02	n.d.	0.03 ± 0.01	0.18 ± 0.05
		H	n.d.	n.d.	n.d.				n.d.		n.d.	n.d.
		C	6.71 ± 0.90	3.88 ± 1.07	0.20 ± 0.03				0.07 ± 0.01		0.01 ± 0.01	0.18 ± 0.05
FP005ME	day 3	L	6.32 ± 0.39	3.01 ± 0.80	0.20 ± 0.02	n.d.	n.d.	n.d.	0.09 ± 0.01*	n.d.	0.03 ± 0.02	0.19 ± 0.03
		H	n.d.	n.d.	n.d.				n.d.		n.d.	n.d.
		C	4.59 ± 0.72	2.94 ± 1.07	0.19 ± 0.05				0.07 ± 0.01		0.01 ± 0.01	0.21 ± 0.05
	day 14	L	4.42 ± 0.27	1.91 ± 0.40	0.20 ± 0.04	n.d.	n.d.	n.d.	0.07 ± 0.01	n.d.	0.03 ± 0.02	0.19 ± 0.05
		H	5.18 ± 1.55	1.18 ± 0.41**	0.22 ± 0.06				0.40 ± 0.32*		0.08 ± 0.04**	0.32 ± 0.04
		C	0.55 ± 0.09	0.39 ± 0.09	0.18 ± 0.03	0.62 ± 0.04	0.11 ± 0.01	0.03 ± 0.01	0.08 ± 0.02	0.02 ± 0.02	0.006 ± 0.006	0.07 ± 0.05
	day 1	L	0.50 ± 0.06	0.31 ± 0.05	0.20 ± 0.07	0.62 ± 0.11	0.11 ± 0.01	0.03 ± 0.01	0.07 ± 0.01	0.04 ± 0.01	0.002 ± 0.001	0.21 ± 0.03***
		H	0.31 ± 0.09***	0.21 ± 0.06**	0.15 ± 0.03	0.37 ± 0.12**	0.06 ± 0.08	0.03 ± 0.01	0.05 ± 0.01*	0.02 ± 0.02	0.002 ± 0.002	0.36 ± 0.03***
		C	1.26 ± 1.80	0.85 ± 1.08	0.37 ± 0.47	1.51 ± 2.08	0.20 ± 0.28	0.06 ± 0.08	0.19 ± 0.27	0.08 ± 0.11	0.007 ± 0.005	0.15 ± 0.02
FP007SE	day 3	L	0.48 ± 0.10	0.31 ± 0.07	0.24 ± 0.10	0.61 ± 0.07	0.08 ± 0.05	0.03 ± 0.01	0.07 ± 0.01	0.04 ± 0.01	0.002 ± 0.001	0.23 ± 0.01
		H	0.35 ± 0.04	0.27 ± 0.06	0.20 ± 0.04	0.29 ± 0.20	0.03 ± 0.04	0.04 ± 0.02	0.05 ± 0.01	0.09 ± 0.08	0.002 ± 0.001	0.34 ± 0.12
		C	0.36 ± 0.05	0.28 ± 0.07	0.11 ± 0.03	0.54 ± 0.04	0.07 ± 0.04	0.02 ± 0.01	0.06 ± 0.01	0.01 ± 0.02	0.005 ± 0.006	0.05 ± 0.02
	day 14	L	0.41 ± 0.05	0.22 ± 0.07	0.17 ± 0.05	0.57 ± 0.09	0.04 ± 0.06	0.03 ± 0.01	0.07 ± 0.01	0.03 ± 0.03	0.001 ± 0.001	0.24 ± 0.02**
		H	0.30 ± 0.10	0.25 ± 0.14	0.10 ± 0.07	0.32 ± 0.19*	0.02 ± 0.04	0.07 ± 0.05*	0.21 ± 0.17*	0.18 ± 0.22	0.001 ± 0.001	0.28 ± 0.11***

[1]2-OG, 2-oxoglutarate; [2]1-MNA, 1-methylnicotinamide; [3]3-IS, 3-indoxylsulfate; [4]n.d., not determined;

***Table 10.1.1 (continued)**: Urinary metabolites [µg/mg creatinine] of the BDN studies FP004BA, FP005ME and FP007SE quantified with the Chenomx NMR Suite. Values are given in mean ± SD, statistically significantly altered (ANOVA + Dunnett's post hoc test) metabolites are marked with * (*, p<0.05; **, p< 0.01; ***, p<0.001).*

			Osmolytes				Gut flora metabolites					
			Betaine	[1]TMAO	Taurine	Trigonelline	[2]4-HPA	Hippurate	[3]PAG	[4]DMG	Methylamine	[5]DMA
		C	0.28 + 0.28	0.12 + 0.02	0.12 + 0.10	0.06 + 0.02	0.07 + 0.01	1.08 + 0.20	0.18 + 0.07	0.12 + 0.07	0.06 + 0.02	0.15 + 0.03
	day 1	L	0.27 + 0.16	0.11 + 0.02	0.11 + 0.13	0.06 + 0.01	0.05 + 0.01	0.91 + 0.08	0.16 + 0.04	0.10 + 0.03	0.06 + 0.01	0.12 + 0.01
		H	0.17 + 0.09	0.13 + 0.03	0.07 + 0.11	0.05 + 0.01	0.06 + 0.01	0.89 + 0.15	0.20 + 0.06	0.10 + 0.04	0.06 + 0.01	0.13 + 0.02
		C	0.28 + 0.20	0.10 + 0.02	0.14 + 0.11	0.06 + 0.01	0.04 + 0.01	0.96 + 0.13	0.09 + 0.02	0.13 + 0.07	0.06 + 0.01	0.13 + 0.02
FP004BA	day 3	L	0.19 + 0.08	0.11 + 0.03	0.12 + 0.05	0.06 + 0.01	0.06 + 0.01**	0.95 + 0.12	0.15 + 0.04*	0.10 + 0.02	0.06 + 0.01	0.13 + 0.02
		H	0.07 + 0.02*	0.13 + 0.06	0.06 + 0.06	0.03 + 0.01**	0.06 + 0.01*	0.66 + 0.20*	0.15 + 0.05	0.07 + 0.02	0.06 + 0.06	0.13 + 0.01
		C	0.17 + 0.12	0.07 + 0.01	0.24 + 0.06	0.05 + 0.01	0.05 + 0.01	0.80 + 0.08	0.12 + 0.03	0.08 + 0.04	0.05 + 0.01	0.10 + 0.01
	day 14	L	0.11 + 0.04	0.06 + 0.01	0.37 + 0.10	0.04 + 0.01	0.04 + 0.01	0.67 + 0.10	0.14 + 0.04	0.06 + 0.01	0.04 + 0.01	0.09 + 0.02
		H	0.28 + 0.11	0.15 + 0.03***	0.44 + 0.15*	0.05 + 0.01	0.07 + 0.01**	0.94 + 0.14	0.24 + 0.06**	0.13 + 0.04*	0.07 + 0.02*	0.12 + 0.01*
		C	0.10 + 0.08	0.17 + 0.06	1.14 + 0.22	0.10 + 0.01	n.q.[6]	1.56 + 0.22	0.20 + 0.03	0.06 + 0.02	0.05 + 0.02	0.11 + 0.02
	day 1	L	0.14 + 0.10	0.18 + 0.02	1.31 + 0.40	0.10 + 0.01	0.11 + 0.01	1.56 + 0.25	0.23 + 0.03	0.11 + 0.03	0.05 + 0.01	0.14 + 0.04
		H	n.d.[7]	n.d.	n.d.	n.d.	n.d.	n.d.	n.d.	n.d.	n.d.	n.d.
		C	0.11 + 0.06	0.19 + 0.06	1.31 + 0.22	0.10 + 0.01	n.q.	1.80 + 0.10	0.18 + 0.03	0.08 + 0.04	0.05 + 0.02	0.14 + 0.03
FP005ME	day 3	L	0.20 + 0.16	0.18 + 0.03	1.37 + 0.25	0.10 + 0.02	0.10 + 0.01	1.60 + 0.17	0.21 + 0.03	0.12 + 0.04	0.04 + 0.02	0.14 + 0.02
		H	n.d.	n.d.	n.d.	n.d.	n.d.	n.d.	n.d.	n.d.	n.d.	n.d.
		C	0.11 + 0.06	0.18 + 0.04	1.12 + 0.27	0.08 + 0.01	0.13 + 0.02	1.35 + 0.12	0.27 + 0.10	0.07 + 0.03	0.07 + 0.02	0.12 + 0.03
	day 14	L	0.18 + 0.12	0.18 + 0.05	1.15 + 0.23	0.09 + 0.01	0.14 + 0.07	1.06 + 0.52	0.20 + 0.02	0.11 + 0.03	0.05 + 0.01	0.12 + 0.01
		H	0.74 + 0.78	0.37 + 0.11**	1.36 + 0.30	0.09 + 0.01	0.17 + 0.04	0.98 + 0.47	0.41 + 0.03*	0.10 + 0.01	0.27 + 0.09***	0.15 + 0.03
		C	0.26 + 0.08	0.18 + 0.02	1.10 + 0.18	0.08 + 0.01	0.14 + 0.04	0.60 + 0.22	0.14 + 0.03	0.17 + 0.03	0.07 + 0.02	0.07 + 0.07
	day 1	L	0.21 + 0.15	0.15 + 0.01	1.23 + 0.16	0.07 + 0.01	0.14 + 0.05	0.61 + 0.22	0.32 + 0.04**	0.14 + 0.04	0.07 + 0.01	0.11 + 0.06
		H	0.13 + 0.12	0.14+ 0.05	1.39 + 0.28	0.04 + 0.03**	0.25 + 0.04**	0.44 + 0.21	0.62 + 0.09***	0.07 + 0.03**	0.09 + 0.03	0.09 + 0.05
		C	0.46 + 0.49	0.31 + 0.32	3.38 + 4.84	0.21 + 0.29	0.39 + 0.59	1.09 + 1.41	0.30 + 0.41	0.41 + 0.55	0.15 + 0.20	0.25 + 0.39
FP007SE	day 3	L	0.18 + 0.14	0.15 + 0.03	1.45 + 0.18	0.07 + 0.01	0.17 + 0.08	0.42 + 0.24	0.32 + 0.02	0.12 + 0.05	0.10 + 0.02	0.12 + 0.02
		H	0.11 + 0.11	0.11 + 0.07	2.45 + 1.46	0.05 + 0.02	0.21 + 0.08	0.20 + 0.12	0.35 + 0.12	0.07 + 0.02	0.10 + 0.04	0.06 + 0.05
		C	0.16 + 0.04	0.12 + 0.03	1.12 + 0.05	0.07 + 0.01	0.10 + 0.03	0.54 + 0.20	0.12 + 0.01	0.10 + 0.02	0.06 + 0.02	0.08 + 0.03
	day 14	L	0.13 + 0.06	0.15 + 0.02	1.25 + 0.39	0.07 + 0.01	0.18 + 0.03*	0.36 + 0.11	0.32 + 0.09**	0.07 + 0.02	0.10 + 0.01	0.10 + 0.03
		H	0.19 + 0.06	0.21 + 0.21	3.01 + 1.41**	0.04 + 0.03	0.17 + 0.07	0.31 + 0.19	0.27 + 0.10*	0.07 + 0.01	0.18 + 0.09**	0.11 +0.03

[1]TMAO, trimethylamine-N-oxide; [2]4-HPA, 4-hydroxyphenylacetate; [3]PAG, phenylacetylglycine; [4]DMG, N,N-dimethylglycine; [5]DMA, dimethylamine; [6]n.q., not quantifyable; [7]n.d., not determined

10.2 Single Study analysis with GC/MS

10.2.1 FP004BA

The PCA model of all animals at all time points showed a separation of day 3 and day 12 high dose samples from controls (Fig. 10.2.1a). Especially the day 3 high dose samples were distinctly separated from the rest of the plot. A subsequent OPLS-DA analysis showed a separation of controls from dosed animal along the discriminating component t[1]p, but low dose samples separated from high dose samples along the orthogonal component t[2]O (Fig. 10.2.1d). S-plot analysis [41] revealed mainly a decrease in urinary citrate and 2-oxoglutarate to be responsible for the separation of treated animals from controls. Additionally, minor increases in short-chained alkylamines (propylamine, *n*-butylamine, putrescine), gluconic acid and *myo*-inositol could be observed as well.

10.2.2 FP005ME

The PCA model of all animals at all time points clearly separated high dose samples from controls along the first two PCs, with the low dose samples situated inbetween (Fig. 10.2.1b). The subsequent OPLS-DA separated controls from treated animals in a dose-dependent manner, with the controls and high dose samples on both sides of the scores plot and the low dose samples situated inbetween (Fig. 10.2.1e). S-plot analysis [41] revealed the urinary excretion of the Krebs cycle intermediates citrate, 2-oxoglutatate and malic acid to be decreased while concentrations of short-chained alkylamines (propylamine, *n*-butylamine), 5-hydroxyindole, hippurate and gluconic acid were increased.

10.2.3 FP007SE

The PCA model partially separated controls from dosed animals, but the model contained a large variance, presumably introduced by sample work-up and derivatization necessary for GC/MS analysis (Fig. 10.2.1.c). The OPLS-DA model separates controls from treated animals, and a trend to a dose-dependent separation is visible (in general, the high dose samples are situated more to the right side of the plot than the low dose samples), however, the plot is still dominated by a large variance not reflecting any dose- or time-dependent trends (Fig. 10.2.1f). S-plot analysis [41] revealed the separation to be driven by a decrease in urinary citrate and 2-oxoglutarate in dosed animals. Further

analysis after removal of citrate and 2-oxoglutarate signals from the model revealed a decrease in malic acid and *cis*-aconitate, which are both Krebs cycle intermediates, and gluconic acid, as well as an increase in the excretion of 5-hydroxyindole and 4-hydroxyphenylacetate.

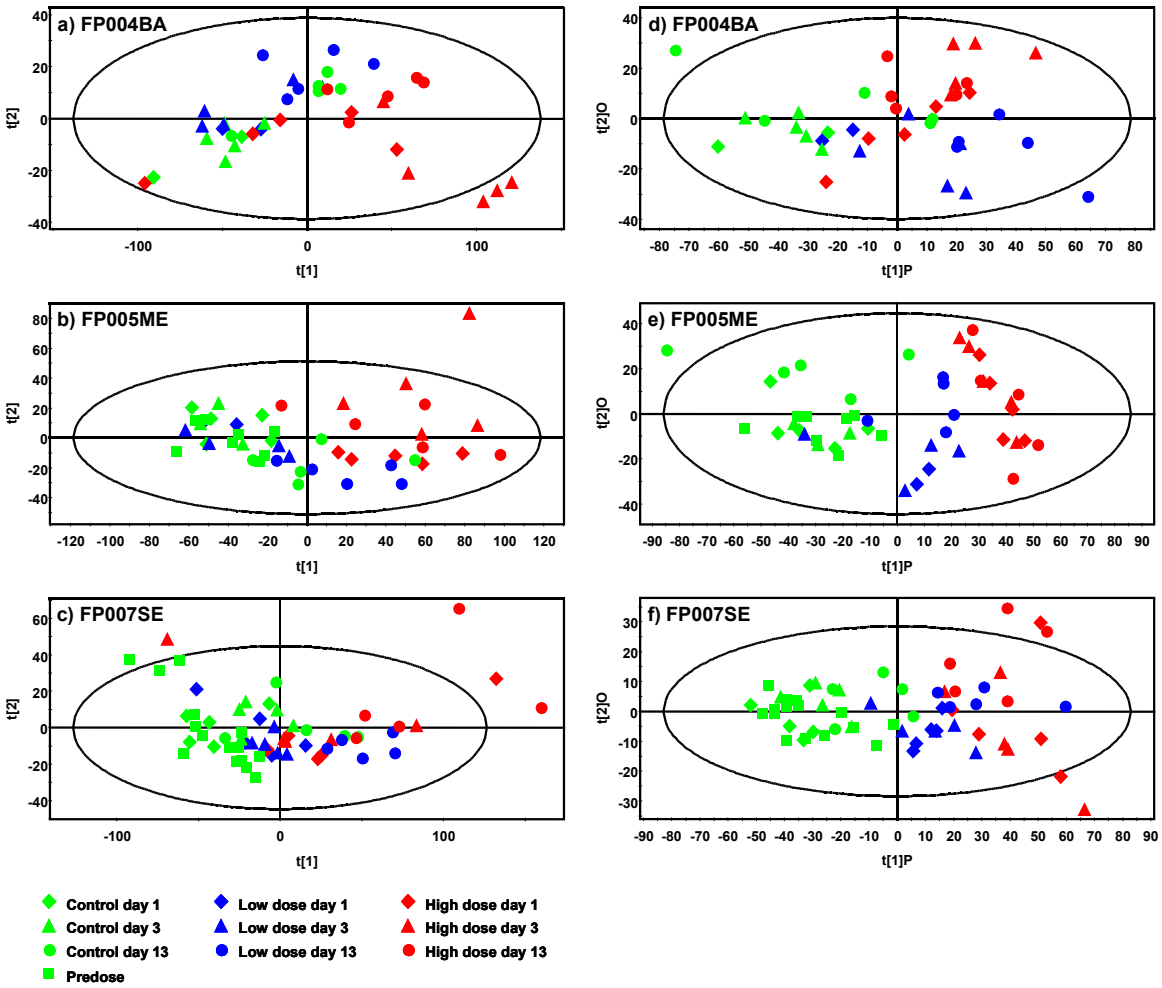

Figure 10.2.1*: Scores plots of multivariate models of FP004BA, FP005ME and FP007SE GC/MS data. (a) PCA of FP004BA, all time points. (b) PCA of FP005ME, all time points. (c) PCA of FP007SE, all time points. (d) OPLS-DA of FP004BA, all time points. (e) OPLS-DA of FP005ME, all time points. (f) OPLS-DA of FP007SE, all time points. Model characteristics are (a) $R^2X(cum) = 0.84$, $Q^2(cum) = 0.69$, 3 significant components; (b) $R^2X(cum) = 0.85$, $Q^2(cum) = 0.43$, 6 significant components; (c) $R^2X(cum) = 0.94$ $Q^2(cum) = 0.80$, 8 significant components; (d) $R^2X(cum) = 0.77$, $R^2Y(cum) = 0.46$ $Q^2(cum) = 0.04$, 1 significant component; (e) $R^2X(cum) = 0.64$, $R^2Y(cum) = 0.68$ $Q^2(cum) = 0.54$, 1 + 1 significant components; (e) $R^2X(cum) = 0.80$, $R^2Y(cum) = 0.73$ $Q^2(cum) = 0.65$, 1 + 2 significant components.*

Separate analysis of the high dose day 13 sample A41-4 showing strong renal inflammation revealed a strong increase in urinary concentrations of 5-oxoproline, glutamine, glycine, and creatine as compared to controls.

10.3 Comparison of ^{1}H NMR and GC/MS metabonomics for single study analysis

GC/MS metabonomics is able to discriminate treated animals from controls in the same manner as ^{1}H NMR metabonomics. While ^{1}H NMR is a fast and efficient screening method for a quick overlook of data structure, it is however limited to a maximum of around 40 quantifiable metabolites. Even though GC/MS requires more extensive sample work-up, it is however more sensitive and allows the analysis of a wider range of metabolites. Further maturation of the technology, i.e. the combination of automated sample preparation with GC/TOF-MS has great potential for metabonomics applications [29].

Table 10.3.1*: Comparison of urinary metabolites found to be changed upon treatment with multivariate analysis of ^{1}H NMR and GC/MS data.↑ indicates increased, ↓ indicates decreased excretion as compared to controls.*

	^{1}H NMR			GC/MS		
	FP004BA	**FP005ME**	**FP007SE**	**FP004BA**	**FP005ME**	**FP007SE**
3-indoxylsulfate	↑	--	↑	--	--	--
4-hydroxyphenylacetate	↑	--	--	--	↑	↑
5-hydroxyindole	--	--	--	↑	↑	↑
betaine	--	--	↓	--	--	--
butylamine	--	--	--	↑	↑	↑
cis-aconitate	--	--	--	--	--	↓
citrate	↓	‾	↓	↓	↓	↓
creatinine	↑	--	--	↑	--	--
gluconic acid	--	--	--	↑	↑	↑
glucose	↑	↑	--	--	--	--
hippurate	↓	↓	↓	--	↓	--
lactate	↑	--	--	--	--	--
malic acid	--	--	--	--	↓	‾
methylamine	--	↑	--	--	--	--
oxoglutarate	↓	↓	↓	↓	↓	↓
phenylacetylglycine	↑	↑	↑	--	--	--
propylamine	--	--	--	↑	↑	↑
taurine	↑	↑	--	--	--	--
TMAO[1]	↑	↑	--	--	--	--

[1]TMAO, trimethylamine-*N*-oxide

Single study metabonomic analysis of three compounds inducing bile duct necrosis (FP004BA, FP005ME, FP007SE, BDN group) revealed as main discriminating factor a decrease of the Krebs cycle intermediates citrate and 2-oxoglutarate. Furthermore, alterations in the excretion of aromatic metabolites probably originating from dietary polyphenols degraded by the gut flora, as well as some other "usual suspects" [15] were observed. These alterations could discriminate between treated animals and controls, however they are found in most toxicity-related metabonomics studies. Therefore, they cannot be used as site- or mechanism-specific biomarkers. However, they appear useful as

general indicators of toxicity. To obtain a quick overview over the urinary profiles, ^{1}H NMR and GC/MS are equally well suited.

One problem with single study analysis is that compound metabolites present in urine may strongly bias the results by contributing to group separation. This is especially the case for novel compounds, where metabolism is not fully elucidated. Besides, effects related to the pharmacological action of a compound or to adaptive processes can be distinguished from toxicity-related effects only with difficulty. For biomarker discovery, therefore, a cross study analysis has to be performed, and only those alterations occurring across all studies with the same toxicity should be considered. Moreover, the classification of the samples should be phenotypically anchored. Groups should not be classified by "dose" and "control" but rather by "toxic lesion" and "no toxicity" as observed by the reference procedure histopathology.

10.4 Cross study analysis with ^{1}H NMR

One problem in single study analyses is the fact that the models differentiate between treated and control animals in the respective study but may not necessarily be generally predictive for the toxicity observed. To eliminate these problems of single study analyses, a multivariate analysis across several studies showing the same histopathological endpoint was applied. This cross study analysis was carried out by two different multivariate statistical approaches, leading to two lists of ^{1}H NMR buckets containing potential markers for the respective toxicity endpoint. The identified bins had to be specific for the respective toxicological endpoint, i.e they should be significantly altered only in the urine of those animals showing the respective toxicity, but not in the others.

Three liver pathology groups were defined and studies showing the respective pathology were assigned to these groups: Bile duct necrosis, hepatocellular cell death and hepatocellular hypertrophy. Bile duct necrosis (BDN, FP004BA, FP005ME, FP007SE) was characterized phenotypically by apoptosis or necrosis of bile duct epithelial cells, inflammation, fibrosis and cholestasis. Hepatocellular cell death (HCD, FP004BA, FP014SC, FP015NN) was characterized by increased liver enzyme activity (AST, ALT), inflammation, apoptosis or necrosis of hepatocytes. Hepatocellular hypertrophy (HCH, FP001RO, FP003SE, FP0008AL, FP010SG, FP011OR, FP016LY) was characterized phenotypically by an increased liver weight and microscopically observable hypertrophic hepatocytes. Mechanistically, hepatocyte hypertrophy origins from an extensive

proliferation of the smooth endoplasmatic reticulum due to the induction of xenobiotic metabolizing enzymes and peroxisome proliferation. These findings were also confirmed by transcriptomics data.

One approach used a t-test corrected for non-independent variables on the data of each pathology group (Genedata), and then selected the "ten best variables" which had the lowest p-value and were only significantly altered in one histopathology group and not in the other groups. The second approach used the shared and unique structure (SUS)-plot for OPLS-DA [41]. This approach requires separate OPLS-DA models for each toxicity group to begin with. Then, the correlations p(corr) of the predictive component t[1]p of each model are plotted against each other. Variables that are either positively or negatively correlated appear in the corners of the plot, while those variables associated uniquely with the discrimination of one model are situated along the axes of the plot [41].

Table 10.4.1*: Variables and putative markers specifically altered in the ^{1}H NMR spectra of the bile duct necrosis (BDN) group. Altered bins were identified either by SIMCA analysis or by t-test corrected for non-independent variables. Changes in excretion levels are marked with arrows, (↑) up and (↓) down as compared to controls. Metabolites that could only be assigned speculatively are marked with (?).*

BDN	Variable ID bin [ppm]	Metabolite ID	Change	p-value (t-test)	Ratio of Medians
SIMCA model	7.84	Hippurate	↓	1.17×10^{-3}	n.a.[1]
	7.72	3-Indoxylsulfate	↑	2.27×10^{-8}	6.48
	7.66	Hippurate	↓	1.27×10^{-9}	n.a.
	7.38	Phenylacetylglycine	↑	2.83×10^{-8}	7.60
	7.37	Phenylacetylglycine	↑	3.25×10^{-7}	5.36
	7.36	Phenylacetylglycine	↑	3.62×10^{-9}	6.16
	7.18	4-Hydroxyphenylacetate	↑	5.72×10^{-11}	3.80
	7.17	4-Hydroxyphenylacetate	↑	3.03×10^{-8}	7.40
	3.69	Phenylacetylglycine	↑	1.39×10^{-9}	3.79
	3.68	Phenylacetylglycine	↑	5.90×10^{-4}	3.85
	2.94	N,N-Dimethylglycine	↓	5.33×10^{-9}	n.a.
	2.14	Bile acid(s) (?)	↑	4.49×10^{-10}	6.01
Best ten (T-test)	8.85	Trigonelline	↓	6.44×10^{-10}	n.a.
	7.43	Phenylacetylglycine	↑	6.23×10^{-10}	7.08
	7.42	Phenylacetylglycine	↑	7.88×10^{-10}	5.94
	7.29	3-Indoxylsulfate	↑	4.57×10^{-10}	3.42
	7.18	4-Hydroxyphenylacetate	↑	5.72×10^{-11}	3.80
	3.99	Hippurate	↓	3.66×10^{-10}	n.a.
	2.79	5-Aminolevulinate (?)	↓	3.57×10^{-12}	n.a.
	2.77	5-Aminolevulinate (?)	↓	7.40×10^{-10}	n.a.
	2.55	Citrate	↓	2.05×10^{-10}	n.a.
	2.49	5-Aminolevulinate (?)	↓	1.42×10^{-12}	n.a.

[1]n.a., not applicable

Both approaches resulted in two sets of ^{1}H NMR buckets for bile duct necrosis (Tab. 10.4.1), hepatocellular hypertrophy (Tab. 10.4.2) and hepatocellular cell death (Tab. 10.4.3). These buckets were then assigned with the spectral database of the Chenomx

NMR Suite. While for most buckets, the corresponding metabolites could be quantified, for some, the corresponding metabolite could only be assigned speculatively by the concordant chemical shifts of the resonances of the compound.

Although there was virtually no overlap between the buckets identified by the different statistical analyses, the compounds identified in these bins overlapped substantially. For example, hippurate was found by both multivariate approaches as putative marker of bile duct necrosis, but the aromatic resonances of hippurate were found only with the SUS-plot analysis and the resonance at 3.99 ppm only with the t-test approach (Tab. 10.4.1). This can probably be attributed to the arbitrarily set cut-off values for bucket selection, were minor changes in rank cause the buckets to be included in the analysis or not.

***Table 10.4.2**: Variables and putative markers specifically altered in the ^{1}H NMR spectra of the hepatocellular hypertrophy (HCH) group. Altered bins were identified with SIMCA analysis and t-test corrected for non-independent variables. Changes in excretion levels are marked with arrows, (↑) up and (↓) down as compared to controls. Metabolites that could only be assigned speculatively are marked with (?).*

HCH	Variable ID bin [ppm]	Metabolite ID	Change	p-value (t-test)	Ratio of Medians
SIMCA model	7.37	Phenylacetylglycine	↑	2.59×10^{-02}	3.72
	7.36	Phenylacetylglycine	↑	6.66×10^{-08}	4.55
	4.15	Proline (?), Gluconate (?)	↑	8.87×10^{-18}	17.03
	3.94	Creatine	↑	4.73×10^{-03}	2.77
	3.89	Glucose, Glycocholate	↑	2.04×10^{-07}	3.48
	3.78	Glucose, Alanine	↑	5.31×10^{-09}	4.41
	3.77	Glucose, Glycocholate, Phenylacetylglycine	↑	5.63×10^{-14}	6.08
	3.76	Glucose, Alanine	↑	1.13×10^{-29}	9.42
	3.75	Glucose, Glycocholate, Phenylacetylglycine	↑	1.33×10^{-26}	9.97
	3.74	Glucose, Glycocholate, Phenylacetylglycine	↑	6.25×10^{-26}	7.84
	3.73	Glucose, Glycocholate, Phenylacetylglycine	↑	2.05×10^{-23}	3.02
	3.72	Glucose, Glycocholate	↑	3.21×10^{-07}	8.74
	3.71	Glucose, N,N-dimethylglycine	↑	7.43×10^{-07}	3.87
	3.7	Sucrose (?)	↑	1.46×10^{-06}	3.32
	3.69	Glucose	↑	1.19×10^{-07}	4.57
	3.68	Phenylacetylglycine	↑	5.96×10^{-11}	6.05
	3.67	Phenylacetylglycine	↑	2.08×10^{-26}	6.02
	3.66	Phenylacetylglycine	↑	1.57×10^{-24}	8.60
	3.65	Isoleucine (?), myo-Inositol (?), Valine (?)	↑	2.05×10^{-23}	11.91
	3.64	Isoleucine (?), myo-Inositol (?), Valine (?)	↑	2.72×10^{-19}	4.81
	3.05	Creatinine, Creatine	↑	5.70×10^{-02}	1.07
Best ten T-test	3.76	Phenylacetylglycine	↑	1.13×10^{-29}	9.42
	3.75	Phenylacetylglycine, Glucose	↑	1.33×10^{-26}	9.97
	3.74	Glucose (?)	↑	6.25×10^{-26}	7.84
	3.67	Phenylacetylglycine	↑	2.08×10^{-26}	6.02
	3.66	Isoleucine (?), myo-Inositol (?), Valine (?)	↑	1.57×10^{-24}	8.60
	3.65	Isoleucine (?), myo-Inositol (?), Valine (?)	↑	2.05×10^{-23}	11.91
	3.64	Isoleucine (?), myo-Inositol (?), Valine (?)	↑	2.72×10^{-19}	4.81
	2.69	Citrate	↓	1.82×10^{-20}	n.a.[1]
	2.55	Citrate	↓	9.83×10^{-19}	n.a.
	1.83	Cholate, Glycocholate, 4-Hydroxybutyrate (?) Glutarate (?)	↓	1.56×10^{-19}	n.a.

[1]n.a., not applicable

Quantified metabolite data is summarized in tables for the bile duct necrosis, hepatocellular hypertrophy and hepatocellular cell death groups (Tabs. 10.4.4, 10.4.5 and 10.4.6 respectively). Lack of time and human resources did not allow the complete quantification of all putative metabolite markers across all studies with all dose levels and time points. Instead, for the bile duct necrosis group, the seven putative metabolite markers were quantified for all studies at the 13 day timepoint to assure that the concentration of these metabolites was only changed in those studies showing bile duct necrosis but not in the others. For the hepatocellular hypertrophy and hepatocellular cell death groups, only control and high dose samples of the respective studies were quantified at the time point showing the greatest effect in histopathology.

***Table 10.4.3**: Variables and putative markers specifically altered in the ^{1}H NMR spectra of the hepatocellular cell death (HCD) group. Altered bins were identified with SIMCA analysis and t-test corrected for non-independent variables. Changes in excretion levels are marked with arrows, (↑) up and (↓) down as compared to controls. Metabolites that could only be assigned speculatively are marked with (?).*

HCD	Variable ID bin [ppm]	Metabolite ID	Change	p-value (t-test)	Ratio of Medians
SIMCA model	3.82	?	↑	3.110×10^{-03}	1.21
	2.44	2-Oxoglutarate	↓	2.710×10^{-03}	1.09
	2.20	?	↑	4.850×10^{-02}	3.71
	1.57	?	↑	1.147×10^{-03}	2.90
	1.56	?	↑	1.850×10^{-04}	3.72
	1.55	?	↑	2.995×10^{-05}	3.74
Best ten T-test	8.84	Trigonelline	↑	1.87849×10^{-06}	2.35
	7.93	?	↑	2.60195×10^{-05}	6.70
	3.69	Phenylacetylglycine	↑	3.08136×10^{-05}	4.29
	2.69	Citrate	↑	1.12342×10^{-05}	1.20
	2.55	Citrate	↑	7.39211×10^{-06}	1.02
	1.55	?	↑	2.99521×10^{-05}	3.74
	1.54	?	↑	1.80665×10^{-05}	2.79
	1.38	?	↑	1.2518×10^{-05}	5.21
	0.45	?	↓	2.38169×10^{-05}	1/2.63
	0.44	?	↑	2.14593×10^{-05}	1.12

For further testing of the identified markers, PCA models were constructed for each histopathology endpoint using the quantified metabolite concentrations as variables (Fig. 10.4.1). Although the levels of the metabolite concentrations in urine varies strongly between the control groups in individual studies, control and high does animals of individual studies can be discriminated with multivariate models on the basis of the selected putative markers.

***Table 10.4.4**: All bile duct necrosis (BDN) markers were quantified in the original [1]H NMR spectra of the day 13 urine samples, using the Chenomx NMR Suite. Values are given as mean ± SD in mM/mM creatinine, statistically significantly altered (ANOVA + Dunnett's post hoc test) metabolites are marked with * (*, p<0.05; **, p< 0.01; ***, p<0.001). Studies showing BDN findings are marked in yellow.*

		3-IS[1]	4-HPA[2]	Citrate	Hippurate	DMG[3]	PAG[4]	Trigonelline
FP001RO	C	0.15 ± 0.07	0.11 ± 0.05	4.06 ± 0.79	1.08 ± 0.53	0.11 ± 0.06	0.16 ± 0.05	0.07 ± 0.01
	L	0.22 ± 0.07	0.11 ± 0.01	4.61 ± 0.66	1.39 ± 0.24	0.07 ± 0.03	0.21 ± 0.06	0.08 ± 0.01
	H	0.22 ± 0.09	0.13 ± 0.04	4.33 ± 1.10	1.13 ± 0.80	0.03 ± 0.03*	0.29 ± 0.15	0.07 ± 0.02
FP002BI	C	0.30 ± 0.06	0.11 ± 0.02	2.27 ± 0.75	1.14 ± 0.25	0.11 ± 0.02	0.49 ± 0.12	0.10 ± 0.02
	L	0.25 ± 0.05	0.10 ± 0.01	3.06 ± 0.76	1.32 ± 0.14	0.14 ± 0.04	0.27 ± 0.18	0.11 ± 0.02
	H	0.24 ± 0.17	0.10 ± 0.01	2.80 ± 0.81	0.86 ± 0.16	0.13 ± 0.02	0.46 ± 0.15	0.08 ± 0.01
FP003SE	C	0.07 ± 0.02	0.08 ± 0.02	3.96 ± 0.71	1.01 ± 0.06	0.11 ± 0.03	0.19 ± 0.03	0.09 ± 0.01
	L	0.17 ± 0.01	0.11 ± 0.03	4.46 ± 1.20	1.00 ± 0.34	0.16 ± 0.03	0.36 ± 0.06	0.09 ± 0.01
	H	0.24 ± 0.13*	0.11 ± 0.02	4.48 ± 1.29	1.10 ± 0.19	0.17 ± 0.03*	0.55 ± 0.26**	0.09 ± 0.01
FP004BA day 03	C	0.11 ± 0.02	0.04 ± 0.01	2.26 ± 0.29	0.96 ± 0.13	0.13 ± 0.07	0.09 ± 0.02	0.06 ± 0.01
	L	0.15 ± 0.05	0.06 ± 0.01**	2.25 ± 0.63	0.95 ± 0.12	0.10 ± 0.02	0.15 ± 0.04*	0.06 ± 0.01
	H	0.11 ± 0.04	0.06 ± 0.01*	0.99 ± 0.58**	0.66 ± 0.20*	0.07 ± 0.02	0.15 ± 0.05	0.03 ± 0.01**
FP004BA day 14	C	0.19 ± 0.04	0.08 ± 0.01	2.85 ± 0.27	1.38 ± 0.12	0.14 ± 0.06	0.22 ± 0.04	0.08 ± 0.01
	L	0.19 ± 0.04	0.08 ± 0.01	2.22 ± 0.62	1.16 ± 0.10*	0.11 ± 0.04	0.24 ± 0.03	0.07 ± 0.01*
	H	0.22 ± 0.02**	0.11 ± 0.01***	2.95 ± 0.77	1.49 ± 0.13	0.21 ± 0.04	0.38 ± 0.09**	0.08 ± 0.01
FP005ME	C	0.08 ± 0.12	0.05 ± 0.07	4.59 ± 0.72	1.35 ± 0.12	0.07 ± 0.03	0.27 ± 0.10	0.08 ± 0.01
	L	0.19 ± 0.05	0.08 ± 0.09	4.42 ± 0.27	1.06 ± 0.52	0.11 ± 0.03	0.20 ± 0.02	0.09 ± 0.01
	H	0.16 ± 0.18	0.09 ± 0.10	4.83 ± 1.53	0.89 ± 0.50	0.10 ± 0.01	0.30 ± 0.20	0.09 ± 0.01
FP006JJ	C	0.14 ± 0.02	0.09 ± 0.03	1.34 ± 0.37	0.50 ± 0.07	0.04 ± 0.01	0.36 ± 0.07	0.02 ± 0.01
	L	0.12 ± 0.02	0.08 ± 0.01	0.74 ± 0.26*	0.44 ± 0.09	0.04 ± 0.01	0.36 ± 0.07	0.02 ± 0.01
	H	0.13 ± 0.03	0.09 ± 0.02	0.67 ± 0.23**	0.47 ± 0.15	0.04 ± 0.03	0.34 ± 0.10	0.02 ± 0.01
FP007SE	C	0.06 ± 0.02	0.13 ± 0.04	4.70 ± 0.31	0.70 ± 0.24	0.13 ± 0.03	0.16 ± 0.02	0.09 ± 0.01
	L	0.28 ± 0.05**	0.21 ± 0.03	4.92 ± 1.22	0.40 ± 0.04	0.09 ± 0.02*	0.36 ± 0.06**	0.08 ± 0.01
	H	0.35 ± 0.13***	0.21 ± 0.09	3.74 ± 1.09	0.39 ± 0.22*	0.09 ± 0.02	0.34 ± 0.12**	0.05 ± 0.03*
FP008AL	C	n.d.[5]	n.d.	n.d.	n.d.	n.d.	n.d.	n.d.
	L	0.30 ± 0.04	0.10 ± 0.01	1.82 ± 0.68	1.06 ± 0.11	0.11 ± 0.03	0.68 ± 0.06	0.08 ± 0.01
	H	0.25 ± 0.08	0.16 ± 0.03*	0.78 ± 0.31	1.15 ± 0.12	0.08 ± 0.02	0.86 ± 0.30***	0.08 ± 0.01
FP009SF	C	0.10 ± 0.10	0.11 ± 0.02	6.61 ± 0.88	1.48 ± 0.17	0.18 ± 0.02	0.19 ± 0.04	0.14 ± 0.01
	L	0.06 ± 0.02	0.21 ± 0.07**	8.20 ± 1.06*	0.91 ± 0.94	0.31 ± 0.09*	0.23 ± 0.06	0.17 ± 0.02***
	H	0.09 ± 0.02	0.28 ± 0.03***	8.09 ± 0.79*	0.10 ± 0.04**	0.32 ± 0.05**	0.22 ± 0.04	0.13 ± 0.01
FP010SG	C	0.09 ± 0.03	0.10 ± 0.01	9.76 ± 1.23	1.97 ± 0.20	0.21 ± 0.05	0.20 ± 0.02	0.16 ± 0.01
	L	0.13 ± 0.04	0.12 ± 0.02	9.41 ± 1.58	1.71 ± 0.13	0.25 ± 0.06	0.25 ± 0.04	0.19 ± 0.02**
	H	0.20 ± 0.04**	0.16 ± 0.02***	10.44 ± 1.45	1.65 ± 0.22*	0.39 ± 0.15*	0.26 ± 0.05	0.19 ± 0.01 *
FP011OR	C	0.14 ± 0.02	0.07 ± 0.01	4.05 ± 1.14	1.13 ± 0.05	0.13 ± 0.02	0.19 ± 0.05	0.11 ± 0.01
	L	0.14 ± 0.03	0.08 ± 0.01	4.47 ± 2.03	1.38 ± 0.09**	0.15 ± 0.02	0.22 ± 0.03	0.12 ± 0.01
	H	0.25 ± 0.09*	0.09 ± 0.01*	3.88 ± 1.08	1.07 ± 0.11	0.14 ± 0.04	0.36 ± 0.11**	0.10 ± 0.01
FP014SC	C	0.13 ± 0.05	0.12 ± 0.05	6.69 ± 2.30	1.35 ± 0.19	0.32 ± 0.19	0.24 ± 0.10	0.14 ± 0.02
	L	0.13 ± 0.03	0.10 ± 0.01	8.63 ± 1.72	1.85 ± 0.40*	0.32 ± 0.11	0.28 ± 0.04	0.19 ± 0.04*
	H	0.2 ± 0.06	0.11 ± 0.03	6.33 ± 0.48	1.62 ± 0.12	0.21 ± 0.03	0.27 ± 0.11	0.19 ± 0.02
FP016LY	C	0.09 ± 0.03	0.10 ± 0.02	9.10 ± 1.12	1.44 ± 0.13	0.14 ± 0.31	0.16 ± 0.03	0.14 ± 0.01
	L	0.12 ± 0.03	0.11 ± 0.03	7.82 ± 0.73	1.41 ± 0.47	0.18 ± 0.06	0.25 ± 0.07	0.14 ± 0.01
	H	0.15 ± 0.07	0.09 ± 0.01	3.74 ± 2.54***	0.95 ± 0.37	0.09 ± 0.02	0.37 ± 0.13**	0.09 ± 0.05*

[1]3-IS, 3-indoxylsulfate; [2]4-HPA, 4-hydroxyphenylacetate; [3]DMG, N,N-dimethylglycine; [4]PAG, phenylacetylglycine; [5]n.d., not determined

For the bile duct necrosis group, increased 3-indoxylsulfate, phenylacetylglycine (PAG), and 4-hydroxyphenylacetate excretion as well as decreased *N*,*N*-dimethylglycine, trigonelline and citrate excretion were found, as well as a putative increase in urinary levels of bile acids and 5-aminolevulinate (Tab. 10.4.1). For the hepatocellular hypertrophy

group, increased phenylacetylglycine, glucose, alanine, *N*,*N*-dimethylglycine and creatine excretion as well as decreased citrate excretion were found, as well as putative alterations in amino acid excretion (Tab. 10.4.2). For the hepatocellular cell death group, increased phenylacetylglycine, citrate and trigonelline excretion and decreased 2-oxoglutarate excretion were found, as well as an alteration of various buckets to which no metabolites could be assigned with the Chenomx NMR Suite spectral database.

***Table 10.4.5**: All hepatocellular cell death (HCD) markers were quantified in the original ^{1}H NMR spectra using the Chenomx NMR Suite. Values are given as mean ± SD in mM/mM creatinine, statistically significantly altered (Student's t-test) metabolites are marked with * (*, p<0.05; **, p< 0.01; ***, p<0.001). Creatine occurred in individual high dose samples (1x in FP004BA, 3x in FP014SC, 2x in FP015NN).*

		2-Oxoglutarate	Citrate	Glucose	PAG[1]	Trigonelline	Creatinine [mmol]
FP004BA day 13	**C**	1.48 ± 0.52	2.85 ± 0.27	0.40 ± 0.09	0.22 ± 0.04	0.08 ± 0.01	4.29 ± 1.34
	H	1.33 ± 0.55	2.95 ± 0.77	0.41 ± 0.09	0.38 ± 0.09**	0.08 ± 0.01	1.86 ± 0.26*
FP014SC day 1	**C**	5.57 ± 0.53	6.24 ± 1.04	n.q.[2]	0.27 ± 0.08	0.20 ± 0.02	3.41 ± 2.08
	H	4.69 ± 1.34	2.58 ± 1.22**	n.q.	0.26 ± 0.07	0.11 ± 0.03**	1.51 ± 0.72
FP015NN day 1	**C**	7.87 ± 2.71	9.18 ± 2.53	n.q.	0.29 ± 0.10	0.19 ± 0.03	5.22 ± 1.49
	H	0.98 ± 0.59*	4.17 ± 1.33*	0.64 ± 0.75	0.56 ± 0.24	0.13 ± 0.02*	2.13 ± 0.76*

[1]PAG, phenylacetylglycine; [2]n.q. not quantifiable

Considering the marker panel of the hepatocellular cell death group, the results should be regarded with care. First of all, since only three studies are belonging to this group, the data base is very small for detection of a general marker of hepatocellular cell death. Besides, the metabolites identified as putative markers of hepatocellular cell death are probably not specific. Citrate and 2-oxoglutarate excretion are very variable and are often found to be altered in metabonomics studies [15]. Phenylacetylglycine was found as potential marker for all three histopathology groups and must thus be subjected to a closer investigation. Trigonelline is part of the nicotinate metabolism responsible for NADH and NADPH synthesis, but no mechanistic link to hepatocellular cell death is known.

The situation is similar for the hepatocellular hypertrophy group. Besides PAG, glucose was found to be increased in the urine of animals showing hepatocellular hypertrophy. However, increased glucose excretion is used routinely as a biomarker of nephrotoxicity in clinical chemistry analyses. Increased excretion of various amino acids was observed as well, however, due to the inherent limit of sensitivity of ^{1}H NMR analysis, a quantitative analysis of urinary amino acid excretion is very difficult.

***Table 10.4.6**: All bile hepatocellular hypertrophy (HCH) markers were quantified in the original ^{1}H NMR spectra of the day 13 urine samples, using the Chenomx NMR Suite. Values are given as mean ± SD in mM/mM creatinine,, statistically significantly altered (Student's t-test) metabolites are marked with * (*, p<0.05; **, p< 0.01; ***, p<0.001). Identity of glycocholate, leucine, isoleucine, proline, gluconate is based solely on ^{1}H NMR shifts and identity could not be confirmed based on ^{1}H NMR spectra since peaks are lost in the baseline.*

		4-HB[1]	Alanine	Ascorbate	Citrate	Glucose	Glutamine
FP001RO	**C**	n.q.[2]	0.031 ± 0.01	0.09 ± 0.04	4.06 ± 0.79	0.37 ± 0.88	0.32 ± 0.02
	H	n.q.	0.048 ± 0.01	0.07 ± 0.08	4.33 ± 1.88	0.64 ± 0.20	0.34 ± 0.03
FP003SE	**C**	0.20 ± 0.02	0.041 ± 0.01	0.14 ± 0.02	3.96 ± 0.71	0.38 ± 0.09	0.36 ± 0.02
	H	n.q.	0.049 ± 0.01	0.15 ± 0.01	4.48 ± 1.29	0.34 ± 0.15	0.39 ± 0.03
FP008AL	**L**	0.11 ± 0.02	0.059 ± 0.01	0.59 ± 0.15	1.82 ± 0.68	0.90 ± 0.31	n.q.
	H	0.08 ± 0.07	0.085 ± 0.01**	0.40 ± 0.13	0.78 ± 0.31*	0.96 ± 0.39	n.q.
FP010SG	**C**	0.33 ± 0.06	0.067 ± 0.01	0.36 ± 0.10	9.76 ± 1.23	0.85 ± 0.23	0.34 ± 0.19
	H	0.31 ± 0.12	0.092 ± 0.01*	0.23 ± 0.14	10.44 ± 1.45	1.03 ± 0.26	n.q.
FP011OR	**C**	0.22 ± 0.03	0.056 ± 0.01	0.23 ± 0.06	4.05 ± 1.14	0.73 ± 0.13	0.35 ± 0.02
	H	0.21 ± 0.02	0.059 ± 0.01	1.85 ± 0.32***	3.88 ± 1.08	0.85 ± 0.07	0.36 ± 0.03
FP016LY	**C**	0.18 ± 0.07	0.041 ± 0.03	0.13 ± 0.02	9.10 ± 1.12	0.50 ± 0.09	0.45 ± 0.11
	H	0.06 ± 0.09	0.037 ± 0.01	0.21 ± 0.03**	3.74 ± 2.54*	0.40 ± 0.10*	0.33 ± 0.05

		DMG[3]	PAG[4]	Sucrose	Trigonelline	Valine	Creatinine [mmol]
FP001RO	**C**	0.11 ± 0.06	0.16 ± 0.05	n.q.	0.069 ± 0.003	0.01 ± 0.011	5.06 ± 1.11
	H	0.03 ± 0.03*	0.29 ± 0.15	n.q.	0.065 ± 0.032	0.02 ± 0.013	5.04 ± 3.60
FP003SE	**C**	0.11 ± 0.03	0.19 ± 0.03	n.q.	0.09 ± 0.01	0.02 ± 0.002	3.59 ± 0.61
	H	0.17 ± 0.03*	0.55 ± 0.26	n.q.	0.09 ± 0.01	0.03 ± 0.004	2.81 ± 0.96
FP008AL	**L**	0.11 ± 0.03	0.68 ± 0.06	0.38 ± 0.11	0.08 ± 0.01	0.03 ± 0.002	5.04 ± 1.70
	H	0.08 ± 0.02*	0.86 ± 0.30	0.61 ± 0.21	0.08 ± 0.01	0.04 ± 0.006*	2.37 ± 1.07*
FP010SG	**C**	0.21 ± 0.05	0.20 ± 0.02	0.21 ± 0.07	0.16 ± 0.01	0.03 ± 0.004	2.68 ± 0.51
	H	0.39 ± 0.15*	0.26 ± 0.05	0.34 ± 0.10*	0.19 ± 0.01**	0.05 ± 0.004***	1.63 ± 0.35**
FP011OR	**C**	0.13 ± 0.02	0.19 ± 0.05	0.18 ± 0.05	0.11 ± 0.01	0.02 ± 0.012	7.62 ± 2.24
	H	0.14 ± 0.04	0.36 ± 0.11*	0.12 ± 0.08	0.10 ± 0.01	0.02 ± 0.012	6.76 ± 1.57
FP016LY	**C**	0.14 ± 0.03	0.16 ± 0.03	n.q.	0.14 ± 0.01	0.010 ± 0.009	4.27 ± 0.81
	H	0.09 ± 0.02*	0.37 ± 0.13*	n.q.	0.09 ± 0.05*	0.02 ± 0.003	4.48 ± 2.33

[1]4-HB, 4-hydroxybutyrate; [2]n.q., not quantifiable; [3]DMG, N,N-dimethylglycine; [4]PAG, phenylacetylglycine;

The bile duct necrosis group marker panel is the most promising that may have predictive value. All buckets could be assigned to specific compounds, and all compounds except two can be quantified in urine. Variations in urinary hippurate, phenylacetylglycine and 4-hydroxyphenylacetate excretion have been associated with alterations in the gut microflora of rats [67; 69], which may be introduced by the altered bile flow into the colon of the rats due to bile duct necrosis.

Trigonelline is part of the nicotinate metabolism for NADH and NADPH synthesis and increased excretion is associated with oxidative stress. Trigonelline is a byproduct of the conversion of *S*-adenosyl-methionine (SAM) to *S*-adenosyl-homocysteine (SAH). A decreased urinary excretion of trigonelline may be related to a depletion of SAM as SAM

is consumed for the regeneration of GSH stores which are consumed by the detoxification of reactive oxygen species [49; 152].

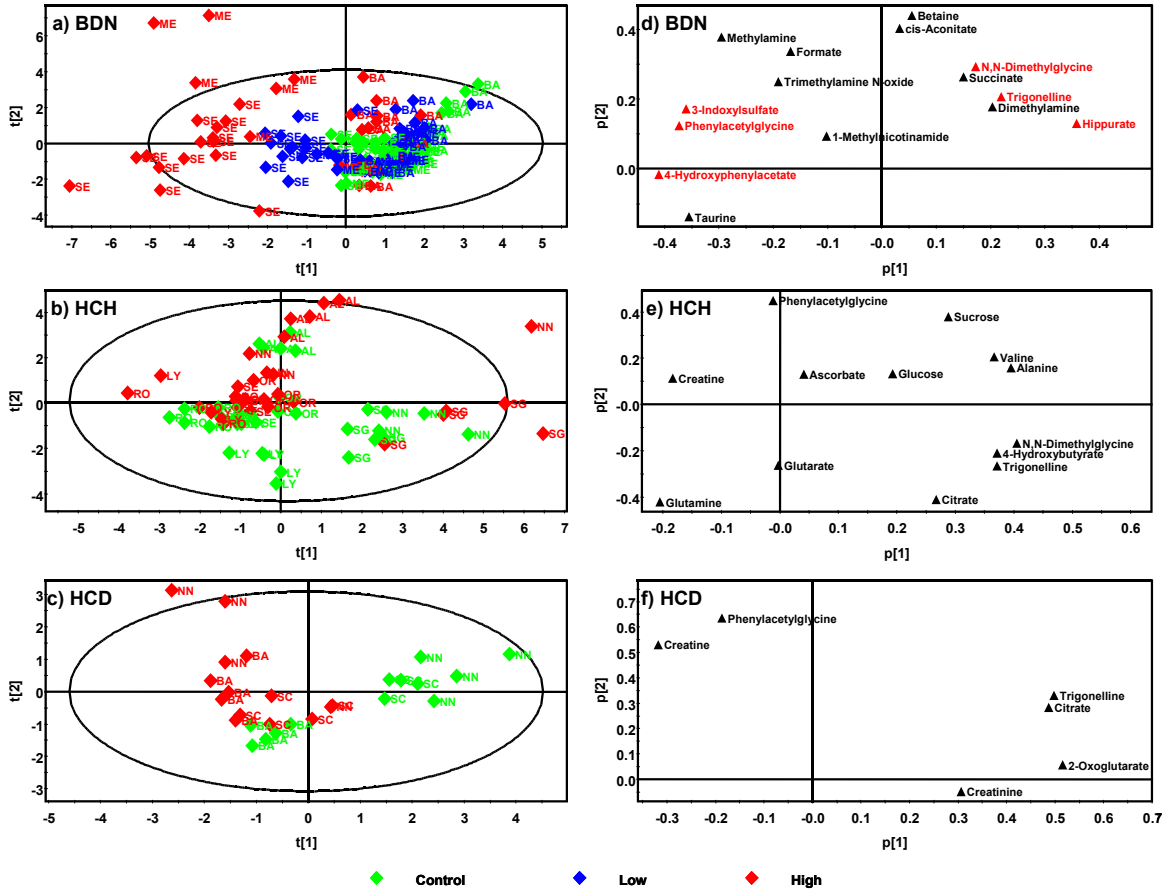

Figure 10.4.1: *Scores plots (a–c) and corresponding loadings plots (d–f) of PCA models constructed with quantitative metabolite data for bile duct necrosis (BDN), hepatocellular hypertrophy (HCH) and hepatocellular cell death (HCD). HCH and HCD models were constructed with markers only, the BDN model contains all quantified metabolites with BDN-specific markers highlighted in red.*

3-Indoxyl sulfate origins from tryptophan metabolism. Tryptophan is a precursor for a variety of biologically important metabolites such as the neurotransmitter serotonin, the hormone melantonin and the NAD precursor nicotinic acid [153]. Tryptophan is metabolized to 3-indoxyl sulfate via indole and indoxyl. It is a circulating protein-bound uremic toxin and associated with the induction of oxidative stress [151; 154]. The mode of action of 3-indoxyl sulfate however is still unclear. Hepatocyte damage may alter the tryptophan metabolism in the liver, thus leading to altered urinary levels of tryptophan metabolites.

5-Aminolevulinate is the first step in heme and bilirubin biosynthesis in the liver. The production of hepatic heme is regulated primarily through the activity of

aminolevulinic acid synthase which is the first and usually rate-limiting enzyme of the pathway. This is, in turn, controlled by a putative regulatory heme pool. The liver catabolizes heme to bilirubin through microsomal heme oxygenase activity and excretes heme into bile along with porphyrins [155]. Bile duct damage may lead to altered heme metabolism and synthesis leading to an increase in urinary 5-aminolevulinate levels.

A problem of the evaluation of the specificity biomarkers is the occurrence in the samples. On one hand, no putative marker is altered significantly in all four studies belonging to the BDN group. On the other hand, several studies not showing bile duct necrosis nonetheless have significantly altered levels of these metabolites.

Although the metabolites determined as putative markers of toxicity, based on histopathological endpoints can be used to discriminate controls from animals showing the pathologic lesions, the number of studies is probably not large enough and the induced toxic lesions not strong enough to build models that are predictive for compounds with unknown histopathology. Only a pattern of various metabolites may be useful for toxicity prediction with ^{1}H NMR. The metabolites accessible with ^{1}H NMR are of such a general nature and alterations of each single metabolite have been associated with so many different clinical symptoms that monitoring of a single marker is probably not successful.

On the other hand, a purely pattern-based classification system carries the danger of modeling artificial or chance correlations between samples, especially with ^{1}H NMR, where no chromatography exists, therefore a number of metabolites may contribute to the same bin. Furthermore, the number of metabolites that can be detected is limited due to the inherent sensitivity of th ^{1}H NMR method. The danger is always that without an understanding of the mechanistic background of the putative marker metabolite, chance correlations are modeled.

11 Conclusion

11.1 Putative markers and biochemistry

In the course of this thesis, urine samples from seven studies were analyzed with a GC/MS- and ^{1}H NMR-based metabonomics approach. Both analytical methods performed well for the separation of controls and treated animal in a time- and dose-dependent manner. Good correlation between alterations in urinary profiles and histopathological changes were observed. For each study, a panel of metabolites with altered excretion levels upon toxin administration could be identified.

A comparison of all urinary metabolites found to be altered upon toxin treatment in the studies analyzed in the course of this thesis reveals that no single one of the metabolites identified is able to serve as an early non-invasive biomarker of toxicity. Comparing the metabolites found to be altered across more than one study, one can conclude that there is no single metabolite characteristic for a specific histopathology.

The Krebs cycle intermediates citrate and oxoglutarate are decreased across all studies, but have been found to be generally quite variable in the course of the analysis of the InnoMed predtox samples. The decrease of Krebs cycle intermediates is attributed to a general sign of toxicity and not to any site-specific or mechanistic reasons [15]. This is an important consideration since these molecules contribute strongly to the ^{1}H NMR and GC/MS analytical profile and thus influence the multivariate data analysis.

Pseudouridine has been found to be altered in the ochratoxin A and aristolochic acid study, both studies that were associated with cell proliferation. This is further evidence that increased urinary pseudouridine excretion may serve as a marker of proliferative processes.

Alterations in aromatic compounds such as hippurate, hydroxyphenylacetic acids and phenylacetylglycine are indicative of altered gut microflora metabolism [68; 69; 156] and therefore only indirectly related to the toxic mechanism. For the aminoglycoside antibiotic gentamicin, an alteration of the gut microflora is clearly a pharmacological effect not linked to its toxicity. For the compounds of bile duct necrosis group of the InnoMed PredTox project, the alteration may only be a secondary effect of the primary lesion in the bile duct region leading to an altered bile flux in the intestine and thereby to alterations of the gut microflora. Correlation of the altered metabolite profiles in the InnoMed PredTox studies to observed toxicities is especially challenging, since the pharmacology and

metabolism of the study compounds is unknown, but may strongly influence the metabolite profiles.

Table 11.1.1: *Summary of metabolites found to be altered across all studies analyzed in the context of this thesis.*

	kidney proximal tubule			liver bile duct necrosis		
	gentamicin	**OTA**	**aristolochic acid**	**FP004BA**	**FP005ME**	**FP007SE**
citrate	↓	↓	↓	↓	↓	↓
2-oxoglutarate	-	↓	↓	↓	↓	↓
lactate	↑	↑	-	↑	-	-
myo-inositol	-	↑	-	↑	-	-
creatinine	↓	↑	-	↑	-	-
hippurate	↓	-	↓	↓	↓	↓
4-hydroxyphenylacetate	-	-	↑	↑	↑	↑
phenylacetylglycine	-	-	-	↑	↑	↑
pseudouridine	-	↑	↑	-	-	-
glucose	↑	↑	↑	↑	↑	-
5-oxoproline	↑	↑	↑	-	-	-
5-hydroxyindole	-	↑	-	↑	↑	↑

[1]TMAO, trimethylamine-*N*-oxide

A finding common to all three kidney toxins was the disturbance of metabolites such as *myo*-inositol related to osmolyte regulation and homeostasis of osmolytic pressure in the kidneys. Alterations in these renal osmolytes could generally be observed quite early after toxin treatment and at low doses. This may be an approach for a targeted screening method, especially with GC/MS, which may be valuable for an early, non-invasive detection of kidney toxicity.

A large part of the metabolites found to be altered upon toxin treatment, such as 5-oxoproline, *N,N*-dimethylglycine and various amino acids, can also be associated with oxidative stress and the detoxification of reactive metabolites via glutathione conjugation. Although the participation of oxidative stress is discussed for a variety of compounds analyzed in the studies of this thesis, the question remains whether oxidative stress should be considered as a consequence of the toxic insult and the responding inflammation rather than the initiating factor. There is also no clear mechanism- or site-specific information obtained from the metabolites. However, for a rapid non-invasive screening method of toxicity, mechanism and site-specificity are of secondary importance, as long as the markers are sensitive enough.

The overall conclusion from the altered metabolites found by the comprehensive metabolite analyses in this thesis is that these metabolites can be brought well into a

mechanistic context when the toxicity of the compound is known. However, the predictive value of these markers, especially regarding site- or organ specificity is rather low, since the biochemistry behind these metabolites is of a very basic nature common to all cell types and organs. Although a classification and separation of controls from treated animals with untargeted screening analyses and PCA-based multivariate data analysis works well, mechanistic information requires further follow-up with targeted experiments.

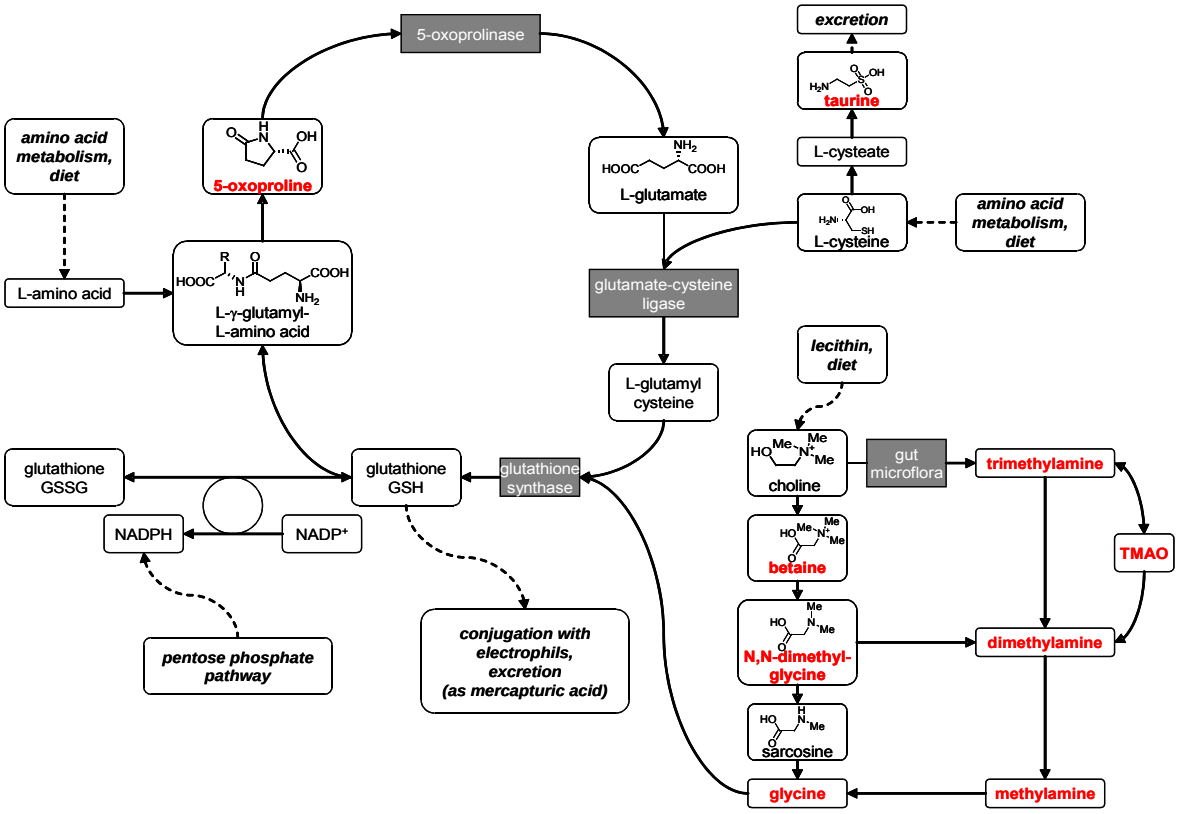

***Figure 11.1.1**: The γ-glutamyl cycle is responsible for the production of glutathione. Metabolites accessible by the GC/MS or ^{1}H NMR analysis methods described here are marked in red.*

11.2 Metabonomics for early noninvasive detection of toxicity

The studies analyzed in the context of this thesis show that metabonomics techniques are able to indicate toxicity at the same time point as histopathology. Effects of compound administration may be observed even before the onset of histopathologic lesions. However, whether these effects are correlated to the adverse effects observed later on or at higher doses, or are more a result of the pharmacological effect of the compound, has to be elucidated before these alterations are considered as toxicity markers. One way to address

this problem is the inclusion of histopathology scores in the metabonomic analysis as demonstrated with the OTA study. Especially the aristolochic acid study showed that it is difficult to distinguish between local and systemic effects and to determine if the observed effects are really indicative of renal damage and not reflecting the irritation of the forestomach mucosa.

These findings show that there is only limited predictivity to be achieved by single compound studies. Even though the multivariate models are predictive for the changes in urinary composition by a certain compound in a single study, this does not mean that this model may predict the toxicity of the compound analyzed. One requirement for good modeling in order to have predictive metabonomics methods is a large data base such as attempted by COMET and COMET2 and the InnoMed PredTox project. The problem is that due to the comprehensive screening method used, the marker metabolites found are of a very basic nature, i.e. playing a role in a large number of processes or being part of very basic biochemistry processes that are not toxin- or organ-specifically altered. For example, the induction of oxidative stress as observed by oxoprolineuria fits well into the toxic mechanisms of gentamicin and ochratoxin A and can be correlated with the onset of kidney damage in the respective studies. However, increased 5-oxoproline excretion upon administration of a test compound does not allow any prediction of site or mechanism even if this effect has to be considered as adverse side effect for this compound. Therefore, the need of a broader data base and probably the modeling of alterations upon toxic insults on a pattern recognition level is necessary. On the other hand, analytical methods have to be developed to access more than the forty metabolites available by standard ^{1}H NMR analysis. For this purpose, the development of sensitive GC/MS methods based on new two-dimensional GC and TOF-detection. (GCxGC/TOF) as well as the development and improvement of databases may be of great value.

The goal of using metabonomics for the early non-invasive prediction of toxicity still requires extensive research by a variety of scientists working fieldsranging from informatics to veterinary pathology. However, the technology is still an emerging one and its power increases with new advances in the fields of analytics and bioinformatics. For future predictive applications, a greater database with large scale projects similar to the COMET or InnoMed PredTox project has to be used.

12 Literature

[1] *Handbook of toxicologic pathology,* 2nd ed.; Academic Press: San Diego, 2002.

[2] Ozer, Josef; Ratner, Marcia; Shaw, Martin; Bailey, Wendy; Schomaker, Shelli. The current state of serum biomarkers of hepatotoxicity. *Toxicology* **2008**, *245* (3) 194–205.

[3] Coca, S. G.; Yalavarthy, R.; Concato, J.; Parikh, C. R. Biomarkers for the diagnosis and risk stratification of acute kidney injury: A systematic review. *Kidney Int.* **2008**, *73* (9) 1008–1016.

[4] Amin, Rupesh P.; Vickers, Alison E.; Sistare, Frank; Thompson, Karol L.; Roman, Richard J.; Lawton, Michael; Kramer, Jeffrey; Hamadeh, Hisham K.; Collins, Jennifer; Grissom, Sherry. Identification of putative gene-based markers of renal toxicity. *Environmental Health Perspectives* **2004**, *112* (4) 465–479.

[5] Wang, Er-Jia; Snyder, Ronald D.; Fielden, Mark R.; Smith, Roger J.; Gu, Yi-Zhong. Validation of putative genomic biomarkers of nephrotoxicity in rats. *Toxicology* **2008**, *246* (2-3) 91–100.

[6] Oliver, S. G.; Winson, M. K.; Kell, D. B.; Baganz, F. Systematic functional analysis of the yeast genome. *Trends Biotechnol.* **1998**, *16* (9) 373–378.

[7] Nicholson, J. K.; Lindon, J. C.; Holmes, E. \"Metabonomics\": understanding the metabolic responses of living systems to pathophysiological stimuli via multivariate statistical analysis of biological NMR spectroscopic data. *Xenobiotica* **1999**, *29* (11) 1181–1189.

[8] Rochfort, Simone. Metabolomics Reviewed: A New \"Omics\" Platform Technology for Systems Biology and Implications for Natural Products Research. *J. Nat. Products* **2005**, *68* (12) 1813–1820.

[9] Dettmer, Katja; Aronov, Pavel A.; Hammock, Bruce D. Mass spectrometry-based metabolomics. *Mass Spec. Rev.* **2007**, *26* (1) 51–78.

[10] Fiehn, Oliver. Combining genomics, metabolome analysis, and biochemical modelling to understand metabolic networks. *Comp. Funct. Genomics* **2001**, *2* (3) 155–168.

[11] Nicholson, Jeremy K.; Timbrell, John A.; Sadler, Peter J. Proton NMR spectra of urine as indicators of renal damage. Mercury-induced nephrotoxicity in rats. *Mol. Pharmacol.* **1985**, *27* (6) 644–651.

[12] Holmes, E.; Bonner, F. W.; Sweatman, B. C.; Lindon, J. C.; Beddell, C. R.; Rahr, E.; Nicholson, J. K. Nuclear magnetic resonance spectroscopy and pattern recognition analysis of the biochemical processes associated with the progression of and recovery from nephrotoxic lesions in the rat induced by mercury(II) chloride and 2-bromoethanamine. *Mol. Pharmacol.* **1992**, *42* (5) 922–930.

[13] Nicholson, Jeremy K.; Higham, Denise P.; Timbrell, John A.; Sadler, Peter J. Quantitative high resolution proton NMR urinalysis studies on the biochemical effects of cadmium in the rat. *Mol. Pharmacol.* **1989**, *36* (3) 398–404.

[14] Gartland, K. P. R.; Bonner, F. W.; Nicholson, J. K. Investigations into the biochemical effects of region-specific nephrotoxins. *Mol. Pharmacol.* **1989**, *35* (2) 242–250.

[15] Robertson, Donald G. Metabonomics in Toxicology: A Review. *Toxicol. Sci.* **2005**, *85* (2) 809–822.

[16] Coen, Muireann; Holmes, Elaine; Lindon, John C.; Nicholson, Jeremy K. NMR-Based Metabolic Profiling and Metabonomic Approaches to Problems in Molecular Toxicology. *Chem. Res. Toxicol.* **2008**, *21* (1) 9–27.

[17] Halket, John M.; Waterman, Daniel; Przyborowska, Anna M.; Patel, Raj K. P.; Fraser, Paul D.; Bramley, Peter M. Chemical derivatization and mass spectral libraries in metabolic profiling by GC/MS and LC/MS/MS. *J. Exp. Bot.* **2005**, *56* (410) 219–243.

[18] Kopka, Joachim. Current challenges and developments in GC-MS based metabolite profiling technology. *J. Biotechnol.* **2006**, *124* (1) 312–322.

[19] Gates, Stephen C.; Sweeley, Charles C. Quantitative metabolic profiling based on gas chromatography. *Clin. Chem.* **1978**, *24* (10) 1663–1673.

[20] Shoemaker, James D.; Elliott, William H. Automated screening of urine samples for carbohydrates, organic and amino acids after treatment with urease. *J. Chromatogr.* **1991**, *562* (1-2) 125–138.

[21] Matsumoto, I.; Kuhara, T. A new chemical diagnostic method for inborn errors of metabolism by mass spectrometry - rapid, practical, and simultaneous urinary metabolites analysis. *Mass Spec. Rev.* **1996**, *15* (1) 43–57.

[22] Kuhara, Tomiko. Noninvasive human metabolome analysis for differential diagnosis of inborn errors of metabolism. *J. Chromatogr. B* **2007**, *855* (1) 42–50.

[23] Ni, Yan; Su, Mingming; Qiu, Yunping; Chen, Minjun; Liu, Yuming; Zhao, Aihua; Jia, Wei. Metabolic profiling using combined GC-MS and LC-MS provides a systems understanding of aristolochic acid-induced nephrotoxicity in rat. *FEBS Lett.* **2007**, *581* (4) 707–711.

[24] Zhang, Qi; Wang, Guangji; Du, Yu; Zhu, Lingling; A, Jiye. GC/MS analysis of the rat urine for metabonomic research. *J. Chromatogr. B* **2007**, *854* (1-2) 20–25.

[25] Little, James L. Artifacts in trimethylsilyl derivatization reactions and ways to avoid them. *J. Chromatogr. A* **1999**, *844* (1 + 2) 1–22.

[26] Pasikanti, Kishore K.; Ho, Paul C.; Chan, Eric C. Y. Development and validation of a gas chromatography/mass spectrometry metabonomic platform for the global profiling of urinary metabolites. *Rapid Commun. Mass Spectrom.* **2008**, *22* (19) 2984–2992.

[27] A, Jiye; Huang, Qing; Wang, Guangji; Zha, Weibin; Yan, Bei; Ren, Hongcan; Gu, Shenghua; Zhang, Ying; Zhang, Qi; Shao, Feng. Global analysis of metabolites in rat and human urine based on gas chromatography/time-of-flight mass spectrometry. *Anal. Biochem.* **2008**, *379* (1) 20–26.

[28] Borner, Jana; Buchinger, Sebastian; Schomburg, Dietmar. A high-throughput method for microbial metabolome analysis using gas chromatography/mass spectrometry. *Anal. Biochem.* **2007**, *367* (2) 143–151.

[29] Pasikanti, Kishore K.; Ho, P. C.; Chan, E. C. Y. Gas chromatography/mass spectrometry in metabolic profiling of biological fluids. *J. Chromatogr. B* **2008**, *871* (2) 202–211.

[30] Wilson, Ian D.; Plumb, Robert; Granger, Jennifer; Major, Hilary; Williams, Rebecca; Lenz, Eva M. HPLC-MS-based methods for the study of metabonomics. *J. Chromatogr. B* **2005**, *817* (1) 67–76.

[31] Lu, Xin; Zhao, Xinjie; Bai, Changmin; Zhao, Chunxia; Lu, Guo; Xu, Guowang. LC-MS-based metabonomics analysis. *J. Chromatogr. B* **2008**, *866* (1-2) 64–76.

[32] Plumb, Robert S.; Granger, Jennifer H.; Stumpf, Chris L.; Johnson, Kelly A.; Smith, Brian W.; Gaulitz, Scott; Wilson, Ian D.; Castro-Perez, Jose. A rapid screening approach to metabonomics using UPLC and oa-TOF mass spectrometry: application to age, gender and diurnal variation in normal/Zucker obese rats and black, white and nude mice. *Analyst* **2005**, *130* (6) 844–849.

[33] Idborg, Helena; Zamani, Leila; Edlund, Per-Olof; Schuppe-Koistinen, Ina; Jacobsson, Sven P. Metabolic fingerprinting of rat urine by LC/MS. Part 1. Analysis by hydrophilic interaction liquid chromatography-electrospray ionization mass spectrometry. *J. Chromatogr. B* **2005**, *828* (1-2) 9–13.

[34] Atherton, Helen J.; Bailey, Nigel J.; Zhang, Wen; Taylor, John; Major, Hilary; Shockcor, John; Clarke, Kieran; Griffin, Julian L. A combined 1H NMR spectroscopy- and mass spectrometry-based metabolomic study of the PPAR-alpha null mutant mouse defines profound systemic changes in metabolism linked to the metabolic syndrome. *Physiol. Genomics* **2006**, *27* (2) 178–186.

[35] Williams, R.; Lenz, E. M.; Wilson, A. J.; Granger, J.; Wilson, I. D.; Major, H.; Stumpf, C.; Plumb, R. A multi-analytical platform approach to the metabonomic analysis of plasma from normal and zucker (fa/fa) obese rats. *Mol. Biosys.* **2006**, *2* (3/4) 174–183.
[36] Trygg, Johan; Holmes, Elaine; Lundstedt, Torbjoern. Chemometrics in Metabonomics. *J. Proteome Res.* **2007**, *6* (2) 469–479.

[37] Eriksson, L.; Johannson, E.; Kettaneh-Wold, N.; Trygg, J.; Wilkstrom, C.; Wold, S. *Multivariate and Megavariate Data Analysis: Basic Principles and Applications (Part I);* Umetrics: 2006.

[38] Trygg, Johan; Wold, Svante. Orthogonal projections to latent structures (O-PLS). *J. Chemometr.* **2002**, *16* (3) 119–128.

[39] Major, Hilary J.; Williams, Rebecca; Wilson, Amy J.; Wilson, Ian D. A metabonomic analysis of plasma from Zucker rat strains using gas chromatography/mass spectrometry and pattern recognition. *Rapid Commun. Mass Spectrom.* **2006**, *20* (22) 3295–3302.

[40] Chan, Eric Chun Yong; Koh, Poh Koon; Mal, Mainak; Cheah, Peh Yean; Eu, Kong Weng; Backshall, Alexandra; Cavill, Rachel; Nicholson, Jeremy K.; Keun, Hector C. Metabolic Profiling of Human Colorectal Cancer Using High-Resolution Magic Angle Spinning Nuclear Magnetic Resonance (HR-MAS NMR) Spectroscopy and Gas Chromatography Mass Spectrometry (GC/MS). *J. Proteome Res.* **2009**, *8* (1) 352–361.

[41] Wiklund, Susanne; Johansson, Erik; Sjoestroem, Lina; Mellerowicz, Ewa J.; Edlund, Ulf; Shockcor, John P.; Gottfries, Johan; Moritz, Thomas; Trygg, Johan. Visualization of GC/TOF-MS-Based Metabolomics Data for Identification of Biochemically Interesting Compounds Using OPLS Class Models. *Anal. Chem.* **2007**, *80* (1) 116–123.

[42] Lommen, A.; van der Weg, G.; van Engelen, M. C.; Bor, G.; Hoogenboom, L. A. P.; Nielen, M. W. F. An untargeted metabolomics approach to contaminant analysis: Pinpointing potential unknown compounds. *Anal. Chim. Acta* **2007**, *584* (1) 43–49.

[43] Katajamaa, Mikko; Miettinen, Jarkko; Oresic, Matej. MZmine: toolbox for processing and visualization of mass spectrometry based molecular profile data. *Bioinformatics* **2006**, *22* (5) 634–636.

[44] Smith, Colin A.; Want, Elizabeth J.; O'Maille, Grace; Abagyan, Ruben; Siuzdak, Gary. XCMS: Processing Mass Spectrometry Data for Metabolite Profiling Using Nonlinear Peak Alignment, Matching, and Identification. *Anal. Chem.* **2006**, *78* (3) 779–787.

[45] Katajamaa, Mikko; Oresic, Matej. Data processing for mass spectrometry-based metabolomics. *J. Chromatogr. A* **2007**, *1158* (1-2) 318–328.

[46] Lange, Eva; Tautenhahn, Ralf; Neumann, Steffen; Gropl, Clemens. Critical assessment of alignment procedures for LC-MS proteomics and metabolomics measurements. *BMC Bioinform.* **2008**, *9*375.

[47] Warrack, Bethanne M.; Hnatyshyn, Serhiy; Ott, Karl-Heinz; Reily, Michael D.; Sanders, Mark; Zhang, Haiying; Drexler, Dieter M. Normalization strategies for metabonomic analysis of urine samples. *J. Chromatogr. B* **2009**, *877* (5-6) 547–552.

[48] Coen, Muireann; Lenz, Eva M.; Nicholson, Jeremy K.; Wilson, Ian D.; Pognan, Francois; Lindon, John C. An Integrated Metabonomic Investigation of Acetaminophen Toxicity in the Mouse Using NMR Spectroscopy. *Chem. Res. Toxicol.* **2003**, *16* (3) 295–303.

[49] Sun, Jinchun; Schnackenberg, Laura K.; Holland, Ricky D.; Schmitt, Thomas C.; Cantor, Glenn H.; Dragan, Yvonne P.; Beger, Richard D. Metabonomics evaluation of urine from rats given acute and chronic doses of acetaminophen using NMR and UPLC/MS. *J. Chromatogr. B* **2008**, *871* (2) 328–340.

[50] Griffin, Julian L.; Walker, Lee A.; Shore, Richard F.; Nicholson, Jeremy K. Metabolic Profiling of Chronic Cadmium Exposure in the Rat. *Chem. Res. Toxicol.* **2001**, *14* (10) 1428–1434.

[51] Waters, Nigel J.; Holmes, Elaine; Williams, Ann; Waterfield, Catherine J.; Farrant, R. Duncan; Nicholson, Jeremy K. NMR and Pattern Recognition Studies on the Time-Related Metabolic Effects of alpha -Naphthyl isothiocyanate on Liver, Urine, and Plasma in the Rat: An Integrative Metabonomic Approach. *Chem. Res. Toxicol.* **2001**, *14* (10) 1401–1412.

[52] Waters, Nigel J.; Waterfield, Catherine J.; Farrant, R. Duncan; Holmes, Elaine; Nicholson, Jeremy K. Integrated Metabonomic Analysis of Bromobenzene-Induced Hepatotoxicity: Novel Induction of 5-Oxoprolinosis. *J. Proteome Res.* **2006**, *5* (6) 1448–1459.

[53] Williams, R. E.; Cottrell, L.; Jacobsen, M.; Bandara, L. R.; Kelly, M. D.; Kennedy, S.; Lock, E. A. 1H-Nuclear magnetic resonance pattern recognition studies with N-phenylanthranilic acid in the rat: time- and dose-related metabolic effects. *Biomarkers* **2003**, *8* (6) 472–490.

[54] Chen, Minjun; Zhao, Liping; Jia, Wei. Metabonomic Study on the Biochemical Profiles of A Hydrocortisone-Induced Animal Model. *J. Proteome Res.* **2005**, *4* (6) 2391–2396.

[55] Feng, Bo; Wu, Shengming; Lv, Sa; Liu, Feng; Chen, Hongsong; Yan, Xianzhong; Li, Yu; Dong, Fangting; Wei, Lai. Metabolic Profiling Analysis of a D-Galactosamine/Lipopolysaccharide-Induced Mouse Model of Fulminant Hepatic Failure. *J. Proteome Res.* **2007**, *6* (6) 2161–2167.

[56] Lee, Sang Hee; Woo, Han Min; Jung, Byung Hwa; Lee, Jeongae; Kwon, Oh Seung; Pyo, Hee Soo; Choi, Man Ho; Chung, Bong Chul. Metabolomic Approach To Evaluate the Toxicological Effects of Nonylphenol with Rat Urine. *Anal. Chem.* **2007**, *79*6102–6110.

[57] Huang, Xin; Shao, Li; Gong, Yifei; Mao, Yong; Liu, Changxiao; Qu, Haibin; Cheng, Yiyu. A metabonomic characterization of CCl4-induced acute liver failure using partial least square regression based on the GC/MS metabolic profiles of plasma in mice. *J. Chromatogr. B* **2008**, *870* (2) 178–185.

[58] Lenz, E. M.; Bright, J.; Knight, R.; Wilson, I. D.; Major, H. A metabonomic investigation of the biochemical effects of mercuric chloride in the rat using 1H NMR and HPLC-TOF/MS: time dependant changes in the urinary profile of endogenous metabolites as a result of nephrotoxicity. *Analyst* **2004**, *129* (6) 535–541.

[59] Lafaye, Alexandra; Junot, Christophe; Ramounet-Le Gall, Beatrice; Fritsch, Paul; Tabet, Jean-Claude; Ezan, Eric. Metabolite profiling in rat urine by liquid chromatography/ electrospray ion trap mass spectrometry. Application to the study of heavy metal toxicity. *Rapid Commun. Mass Spectrom.* **2003**, *17* (22) 2541–2549.

[60] Lafaye, Alexandra; Junot, Christophe; Ramounet-Le Gall, Beatrice; Fritsch, Paul; Ezan, Eric; Tabet, Jean-Claude. Profiling of sulfoconjugates in urine by using precursor

ion and neutral loss scans in tandem mass spectrometry. *J. Mass Spectrom.* **2004**, *39* (6) 655–664.

[61] Lenz, E. M.; Bright, J.; Knight, R.; Wilson, I. D.; Major, H. Cyclosporin A-induced changes in endogenous metabolites in rat urine: a metabonomic investigation using high field 1H NMR spectroscopy, HPLC-TOF/MS and chemometrics. *J. Pharm. Biomed. Anal.* **2004**, *35* (3) 599–608.

[62] Williams, R. E.; Major, H.; Lock, E. A.; Lenz, E. M.; Wilson, I. D. D-Serine-induced nephrotoxicity: a HPLC-TOF/MS-based metabonomics approach. *Toxicology* **2005**, *207* (2) 179–190.

[63] Anthony, M. L.; Sweatman, B. C.; Beddell, C. R.; Lindon, J. C.; Nicholson, J. K. Pattern recognition classification of the site of nephrotoxicity based on metabolic data derived from proton nuclear magnetic resonance spectra of urine. *Mol. Pharmacol.* **1994**, *46* (1) 199–211.

[64] Nicholls, Andrew W.; Holmes, Elaine; Lindon, John C.; Shockcor, John P.; Farrant, R. Duncan; Haselden, John N.; Damment, Stephen J. P.; Waterfield, Catherine J.; Nicholson, Jeremy K. Metabonomic Investigations into Hydrazine Toxicity in the Rat. *Chem. Res. Toxicol.* **2001**, *14* (8) 975–987.

[65] Nicholls, Andrew W.; Nicholson, Jeremy K.; Haselden, John N.; Waterfield, Catherine J. A metabonomic approach to the investigation of drug-induced phospholipidosis: an NMR spectroscopy and pattern recognition study. *Biomarkers* **2000**, *5* (6) 410–423.

[66] Lindon, John C.; Nicholson, Jeremy K.; Holmes, Elaine; Everett, Jeremy R. Metabonomics: metabolic processes studied by NMR spectroscopy of biofluids. *Concepts Magn. Reson.* **2000**, *12* (5) 289–320.

[67] Nicholls, Andrew W.; Mortishire-Smith, Russell J.; Nicholson, Jeremy K. NMR Spectroscopic-Based Metabonomic Studies of Urinary Metabolite Variation in Acclimatizing Germ-Free Rats. *Chem. Res. Toxicol.* **2003**, *16* (11) 1395–1404.

[68] Williams, R. E.; Eyton-Jones, H. W.; Farnworth, M. J.; Gallagher, R.; Provan, W. M. Effect of intestinal microflora on the urinary metabolic profile of rats: a 1H-nuclear magnetic resonance spectroscopy study. *Xenobiotica* **2002**, *32* (9) 783–794.

[69] Phipps, A. N.; Stewart, J.; Wright, B.; Wilson, I. D. Effect of diet on the urinary excretion of hippuric acid and other dietary-derived aromatics in rat. A complex interaction between diet, gut microflora and substrate specificity. *Xenobiotica* **1998**, *28* (5) 527–537.

[70] Bollard, M. E.; Holmes, E.; Lindon, J. C.; Mitchell, S. C.; Branstetter, D.; Zhang, W.; Nicholson, J. K. Investigations into biochemical changes due to diurnal variation and estrus cycle in female rats using high-resolution 1H NMR spectroscopy of urine and pattern recognition. *Anal. Biochem.* **2001**, *295* (2) 194–202.

[71] Shockcor, John P.; Holmes, Elaine. Metabonomic applications in toxicity screening and disease diagnosis. *Curr. Topics Med. Chem.* **2002**, *2* (1) 35–51.

[72] Lindon, John C.; Nicholson, Jeremy K.; Holmes, Elaine; Antti, Henrik; Bollard, Mary E.; Keun, Hector; Beckonert, Olaf; Ebbels, Timothy M.; Reily, Michael D.; Robertson, Donald; et al. Contemporary issues in toxicology the role of metabonomics in toxicology and its evaluation by the COMET project. *Toxicol. Appl. Pharmacol.* **2003**, *187* (3) 137–146.

[73] Ebbels, Timothy M. D.; Keun, Hector C.; Beckonert, Olaf P.; Bollard, Mary E.; Lindon, John C.; Holmes, Elaine; Nicholson, Jeremy K. Prediction and Classification of Drug Toxicity Using Probabilistic Modeling of Temporal Metabolic Data: The Consortium on Metabonomic Toxicology Screening Approach. *J. Proteome Res.* **2007**, *6* (11) 4407–4422.

[74] König, Jochen. A better system. *Drug Discovery Dev.* **2008**, *11* (8) 28–30.

[75] Clayton, T. Andrew; Lindon, John C.; Cloarec, Olivier; Antti, Henrik; Charuel, Claude; Hanton, Gilles; Provost, Jean-Pierre; Le Net, Jean-Loic; Baker, David; Walley, Rosalind J.; et al. Pharmaco-metabonomic phenotyping and personalized drug treatment. *Nature* **2006**, *440* (7087) 1073–1077.

[76] Hagel, Jillian M.; Facchini, Peter J. Plant metabolomics: analytical platforms and integration with functional genomics. *Phytochem. Rev.* **2008**, *7* (3) 479–497.

[77] Viant, Mark R.; Pincetich, Christopher A.; Hinton, David E.; Tjeerdema, Ronald S. Toxic actions of dinoseb in medaka (Oryzias latipes) embryos as determined by in vivo 31P NMR, HPLC-UV and 1H NMR metabolomics. *Aquat. Toxicol.* **2006**, *76* (3-4) 329–342.

[78] Gottschalk, M.; Ivanova, G.; Collins, D. M.; Eustace, A.; O'Connor, R.; Brougham, D. F. Metabolomic studies of human lung carcinoma cell lines using in vitro 1H NMR of whole cells and cellular extracts. *NMR Biomed.* **2008**, *21* (8) 809–819.

[79] Wishart, David S. Metabolomics: applications to food science and nutrition research. *Trends Food Sci. Technol.* **2008**, *19* (9) 482–493.

[80] Nagai, Junya; Takano, Mikihisa. Molecular aspects of renal handling of aminoglycosides and strategies for preventing the nephrotoxicity. *Drug Metab. Pharmacokinet.* **2004**, *19* (3) 159–170.

[81] Servais, H.; Ortiz, A.; Devuyst, O.; Denamur, S.; Tulkens, P. M.; Migeot-Leclercq, M. P. Renal cell apoptosis induced by nephrotoxic drugs: cellular and molecular mechanisms and potential approaches to modulation. *Apoptosis* **2008**, *13* (1) 11–32.

[82] European Food Safety Authority. Opinion of the CONTAM panel related to to ochratoxin A in food. *EFSA J.* **2006**, *365*, http://www.efsa.europa.eu/contam_op_ej365_ochratoxin_a_food_en,3.pdf.

[83] Mally, A.; Hard, G. C.; Dekant, W. Ochratoxin A as a potential etiologic factor in endemic nephropathy: Lessons from toxicity studies in rats. *Food Chem. Toxicol.* **2007**, *45* (11) 2254–2260.

[84] Mally, Angela; Voelkel, Wolfgang; Amberg, Alexander; Kurz, Michael; Wanek, Paul; Eder, Erwin; Hard, Gordon; Dekant, Wolfgang. Functional, Biochemical, and Pathological Effects of Repeated Oral Administration of Ochratoxin A to Rats. *Chem. Res. Toxicol.* **2005**, *18* (8) 1242–1252.

[85] National Toxicology Program. Toxicology and carcinogenesis studies of ochratoxin A (CAS No.303-47-9) in F344/N rats (gavage studies). *NTP - Technical Report Series* **1989**, *358*, http:/ntp.niehs.nih.gov/ntp/htdocs/LT_rpts/tr358.pdf.

[86] Boorman, G. A.; McDonald, M. R.; Imoto, S.; Persing, R. Renal lesions induced by ochratoxin A exposure in the F344 rat. *Toxicol. Pathol.* **1992**, *20* (2) 236–245.

[87] Marin-Kuan, Maricel; Cavin, Christophe; Delatour, Thierry; Schilter, Benoit. Ochratoxin A carcinogenicity involves a complex network of epigenetic mechanisms. *Toxicon* **2008**, *52* (2) 195–202.

[88] *IARC monographs on the evaluation of carcinogenic risks to humans: Some traditional herbal medicines, some mycotoxins, naphtalene and styrene.* IARC monographs on the evaluation of carcinogenic risks to humans; IARC Press, Lyon, France: 2002, Vol. 82.

[89] Debelle, Frederic D.; Vanherweghem, Jean-Louis; Nortier, Joelle L. Aristolochic acid nephropathy: A worldwide problem. *Kidney Int.* **2008**, *74* (2) 158–169.

[90] Mengs, U.; Lang, W.; Poch, J. A. The carcinogenic action of aristolochic acid in rats. *Arch. Toxicol.* **1982**, *51* (2) 107–119.

[91] National Toxicology Program. Toxicology and carcinogenesis studies of furan in F344 rats and B6C3F1 mice. *NTP - Technical Report Series* **1993**, *402*, http:/ntp.niehs.nih.gov/ntp/htdocs/LT_rpts/tr402.pdf.

[92] European Food Safety Authority. Report of the scientific panel on contaminants in the food chain on furan in food. *EFSA J.* **2004**, *137*, http://www.efsa.europa.eu /EFSA/Scientific_Document/contam_furan_report7-11-051,0.pdf.

[93] Kellert, Marco; Wagner, Silvia; Lutz, Ursula; Lutz, Werner K. Biomarkers of Furan Exposure by Metabolic Profiling of Rat Urine with Liquid Chromatography-Tandem Mass Spectrometry and Principal Component Analysis. *Chem. Res. Toxicol.* **2008**, *21* (3) 761–768.

[94] Mulrane, Laoighse; Rexhepaj, Elton; Smart, Valerie; Callanan John, J.; Orhan, Diclehan; Eldem, Turkan; Mally, Angela; Schroeder, Susanne; Meyer, Kirstin; Wendt, Maria. Creation of a digital slide and tissue microarray resource from a multi-institutional predictive toxicology study in the rat: an initial report from the PredTox group. *Exp. Toxicol. Pathol.* **2008**, *60* (4-5) 235–245.

[95] Lenz, E. M.; Bright, J.; Knight, R.; Westwood, F. R.; Davies, D.; Major, H.; Wilson, I. D. Metabonomics with 1H NMR spectroscopy and liquid chromatography-mass

spectrometry applied to the investigation of metabolic changes caused by gentamicin-induced nephrotoxicity in the rat. *Biomarkers* **2005**, *10* (2-3) 173–187.

[96] Rached, Eva; Hard Gordon, C.; Blumbach, Kai; Weber, Klaus; Draheim, Regina; Lutz Werner, K.; Ozden, Sibel; Steger, Ulrich; Dekant, Wolfgang; Mally, Angela. Ochratoxin a: 13-week oral toxicity and cell proliferation in male f344/n rats. *Toxicol. Sci.* **2007**, *97* (2) 288–298.

[97] Mengs, U. On the histopathogenesis of rat forestomach carcinoma caused by aristolochic acid. *Arch. Toxicol.* **1983**, *52* (3) 209–220.

[98] Mally, A.; Graff, C.; Moro, S.; Hamberger, C.; Schauer, U. M.; Brück, J.; Özden, S.; Sieber, M.; Steger, U.; Hard, G. C. Furan in Food: 28 day oral toxicity and cell proliferation in male F344/N rats. Abstract No. 744. *Toxicologist* **2009**, *102* (1) 154.

[99] Sangster, Timothy; Major, Hilary; Plumb, Robert; Wilson, Amy J.; Wilson, Ian D. A pragmatic and readily implemented quality control strategy for HPLC-MS and GC-MS-based metabonomic analysis. *Analyst* **2006**, *131* (10) 1075–1078.

[100] Kuhara, T. Diagnosis of inborn errors of metabolism using filter paper urine, urease treatment, isotope dilution and gas chromatography-mass spectrometry. *J. Chromatogr. B* **2001**, *758* (1) 3–25.

[101] Kind, Tobias; Tolstikov, Vladimir; Fiehn, Oliver; Weiss, Robert H. A comprehensive urinary metabolomic approach for identifying kidney cancer. *Anal. Biochem.* **2007**, *363* (2) 185–195.

[102] R Development Core Team. *R: A language and environment for statistical computing.;* R Foundation for Statistical Computing: Vienna, Austria, 2007.

[103] Martinez-Salgado, Carlos; Lopez-Hernandez, Francisco J.; Lopez-Novoa, Jose M. Glomerular nephrotoxicity of aminoglycosides. *Toxicol. Appl. Pharmacol.* **2007**, *223* (1) 86–98.

[104] Wiklund, Susanne; Johansson, Erik; Sjoestroem, Lina; Mellerowicz, Ewa J.; Edlund, Ulf; Shockcor, John P.; Gottfries, Johan; Moritz, Thomas; Trygg, Johan. Visualization of GC/TOF-MS-Based Metabolomics Data for Identification of Biochemically Interesting Compounds Using OPLS Class Models. *Anal. Chem.* **2007**, *80* (1) 116–123.

[105] Narayana, Kilarkaje. An aminoglycoside antibiotic gentamycin induces oxidative stress, reduces antioxidant reserve and impairs spermatogenesis in rats. *J. Toxicol. Sci.* **2008**, *33* (1) 85–96.

[106] Kiyatake, Ikuo; Nakamura, Tsukasa; Koide, Hikaru. Urinary Guanidinoacetic Acid Excretion as an Indicator of Gentamicin Nephrotoxicity in Rats. *Ren. Fail.* **2004**, *26* (4) 339–344.

[107] Xu, Ethan Yixun; Perlina, Ally; Vu, Heather; Troth, Sean P.; Brennan, Richard J.; Aslamkhan, Amy G.; Xu, Qiuwei. Integrated Pathway Analysis of Rat Urine Metabolic

Profiles and Kidney Transcriptomic Profiles To Elucidate the Systems Toxicology of Model Nephrotoxicants. *Chem. Res. Toxicol.* **2008**, *21* (8) 1548–1561.

[108] Pierce, Karisa M.; Hoggard, Jamin C.; Mohler, Rachel E.; Synovec, Robert E. Recent advancements in comprehensive two-dimensional separations with chemometrics. *J. Chromatogr. A* **2008**, *1184* (1-2) 341–352.

[109] Lenz, Eva Maria; Wilson, Ian D. Analytical Strategies in Metabonomics. *J. Proteome Res.* **2007**, *6* (2) 443–458.

[110] Aleo, Michael D.; Wyatt, Roger D.; Schnellmann, Rick G. Mitochondrial dysfunction is an early event in ochratoxin A but not oosporein toxicity to rat renal proximal tubules. *Toxicol. Appl. Pharmacol.* **1991**, *107* (1) 73–80.

[111] Gautier, J. C.; Holzhaeuser, D.; Markovic, J.; Gremaud, E.; Schilter, B.; Turesky, R. J. Oxidative damage and stress response from ochratoxin A exposure in rats. *Free Radical Biol. Med.* **2001**, *30* (10) 1089–1098.

[112] Hoehler, D.; Marquardt, R. R.; McIntosh, A. R.; Hatch, G. M. Induction of free radicals in hepatocytes, mitochondria and microsomes of rats by ochratoxin A and its analogs. *Biochim. Biophys. Acta* **1997**, *1357* (2) 225–233.

[113] Rached, Eva; Pfeiffer, Erika; Dekant, Wolfgang; Mally, Angela. Ochratoxin A: Apoptosis and Aberrant Exit from Mitosis due to Perturbation of Microtubule Dynamics? *Toxicol. Sci.* **2006**, *92* (1) 78–86.

[114] Skordi, Eleni; Yap, Ivan K. S.; Claus, Sandrine P.; Martin, Francois-Pierre J.; Cloarec, Olivier; Lindberg, Johan; Schuppe-Koistinen, Ina; Holmes, Elaine; Nicholson, Jeremy K. Analysis of Time-Related Metabolic Fluctuations Induced by Ethionine in the Rat. *J. Proteome Res.* **2007**, *6* (12) 4572–4581.

[115] Larsson, Agne; Mattsson, Barbro. On the mechanism of 5-oxoproline overproduction in 5-oxoprolinuria. *Clin. Chim. Acta* **1976**, *67* (3) 245–253.

[116] Waters, Nigel J.; Waterfield, Catherine J.; Farrant, R. Duncan; Holmes, Elaine; Nicholson, Jeremy K. Integrated Metabonomic Analysis of Bromobenzene-Induced Hepatotoxicity: Novel Induction of 5-Oxoprolinosis. *J. Proteome Res.* **2006**, *5* (6) 1448–1459.

[117] Ghauri, Farida Y. K.; McLean, Andre E. M.; Beales, Denis; Wilson, Ian D.; Nicholson, Jeremy K. Induction of 5-oxoprolinuria in the rat following chronic feeding with N-acetyl 4-aminophenol (paracetamol). *Biochem. Pharmacol.* **1993**, *46* (5) 953–957.

[118] Cavin, Christophe; Delatour, Thierry; Marin-Kuan, Maricel; Holzhaeuser, Daisy; Higgins, Larry; Bezencon, Claudine; Guignard, Gabriela; Junod, Sylviane; Richoz-Payot, Janique; Gremaud, Eric; et al. Reduction in Antioxidant Defenses may Contribute to Ochratoxin A Toxicity and Carcinogenicity. *Toxicol. Sci.* **2007**, *96* (1) 30–39.

[119] Friesen, Russell W.; Novak, Elizabeth M.; Hasman, David; Innis, Sheila M. Relationship of dimethylglycine, choline, and betaine with oxoproline in plasma of pregnant women and their newborn infants. *J. Nutr.* **2007**, *137* (12) 2641–2646.

[120] Boesch-Saadatmandi, C.; Loboda, A.; Jozkowicz, A.; Huebbe, P.; Blank, R.; Wolffram, S.; Dulak, J.; Rimbach, G. Effect of ochratoxin A on redox-regulated transcription factors, antioxidant enzymes and glutathione-S-transferase in cultured kidney tubulus cells. *Food Chem. Toxicol.* **2008**, *46* (8) 2665–2671.

[121] Han, X.; Patters, A. B.; Jones, D. P.; Zelikovic, I.; Chesney, R. W. The taurine transporter: mechanisms of regulation. *Acta Physiol.* **2006**, *187* (1/2) 61–73.

[122] Nakanishi, T.; Balaban, R. S.; Burg, M. B. Survey of osmolytes in renal cell lines. *Am. J. Physiol.* **1988**, *255* (2) 181–191.

[123] Grunewald, R. Willi; Kinne, Rolf K. H. Osmoregulation in the mammalian kidney: the role of organic osmolytes. *J. Exp. Zool.* **1999**, *283* (7) 708–724.

[124] Lahjouji, Karim; Aouameur, Rym; Bissonnette, Pierre; Coady, Michael J.; Bichet, Daniel G.; Lapointe, Jean-Yves. Expression and functionality of the Na+/myo-inositol cotransporter SMIT2 in rabbit kidney. *Biochim. Biophys. Acta* **2007**, *1768* (5) 1154–1159.

[125] Schrickx, Jan; Lektarau, Yuri; Fink-Gremmels, J. Ochratoxin A secretion by ATP-dependent membrane transporters in Caco-2 cells. *Arch. Toxicol.* **2006**, *80* (5) 243–249.

[126] Tebib, J. G.; Reynaud, C.; Cedoz, J. P.; Letroublon, M. C.; Niveleau, A. Relationship between urinary excretion of modified nucleosides and rheumatoid arthritis process. *Br. J. Rheumatol.* **1997**, *36* (9) 990–995.

[127] Viola, Antonella; Bronte, Vincenzo. Metabolic mechanisms of cancer-induced inhibition of immune responses. *Semin. Cancer Biol.* **2007**, *17* (4) 309–316.

[128] Marklova, E.; Makovickova, H.; Krakorova, I. Screening for defects in tryptophan metabolism. *J. Chromatogr. A* **2000**, *870* (1+2) 289–293.

[129] Mengs, U.; Stotzem, C. D. Toxicity of aristolochic acid. A subacute study in male rats. *Med. Sci. Res.* **1992**, *20* (6) 223–224.

[130] Mengs, U. Acute toxicity of aristolochic acid in rodents. *Arch. Toxicol.* **1987**, *59* (5) 328–331.

[131] Stiborová, Marie; Frei, Eva; Arlt, Volker M.; Schmeiser, Heinz H. Metabolic activation of carcinogenic aristolochic acid, a risk factor for Balkan endemic nephropathy. *Rev. Mutat. Res.* **2008**, *658* (1-2) 55–67.

[132] Chen, Minjun; Su, Mingming; Zhao, Liping; Jiang, Jian; Liu, Ping; Cheng, Jiye; Lai, Yijiang; Liu, Yumin; Jia, Wei. Metabonomic Study of Aristolochic Acid-Induced Nephrotoxicity in Rats. *J. Proteome Res.* **2006**, *5* (4) 995–1002.

[133] Chan, Wan; Cai, Zongwei. Aristolochic acid induced changes in the metabolic profile of rat urine. *J. Pharm. Biomed. Anal.* **2008**, *46* (4) 757–762.

[134] Chan, Wan; Lee, Kim-Chung; Liu, Ning; Wong Ricky, N. S.; Liu, Huwei; Cai, Zongwei. Liquid chromatography/mass spectrometry for metabonomics investigation of the biochemical effects induced by aristolochic acid in rats: the use of information-dependent acquisition for biomarker identification. *Rapid Commun. Mass Spectrom.* **2008**, *22* (6) 873–880.

[135] Ni, Yan; Su, Mingming; Qiu, Yunping; Chen, Minjun; Liu, Yuming; Zhao, Aihua; Jia, Wei. Metabolic profiling using combined GC-MS and LC-MS provides a systems understanding of aristolochic acid-induced nephrotoxicity in rat. *FEBS Lett.* **2007**, *581* (4) 707–711.

[136] Zhang, Xiaoyu; Wu, Huifeng; Liao, Peiqiu; Li, Xiaojing; Ni, Jiazuan; Pei, Fengkui. NMR-based metabonomic study on the subacute toxicity of aristolochic acid in rats. *Food Chem. Toxicol.* **2006**, *44* (7) 1006–1014.

[137] Sander, G.; Topp, H.; Wieland, J.; Heller-Schoech, G.; Schoech, G. Possible use of urinary modified RNA metabolites in the measurement of RNA turnover in the human body. *Hum. Nutr.: Clin. Nutr.* **1986**, *40* (2) 103–118.

[138] Sander, G.; Topp, H.; Heller-Schoch, G.; Wieland, J.; Schoch, G. Ribonucleic acid turnover in man:RNA catabolites in urine as measure for the metabolism of each of the three major species of RNA. *Clin. Sci.* **1986**, *71* (4) 367–374.

[139] Pozdzik, A. A.; Salmon, I. J.; Debelle, F. D.; Decaestecker, C.; Van den Branden, C.; Verbeelen, D.; Deschodt-Lanckman, M. M.; Vanherweghem, J. L.; Nortier, J. L. Aristolochic acid induces proximal tubule apoptosis and epithelial to mesenchymal transformation. *Kidney Int.* **2008**, *73* (5) 595–607.

[140] Ejaz, A. Ahsan; Mu, Wei; Kang, Duk-Hee; Roncal, Carlos; Sautin, Yuri Y.; Henderson, George; Tabah-Fisch, Isabelle; Keller, Birgit; Beaver, Thomas M.; Nakagawa, Takahiko; et al. Could uric acid have a role in acute renal failure? *Clin. J. Am. Soc. Nephrol.* **2007**, *2* (1) 16–21.

[141] Nakagawa, Takahiko; Mazzali, Marilda; Kang, Duk-Hee; Sanchez-Lozada, L. Gabriela; Herrera-Acosta, Jaime; Johnson, Richard J. Uric Acid - A Uremic Toxin? *Blood Purif.* **2006**, *24* (1) 67–70.

[142] Robosky, Lora C.; Wells, Dale F.; Egnash, Laura A.; Manning, Matthew L.; Reily, Michael D.; Robertson, Donald G. Metabonomic Identification of Two Distinct Phenotypes in Sprague-Dawley (Crl:CD(SD)) Rats. *Toxicol. Sci.* **2005**, *87* (1) 277–284.

[143] Debelle, Frederic D.; Nortier, Joelle L.; De Prez, Eric G.; Garbar, Christian H.; Vienne, Anne R.; Salmon, Isabelle J.; Deschodt-Lanckman, Monique M.; Vanherweghem, Jean-Louis. Aristolochic acids induce chronic renal failure with interstitial fibrosis in salt-depleted rats. *J. Am. Soc Nephrol.* **2002**, *13* (2) 431–436.

[144] Yeh, Yen-Hung; Lee, Ya-Ting; Hsieh, Hung-Sheng; Hwang, Deng-Fwu. Short-term toxicity of aristolochic acid, aristolochic acid-I and aristolochic acid-II in rats. *Food Chem. Toxicol.* **2008**, *46* (3) 1157–1163.

[145] Shibutani, Shinya; Dong, Huan; Suzuki, Naomi; Ueda, Shiro; Miller, Frederick; Grollman, Arthur P. Selective toxicity of aristolochic acids I and II. *Drug Metab. Dispos.* **2007**, *35* (7) 1217–1222.

[146] Limacher, Anita; Kerler, Josef; Davidek, Tomas; Schmalzried, Frank; Blank, Imre. Formation of Furan and Methylfuran by Maillard-Type Reactions in Model Systems and Food. *J. Agric. Food Chem.* **2008**, *56* (10) 3639–3647.

[147] Thomas, Charles; Pellicciari, Roberto; Pruzanski, Mark; Auwerx, Johan; Schoonjans, Kristina. Targeting bile-acid signalling for metabolic diseases. *Nat. Rev. Drug Discovery* **2008**, *7* (8) 678–693.

[148] Ellinger-Ziegelbauer, H. C.; Mally, A.; Walijew, A.; Schmitt, C.; Hewitt, P.; Matheis, K.; Raschke, M.; Riefke, B.; Brandenburg, A.; Gmuender, H. Combined conventional and 'omics evaluation of 4 hepatotoxicants with bile duct or cholestatic effects. Abstract No. 1028. *Toxicologist* **2009**, *102* (1) 213.

[149] Delaney, Jane; Neville, William A.; Swain, Aubrey; Miles, Adam; Leonard, Michael S.; Waterfield, Catherine J. Phenylacetylglycine, a putative biomarker of phospholipidosis: Its origins and relevance to phospholipid accumulation using amiodarone treated rats as a model. *Biomarkers* **2004**, *9* (3) 271–290.

[150] Zhen, Yueying; Krausz, Kristopher W.; Chen, Chi; Idle, Jeffrey R.; Gonzalez, Frank J. Metabolomic and genetic analysis of biomarkers for peroxisome proliferator-activated receptor alpha expression and activation. *Mol. Endocrinol.* **2007**, *21* (9) 2136–2151.

[151] Dou, L.; Jourde-Chiche, N.; Faure, V.; Cerini, C.; Berland, Y.; Dignat-George, F.; Brunet, P. The uremic solute indoxyl sulfate induces oxidative stress in endothelial cells. *J. Thromb. Haemostasis* **2007**, *5* (6) 1302–1308.

[152] Berglund, Torkel. Nicotinamide, a missing link in the early stress response in eukaryotic cells: a hypothesis with special reference to oxidative stress in plants. *FEBS Lett.* **1994**, *351* (2) 145–149.

[153] Comai, Stefano; Costa, Carlo V. L.; Ragazzi, Eugenio; Bertazzo, Antonella; Allegri, Graziella. The effect of age on the enzyme activities of tryptophan metabolism along the kynurenine pathway in rats. *Clin. Chim. Acta* **2005**, *360* (1-2) 67–80.

[154] Laviano, Alessandro; Meguid, Michael M.; Preziosa, Isabella; Fanelli, Filippo Rossi. Oxidative stress and wasting in cancer. *Curr. Opin. Clin. Nutr. Metab. Care* **2007**, *10* (4) 449–456.

[155] Bloomer, Joseph R. Liver metabolism of porphyrins and heme. *J. Gastroenterol. Hepatol.* **1998**, *13* (3) 324–329.

[156] Rohde, Cynthia M.; Wells, Dale F.; Robosky, Lora C.; Manning, Matthew L.; Clifford, Charles B.; Reily, Michael D.; Robertson, Donald G. Metabonomic Evaluation of Schaedler Altered Microflora Rats. *Chem. Res. Toxicol.* **2007**, *20* (10) 1338–1392.

13 List of abbreviations

3-IS	3-indoxylsulfate
AA	aristolochic acid
ALAT	alanine amino transferase
ALP	alkaline phosphatase
ASAT	aspartate amino transferase
BDN	bile duct necrosis
BrdU	5-bromo-2'-deoxyuridine
BSA	bis-trimethylsilyltrifuoroacetamide
BUN	blood urea nitrogen
bw	body weight
C	control group
DA	discriminant analysis
GC/MS	gas chromatography coupled to mass spectrometry
GGT	gamma glutamyl transferase
GM	gentamicin
GOT	glutamate oxalate transaminase
GPT	glutamate pyruvate transaminase
ESI	electrospray ionization
H	high dose group
HCD	hepatocellular cell death
HCH	hepatocellular hypertrophy
HILIC	hydrophilic interaction liquid chromatography
^{1}H NMR	proton nuclear magnetic resonance
i.p.	intraperitoneal(ly)
i.v.	intravenous(ly)
L	low dose group
LC/MS	liquid chromatography coupled to mass spectrometry
M	mid dose group
MO	methoxime
MS	mass spectrometry
PAG	phenylacetyl glycine

PC	principal component
PCA	principal component analysis
PLS	partial least squares projection to latent structures
p.o.	peroral
OPLS-DA	orthogonal projection to latent structures discriminant analysis
OTA	ochratoxin A
SAH	*S*-adenosyl-homocysteine
SAM	*S*-adenosyl-methionine
SPF	specific pathogen free
TMAO	trimethylamine-*N*-oxide
TMS	trimethylsilyl
TOF	time-of-flight detection
TSP	d_4-trimethylsilylpropionic acid sodium salt
wt	weight

14 List of publications

14.1 Peer reviewed journals

Sieber, M.; Wagner, S.; Rached, E.; Amberg, A.; Mally, A.; Dekant, W. Metabonomic study of ochratoxin A toxicity after repeated administration: Phenotypic anchoring enhances ability for biomarker discovery. Accepted for *Chem. Res. Toxicol.*

Sieber, M.; Hoffmann, D.; Adler, M.; Vaidya, V. S.; Clement, M.; Bonventre, J. V.; Zidek, N.; Rached, E.; Amberg, A.; Dekant, W.; Mally, A. Comparative analysis of novel non-invasive renal biomarkers and metabonomic changes in a rat model of gentamicin nephrotoxicity. Accepted for *Toxicol. Sci.*

Kopp, Eva K.; Sieber, Maximilian; Kellert, Marco; Dekant, Wolfgang. Rapid and Sensitive HILIC-ESI-MS/MS Quantitation of Polar Metabolites of Acrylamide in Human Urine Using Column Switching with an Online Trap Column. *J. Agric. Food Chem.* **2008**, *56* (21) 9828–9834.

Wagner, Silvia; Scholz, Karoline; Sieber, Maximilian; Kellert, Marco; Voelkel, Wolfgang. Tools in Metabonomics: An Integrated Validation Approach for LC-MS Metabolic Profiling of Mercapturic Acids in Human Urine. *Anal. Chem.* **2007**, *79* (7) 2918–2926.

Sieber, M.; Dekant, W.; Faber, J. H.; Bringmann, G. Biotransformation and pharmacokinetics of the antiplasmodial naphthylisoquinoline alkaloid dioncophylline A. *Xenobiotica* **2006**, *36* (9) 750–762.

Broering, Martin; Brandt, Carsten D.; Koehler, Silke; Sieber, Maximilian. Crystallographic evidence for structural diversity in cationic (tripyrrinato)cobalt(II) complexes. *J. Porphyrins Phthalocyanines* **2005**, *9* (10 & 11) 683–690.

14.2 Posters

Sieber, M.; Wagner, S., Amberg, A.r; Mally, A.; Dekant, W. Metabonomic analysis of ochratoxin A toxicity after repeated administration: Phenotypic anchoring enhances model predictivity and biomarker identification. Abstract No. 995. *Toxicologist* **2009**, *102*, (Suppl. 1) 188.

Ellinger-Ziegelbauer, H. C., Mally, A., Walijew, A., Schmitt, C., Hewitt, P., Matheis, K., Raschke, M., Riefke, B., Brandenburg, A., Gmuender, H., Amberg, A., Mulrane, L., Gallagher, W., Sieber, M. and Adler, M. Combined conventional and 'omics evaluation of 4 hepatotoxicants with bile duct or cholestatic effects. Abstract No. 1028. *Toxicologist* **2009**, *102*, (Suppl. 1) 213.

Mally, A., Graff, C., Moro, S., Hamberger, C., Schauer, U. M., Brück, J., Özden, S., Sieber, M., Steger, U., Hard, G. C., Chipman, J. K., Schrenk, D. and Dekant, W. Furan in Food: 28 day oral toxicity and cell proliferation in male F344/N rats. Abstract No. 744. *Toxicologist* **2009**, *102*, (Suppl. 1) 154.

Sieber, M.; Wagner, S.; Rached, E.; Amberg, A.; Mally, A.; Dekant, W. A combined GC-MS, LC-MS and NMR metabonomics approach for early detection of ochratoxin A

nephrotoxicity. Abstract No. 365. *Naunyn-Schiedeberg's Arch. Pharmacol.* **2008**, *377* (Suppl. 1) 74.

Hoffmann, D.; Zidek, N.; Sieber, M.; Dekant, W.; Mally, A. Lipocalin 2, clusterin and Kim 1 as potential early, non-invasive biomarkers of nephrotoxicity. Abstract No.366. *Naunyn-Schiedeberg's Arch. Pharmacol.* **2008**, *377* (Suppl. 1) 74.

Sieber, Maximilian; Dekant, Wolfgang. An integrated GC/MS method for metabonomics of biofluids. Abstract No. 497. *Naunyn-Schiedeberg's Arch. Pharmacol.* **2007**, *375* (Suppl. 1) 98.

Wagner, S.; Simon, K.; Sieber, M.; Kellert, M.; Völkel, W.. Metabolic profiling of mercapturic acids in human urine: a validation approach for LC/MS metabonomics. Abstract No.496. *Naunyn-Schiedeberg's Arch. Pharmacol.* **2007**, *375* (Suppl. 1) 98.

15 Summary/Zusammenfassung

15.1 Summary

Aim of this thesis was the assessment of metabonomics techniques for the early and non-invasive detection of toxicity. For this purpose, the urine collected during various repeated-dose studies of nephro- and hepatotoxins in rats was analyzed with ^{1}H NMR and GC/MS. The samples were obtained from four studies conducted in-house, three studies on the nephrotoxins gentamicin (repeated s.c. administration of 0, 60 and 120 mg/kg bw twice daily for 8 days), ochratoxin A (repeated p.o. administration of 0, 21, 70 and 210 µg/kg bw five days per week for 90 days) and aristolochic acid (repeated p.o. administration of 0, 0.1, 1.0 and 10 mg/kg bw for 12 days), as well as one study on the hepatotoxin furan (repeated p.o. administration of 0, 0.1, 0.5 and 2.0 mg/kg bw for 28 days). The urine samples from 16 studies conducted in the course of the InnoMed PredTox project were analyzed as well, thereby focusing on ^{1}H NMR analysis and bile duct necrosis as histopathological endpoint.

The InnoMed PredTox project within the 6th framework programme of the European Union is a joint industry and academia project which evaluates the combination of results from omics technologies together with the results from more conventional toxicology methods for more informed decision making in preclinical safety evaluation.

^{1}H NMR analysis was carried out using the InnoMed PredTox protocol, i.e. urine buffered with 1 M phosphate buffer, using D_2O as shift lock reagent and D_4-trimethylsilyl-propionic acid as chemical shift reference. The spectra were recorded using the bruker noesygppr1d pulse sequence for water suppression. For multivariate data analysis, spectral intensity was binned into 0.04 ppm wide bins.

GC/MS analysis of urine samples was carried out by a comprehensive methoximation/silylation method. After protein precipitation with methanol, samples were dried, treated with methoxyamine hydrochloride in pyridine and subsequently with methyl(trimethylsilyl)trifluoroacetamide. GC/MS analysis was carried out with split/splitless inlet using a temperature gradient on a DB5-MS column and EI ionization. The chromatograms were prepared for multivariate data analysis using the R-program based peak picking and alignment software XCMS version 2.4.0.

Multivariate data analysis of GC/MS and ^{1}H NMR data was carried out using SIMCA P+ 11.5. Principal component analysis (PCA) was used to detect and visualize time-point and dose-dependent differences between treated animals and controls. Potential molecular markers of toxicity discriminating treated animals from controls were extracted from the data with orthogonal projection to latent structures discriminant analysis (OPLS-DA). ^{1}H NMR-based markers were identified and quantified with the Chenomx NMR Suite, GC/MS based markers were identified using the NIST Mass Spectral Database and by co-elution with authentic reference standards.

PCA of urinary metabolite profiles was able to differentiate treated animals from controls at the same time as histopathology. An advantage over classical clinical chemistry parameters regarding sensitivity could be observed in some cases. However, analysis of the markers responsible for class separation revealed only alterations in the so called “usual suspects” [15]. These metabolites are found to be altered in almost any metabonomics study. They are most abundant in urine and reflect alterations in very general toxicity pathways.

Metabonomic analysis with GC/MS and ^{1}H NMR revealed alterations in the urinary profile of treated animals as soon as one day after start of treatment with 120 mg/kg bw gentamicin, correlating with changes in clinical chemistry parameters and histopathology. These alterations were a decrease in the urinary excretion of citrate, 2-oxoglutarate, hippurate, trigonelline and 3-indoxylsulfate as well as an increase in the excretion of 5-oxoproline, lactate, alanine and glucose.

Ochratoxin A (OTA) treatment caused changes in urinary profiles in single animals observed as early as 2 weeks after start of treatment with 210µg OTA/kg bw, correlating with changes in clinical chemistry parameters and histopathology. These alterations were a decrease in the excretion of citrate, 2-oxoglutarate and hippurate and an increase in the excretion of glucose, *myo*-inositol, *N,N*-dimethylglycine, glycine, alanine and lactate. Integration of histopathology scores increased confidence in the molecular markers discovered.

Aristolochic acid treatment resulted in decreased urinary excretion of citrate, 2-oxoglutarate, hippurate and creatinine as well as increased excretion of 5-oxoproline, *N,N*-dimethylglycine, pseudouridine and uric acid observable after 12 days of treatment

with 10 mg aristolochic acid/kg bw. These changes were not accompanied by alterations in clinical chemistry parameters or histopathology.

Treatment with 2.0 mg furan/kg bw for four weeks did not induce any alterations in urinary profiles observable with the GC/MS and ^{1}H NMR methods applied, correlating with unchanged clinical chemistry parameters and histopathology.

The alterations in metabolite profiles can be associated with mechanisms of toxicity. Decrease in the excretion of hippurate is indicative of alterations in the gut microflora, an effect that is expected as pharmacological action of the aminoglycoside antibiotic gentamicin and that can also be explained by the p.o. administration of xenobiotica. Decreases in the Krebs cycle intermediates citrate and 2-oxoglutarate and an increase in lactate is associated with altered energy metabolism. Increased pseudouridine excretion is associated with cell proliferation and was observed with aristolochic acid and ochratoxin A, for which proliferative processes were observed with histopathology. Various metabolites, such as 5-oxoproline and *N,N*-dimethylglycine can be associated with oxidative stress. Glucose, a marker of renal damage in clinical chemistry, was observed for all three nephrotoxins studied.

Single study analysis with PCA of GC/MS chromatograms and ^{1}H NMR spectra of urine from three studies conducted within the InnoMed PredTox project showing bile duct necrosis revealed alterations in urinary profiles with the onset of changes in clinical chemistry and histopathology. Alterations were mainly decreased Krebs cycle intermediates and changes in the aromatic gut flora metabolites, an effect that may result as a secondary effect from altered bile flow.

A cross study analysis of all 16 InnoMed PredTox studies using urinary ^{1}H NMR spectra was applied to find specific markers for bile duct damage. Even though a marker panel was extracted from the data, these markers were not altered across all studies showing bile duct damage, but also showed changes in studies not showing the respective histopathology. These markers require further evaluation.

In conclusion, metabonomics techniques are able to detect toxic lesions at the same time as histopathology and clinical chemistry. The metabolites found to be altered are common to most toxicities and are not organ-specific. A mechanistic link to the observed toxicity has to be established in order to avoid confounders such as body weight loss,

pharmacological effects etc. For pattern recognition purposes, large databases are necessary.

15.2 Zusammenfassung

Ziel dieser Dissertation war die Bewertung von Metabonomics-Techniken zur frühen, nicht-invasiven Erkennung von Toxizität. Zu diesem Zweck wurde Urin, der im Zuge mehrerer Studien mit wiederholter Gabe verschiedener Nephro- und Hepatotoxine in Ratten mit ^{1}H NMR und GC/MS analysiert. Die Urinproben wurden aus vier Studien erhalten, die am Institut durchgeführt wurden; drei Studien mit den Nephrotoxinen Gentamicin (wiederholte s.c.-Gabe von 0, 60 und 120 mg/kg Körpergewicht (KG) zweimal täglich über 8 Tage), Ochratoxin A (wiederholte p.o.-Gabe von 0, 21, 70 und 210 µg/kg KG fünf mal wöchentlich für 90 Tage) und Aristolochiasäure (wiederholte Gabe von von 0, 0.1, 1.0 und 10 mg/kg KG über 12 Tage), sowie eine Studie mit dem Hepatotoxin Furan (wiederholte p.o.-Gabe von 0, 0.1, 0.5 und 2.0 mg/kg KG über 28 Tage). Die Urinproben von 16 Studien, die im Zuge des InnoMed PredTox Projekts durchgeführt wurden, wurden ebenfalls analysiert. Dabei lag der Schwerpunkt auf der ^{1}H NMR Analytik und dem histopathologischen Endpunkt Gallengangnekrose (BDN).

Das InnoMed PredTox Projekt innerhalb des „6th framework programme“ der Europäischen Union ist ein gemeinschaftliches Projekt von Industrie- und Universitäts-partnern, welche die Ergebnisse von omics-Technologien zusammen mit herkömmlichen Methoden der Toxikologie bewerten, zur besseren Entscheidungsfindung in der präklinischen Sicherheitsbewertung.

^{1}H NMR-Analysen folgten dem InnoMed PredTox Protokoll. Urin wurde mit 1 M Phosphatpuffer gepuffert, D_2O wurde als shift lock Reagenz verwendet und die chemische Verschiebung auf *D*$_4$-Trimethylsilylpropionsäure referenziert. Die Spektren wurden mit Wasserunterdrückung durch die noesygppr1d-Pulssequenz der Bruker-bibliothek aufgenommen. Zur multivariaten Datenanalyse wurden die ^{1}H NMR-Spektren in 0.04 ppm große „bins“ unterteilt.

Zur GC/MS-Analyse der Urinproben wurde eine umfassende Methoximierungs/ Silylierungsmethode verwendet. Nach der Proteinfällung mit Methanol wurden die Urinproben getrocknet und nacheinander mit Methoxyaminhydrochlorid in Pyridin und Methyl(trimethylsilyl)trifluoracetamid derivatisiert. Zur GC/MS-Probenaufgabe wurde ein split/splitless-Einlass mit verwendet. Die Trennung der Analyten erfolgte mit einem

Temperaturgradienten auf einer DB5-MS-Säule. Die Ionisierung zur MS-Detektion erfolgte mit Elektronenstoßionisierung. Die GC/MS-Chromatogramme wurden mit dem R-Programm-basierten XCMS-Softwarepaket Version 2.4.0 zur multivariaten Datenanalyse vorbereitet.

Zur multivariaten Datenanalyse von GC/MS- und ^{1}H NMR-Daten wurde SIMCA P+11.5 verwendet. Hauptkomponentenanalyse (PCA) wurde zur Visualisierung von zeit- und dosisabhängigen Unterschieden zwischen Kontrollen und behandelten Tieren benutzt. Potentielle Toxizitätsmarker wurden mit der „orthogonal projection to latent structures"-Diskriminantenanalyse (OPLS-DA) herausgefiltert. Die Chenomx-NMR-Suite wurde zur Identifizierung und Quantifizierung von ^{1}H NMR-basierten Markern verwendet; GC/MS-basierte Marker wurden mit der „NIST Mass Spectral Database" und durch Koelution mit Referenzstandards identifiziert.

Mittels PCA konnten Kontroll- von behandelten Tieren zum gleichen Zeitpunkt wie mit Histopathologie unterschieden werden. Gegenüber klinisch-chemischen Parametern zeigte sich Metabonomics in einigen Fällen empfindlicher. Eine genauere Betrachtung der Metaboliten, die für die Trennung zwischen Kontroll- und behandelten Tieren verantwortlich waren, zeigte jedoch, dass es sich dabei hauptsächlich um die sog. „Üblichen Verdächtigen" [15] handelt. Diese Metaboliten sind in fast allen Metabonomics-studien verändert. Sie liegen im Urin in der höchsten Konzentration vor und zeigen allgemeine Reaktionen des Organismus auf Toxizität an.

GC/MS- und ^{1}H NMR-Analyse von Urin von Tieren, die mit 120 mg/kg KG Gentamicin behandelt wurden, zeigten bereits nach einem Tag Änderungen in der Urinzusammensetzung an. Diese Beobachtung wurde von geringfügigen Änderungen in klinisch-chemischen Parametern gestützt. Während die Ausscheidung von Citrat, 2-Oxoglutarat, Hippurat, Trigonellin und 3-Indoxylsulfat im Urin erniedrigt war, war die Ausscheidung von Lactat, Alanin, 5-Oxoprolin und Glucose erhöht.

Die durch die Gabe von 210 µg Ochratoxin A/kg KG verursachten Änderungen im Metabolitenprofil des Urins konnten mit Metabonomics-Techniken bereits nach zwei Wochen in einzelnen Tieren beobachtet werden. Diese Beobachtungen wurden durch Veränderungen in klinisch-chemischen Parametern und in der Histopathologie gestützt. Die beobachteten Veränderungen waren eine erniedrigte Ausscheidung von Citrat, 2-Oxoglutarat und Hippurat sowie eine erhöhte Ausscheidung von Glucose, *myo*-Inositol,

N,N-Dimethylglycin, 5-Oxoprolin, Glycin, Alanin und Lactat. Die Miteinbeziehung von Histopathologiedaten in die multivariaten Modelle zur Markeridentifizierung erhöhte die Konfidenz der Marker.

Nach 12 Tagen der Behandlung mit 10 mg Aristolochiasäure/kg KG konnte eine Erniedrigung in der Ausscheidung von Citrat, 2-Oxoglutarat, Hippurat und Creatinin sowie eine Erhöhung der Ausscheidung von 5-Oxoprolin, *N,N*-Dimethylglycin und Pseudouridin beobachtet werden. Diese Veränderungen des Metabolitenprofils im Urin wurden von keinerlei Veränderungen in klinisch-chemischen Parametern oder in der Histopathologie begleitet.

Eine Behandlung mit 2.0 mg/kg KG Furan über vier Wochen verursachte keine Veränderungen im Urinprofil, die mit den hier beschriebenen GC/MS- und ^{1}H NMR-Methoden beobachtet werden konnten. Dies ist im Einklang mit unveränderten klinisch-chemischen Parametern und der Histopathologie.

Die beobachteten Veränderungen der Metabolitenprofile des Urins können mit verschiedenen Mechanismen in Verbindung gebracht werden. Eine Erniedrigung der Ausscheidung von Hippurat weist auf eine Veränderung der Darmmikroflora hin; für das Aminoglykosid-Antibiotikum Gentamicin ist dies ein pharmakologischer Effekt, und für die perorale Gabe von Xenobiotica ist eine Veränderung der Darmflora zu erwarten. Eine erniedrigte Ausscheidung von Citrat und 2-Oxoglutarat zusammen mit einer erhöhten Ausscheidung von Lactat wird mit einer Veränderung des Energiestoffwechsels in Verbindung gebracht. Eine erhöhte Ausscheidung von Pseudouridin ist mit Zell-proliferation assoziiert und wurde nach der Gabe von Ochratoxin A und Aristolochiasäure beobachtet. Beide Stoffe sind kanzerogen und es wurden proliferative Prozesse in der Histopathologie beobachtet. Verschiedene Metaboliten wie 5-Oxoprolin und *N,N*-Dimethylglycin können mit erhöhtem oxidativen Stress in Verbindung gebracht werden. Erhöhte Glucose im Urin, ein Parameter zur Diagnose von Nierenschäden in der klinischen Chemie, wurde in allen drei Studien mit Nephrotoxinen beobachtet.

Die PCA von GC/MS- und ^{1}H NMR-Daten von drei einzelnen Studien aus dem „InnoMed PredTox“ Projekt, welche Gallengangnekrosen als histopathologischen Endpunkt aufwiesen, zeigte eine Veränderung der Urinprofile zur gleichen Zeit wie klinisch-chemische Parameter und die Histopathologie. Die Veränderungen waren hauptsächlich eine erniedrigte Ausscheidung von Citratzyklusintermediaten und

Veränderungen bei Metaboliten, die mit der Darmflora assoziiert sind – ein Effekt, der wahrscheinlich auf den veränderten Gallenfluss zurückzuführen ist.

Eine multivariate Datenanlyse, welche die ^{1}H NMR Urinprofile aller 16 „InnoMed PredTox“-Studien beinhaltete, wurde angewendet, um spezifische Marker für Gallengang-nekrosen zu finden. Obwohl eine Reihe von potentiellen Markern aus den ^{1}H NMR-Spektren extrahiert werden konnte, waren diese Metaboliten nicht in allen Studien mit Gallengangsnekrosen verändert und zeigten außerdem auch Veränderungen in Studien ohne Gallengangbefunde.

Zusammenfassend konnte gezeigt werden, dass Metabonomics prinzipiell zum gleichen Zeitpunkt wie klinisch-chemische Parameter und Histopathologie die Erkennung von toxischen Veränderungen erlauben. Die veränderten Metaboliten sind jedoch zumeist nicht organspezifisch und können mit allgemeinen Toxizitätsmechanismen, wie oxidativem Stress oder Zellproliferation, in Verbindung gebracht werden. Für die Bewertung der Ergebnisse von Metabonomics-Studien ist ein mechanistisches Verständnis der Veränderungen im Urinprofil notwendig, um eine Trennung von toxischen Effekten und solchen, die auf pharmakologische Wirkung, Körpergewichtsverlust etc. zurückzuführen sind, zu erreichen. Für eine Vorhersage von toxischen Mechanismen aufgrund der Urinprofile ist eine größere Datengrundlage notwendig.

16 Acknowledgements

I would like to thank the following persons, without them this thesis would not have been possible:

- Prof. Dr. Wolfgang Dekant, for his supervision and for providing the topic of this thesis.
- Prof. Dr. Ulrike Holzgrabe for supervising my thesis on behalf of the faculty of chemistry and pharmacy.
- Dr. Angela Mally, for correcting the manuscript and for the comments to the work and the fruitful discussions in all scientific belongs.
- Silvia Wagner, for all the joint work concerning the omics and especially for the LC/MS analyses of the OTA project.
- Hannelore Popa-Henning and Gabriella Wehr for all the paperwork.
- Alexander Amberg, Björn Riefke, Marian Raschke and Arndt Brandenburg from the metabonomics subgroup, Phil Hewitt, Heidrun Ellinger-Ziegelbauer and Katja Matheis as well as all other project partners for the great cooperation during the InnoMed PredTox project.
- Heike Keim-Häusler, Ursula Tatsch, Nataly Bittner and Elisabeth Rüb-Spiegel for their help with all experimental procedures.
- My colleagues Marco, Silvia, Sibel, Eva and Karin, for the great atmosphere in room 304.
- All colleagues from the second and third floor and the animal house for the good working atmosphere.
- My parents for their support in all regards.

Part of this work was sponsored by the InnoMed PredTox project within the 6th framework programme of the European Union.